Université de Montréal

Développement et applications d'approches pharmacométriques pour l'individualisation du méthylphénidate dans le traitement du trouble déficitaire de l'attention : de l'occupation des transporteurs à l'effet clinique

Par

Sara Soufsaf

Faculté de Pharmacie

Thèse présentée en vue de l'obtention du grade de Philosophiæ Doctor (Ph.D.)

en Sciences pharmaceutiques

13 Avril 2023

Université de Montréal

Faculté de Pharmacie

Cette thèse intitulée

Développement et applications d'approches pharmacométriques pour l'individualisation du méthylphénidate dans le traitement du trouble déficitaire de l'attention : de l'occupation des transporteurs à l'effet clinique

Présenté par

Sara Soufsaf

A été évalué(e) par un jury composé des personnes suivantes

Amélie Marsot
Président-rapporteur

Fahima Nekka
Directeur de recherche

Philippe Vincent
Membre du jury

Roberto Gomeni
Examinateur externe

Résumé

Le méthylphénidate est un des médicaments les plus prescrits pour les patients ayant un trouble déficitaire de l'attention (TDAH). Comme la réponse au méthylphénidate peut varier d'un patient à l'autre, l'optimisation de la dose passe souvent par une période de titration. Au cours de cette titration, le clinicien, guidé par son expertise, prescrit différents niveaux de dose jusqu'à trouver celle qui convienne au patient. Ceci en fait un processus lourd pour le patient. L'individualisation des doses de méthylphénidate peut donc être améliorée par l'utilisation d'approches pharmacométriques. Ces approches cristallisent les informations connues sur le médicament dans un langage condensé basé sur les mathématiques et statistiques. Ainsi, leur utilisation dans le contexte du méthylphénidate fournit un outil numérique permettant de comprendre sa pharmacocinétique (ce que le corps fait au méthylphénidate) et sa pharmacodynamie (ce que le méthylphénidate fait au corps). Cette thèse se met à la quête de l'enrichissement de ces approches pharmacométriques en trois volets.

La première problématique abordée concerne la grande variabilité interindividuelle dans le traitement du méthylphénidate. Le début de la thèse s'attaque à l'interchangeabilité des médicaments novateurs et génériques ayant une grande variabilité interindividuelle. Une nouvelle méthode est proposée pour comparer efficacement les médicaments selon leur pharmacocinétique. Celle-ci se base sur une méthode établie qui tient compte non seulement de la réponse moyenne d'une population à un médicament, mais aussi de la variabilité interindividuelle dans cette réponse. Cette nouvelle méthode ajoute un paramètre modulable selon le médicament étudié et corrige les problèmes de permissivité des méthodes actuelles.

La pharmacodynamie du méthylphénidate est étudiée dans les deuxième et troisième volets de cette thèse. Il a été rapporté que l'efficacité du méthylphénidate décroît en fin de journée, malgré des concentrations plasmatiques similaires aux premières heures d'administration. Ainsi, suite à la prise de méthylphénidate, une tolérance aigüe se développe dans une même journée. Ce phénomène, observé sur des échelles de mesure cliniques mesurant la réduction des symptômes du TDAH, a déjà été décrit par des approches pharmacométriques. La deuxième partie de cette

thèse explore la présence de cette tolérance aigüe au niveau des cibles thérapeutiques du méthylphénidate : les transporteurs de dopamine et norépinéphrine. Un modèle pharmacométrique est créé, décrivant l'interaction du méthylphénidate avec les transporteurs de dopamine et de norépinéphrine. Ce modèle est utilisé pour calculer la performance de différents régimes posologiques et explore le rôle de la norépinéphrine sur les doses nécessaires pour le traitement du TDAH.

Finalement, le troisième volet ajoute la pharmacodynamie sur une échelle clinique, notamment celle du score SKAMP. Grâce au modèle pharmacométrique du deuxième volet, la dernière partie de cette thèse cherche à répondre à la question : comment l'interaction du méthylphénidate avec les transporteurs de dopamine se traduit en effet clinique? Nos résultats indiquent que l'interaction avec les transporteurs se traduit partiellement en effet clinique et que la relation entre ces deux éléments est plus significative en début de journée comparativement au soir.

En somme, cette thèse a exploré les différentes facettes des méthodes pharmacométriques et leur application dans les prescriptions du méthylphénidate chez les patients atteints de TDAH. Les résultats de cette recherche démontrent l'utilité des approches pharmacométriques et ouvrent la porte à une recherche plus poussée afin de guider l'individualisation du méthylphénidate.

Mots-clés : méthylphénidate, pharmacométrie, pharmacocinétique, pharmacodynamie, bioéquivalence, transporteurs de dopamine, échelles de mesures clinique, modélisation de population

Abstract

Methylphenidate is one of the most prescribed medications for patients with attention deficit hyperactivity disorder (ADHD). Because the response to methylphenidate varies greatly among patients, dose optimization often involves a titration period. During this titration period, the clinicians, guided by their expertise, prescribes different levels of dose until they find the one that works best for the patient. This makes it a burdensome process for the patient. Individualization of methylphenidate doses can be improved by using pharmacometric approaches. These approaches crystallize the known information about the medication into a condensed language based on mathematics and statistics. Thus, their use in the context of methylphenidate provides a digital tool for understanding its pharmacokinetics (what the body does to methylphenidate) and its pharmacodynamics (what methylphenidate does to the body). This thesis seeks to enrich these pharmacometric approaches in three parts.

The first part of this dissertation concerns the high interindividual variability in methylphenidate response. The beginning of the thesis tackles the interchangeability of innovative and generic drugs with high interindividual variability. A new method is proposed to effectively compare drugs based on their pharmacokinetics. This method is based on an established method that takes into account not only the average response of a population to a drug, but also the interindividual variability in that response. This new method adds a modifiable parameter depending on the drug being studied and corrects the problems of permissiveness in current methods.

The pharmacodynamics of methylphenidate are studied in the second and third parts of this thesis. It has been reported that the efficacy of methylphenidate decreases at the end of the day, despite similar plasma concentrations to those in the early hours of administration. Thus, after taking methylphenidate, acute tolerance develops within the same day. This phenomenon, observed on clinical measurement scales measuring the reduction of ADHD symptoms, has already been described by pharmacometric approaches. The second part of this thesis explores the presence of this acute tolerance at the therapeutic targets of methylphenidate: dopamine and norepinephrine transporters. A pharmacometric model is created, describing the interaction

of methylphenidate with dopamine and norepinephrine transporters. This model is used to calculate the performance of different dosage regimens and explore the role of norepinephrine in the doses needed for ADHD treatment.

Finally, the third part adds pharmacodynamics on a macroscopic scale, particularly the clinical effect of methylphenidate. Using the pharmacometric model from the second part, the end of this thesis seeks to answer the question: how does the interaction of methylphenidate with dopamine transporters translate into clinical effects? Our results indicate that the interaction with transporters partially translates into clinical effects and that the relationship between these two elements is more significant in the morning compared to the evening.

Overall, this thesis has explored the various facets of pharmacometric methods and their application in the prescriptions of methylphenidate for patients with ADHD. The results of this research demonstrate the utility of pharmacometrics approaches and open the door to further research to guide the individualization of methylphenidate.

Keywords: methylphenidate, pharmacometrics, pharmacokinetic, pharmacodynamic, bioequivalence, dopamine transporter, clinical rating scales, population modeling.

Table des matières

Liste des tableaux

Liste des figures

Liste des sigles et abréviations

ABE : bioéquivalence moyenne (*Average bioequivalence*)

ADHD-RS-5: Échelle de mesure clinique basée sur le DSM-5 *ADHD Rating Scale–DSM-5*

ANDA : soumission abrégée d'une nouvelle formulation (*Abbreviated New Drug Submission* au Canada ou *Abbreviated New Drug Application* - ANDA aux États-Unis)

AUC : aire sous la courbe pharmacocinétique (*area under the curve*)

BHE : barrière hématoencéphalique

C_{max} : concentration maximale

CV : coefficient de variation

DA : dopamine

DAT : transporteur de dopamine

DBDS : Système de libération par billes Diffucaps (*Diffucaps Bead-Delivery System*)

DSM : Manuel diagnostique et statistique des troubles mentaux (*Diagnostic and Statistical Manual of Mental Disorders)*

EC50 : concentration menant à la moitié de l'effet maximal

ED50 : dose menant à la moitié de l'effet maximal

ER : formulations à libération prolongée (*Extended Release*)

FDA : Food and Drug Administration

IBE : bioéquivalence individuelle

IIV : variabilité interindividuelle (*interindividual variability*)

IR : formulations à libération immédiate (*Immediate Release*)

IMRf : Imagerie par résonance magnétique fonctionnelle

Ki : constante d'inhibition

MTA : Étude des traitements multimodes des enfants ayant un TDAH

MPH : méthylphénidate

NE : norépinéphrine (noradrénaline)

NET : transporteur de norépinéphrine

NLME : modèles non linéaires à effets mixtes

OROS*:* système oral à libération contrôlée par osmose *(Osmotically Controlled-Release Oral System*)

pAUC : aire sous la courbe partielle

PBE : bioéquivalence de population

PBPK : modélisation pharmacocinétique basée sur la physiologie (*Physiolocally based pharmacokinetic modeling*)

PERMP : Mesure permanente de la performance d'un produit

PK : Pharmacocinétique

PD : Pharmacodynamie

PET : tomographie par émission de positrons *(positron emission tomography)*

POP-PKPD : modélisation populationnelle pharmacocinétique-pharmacodynamique

QSP : modélisation quantitative des systèmes pharmacologiques (*Quantitative Systems* Pharmacology)

RCE : effet de montagnes russes (*roller coaster effect)*

RMSE : erreur quadratique moyenne (Root mean square error)

SKAMP : Échelle de mesure clinique Swanson, Kotkin, Agler, M-Flynn, and Pelham

SODAS: Système sphéroïdal d'absorption du médicament oral (*Spheroidal Oral Drug Absorption System*)

$t_{1/2}$: temps de demi-vie

TBE: bioéquivalence trapézoïdale

TDAH : Trouble du Déficit de l'Attention avec/sans Hyperactivité

t_{max} : temps pour atteindre la concentration maximale

VPC: Inspection graphique du pouvoir prédictif du modèle *(Visual Predictive Check)*

À *jeddo* Mikhael et *jeddo* Youssef,

les seuls que je ne pourrai pas enlacer dans mes bras

Remerciements

Si tu veux aller vite, marche seul ; mais si tu veux aller loin, marchons ensemble.

Cette thèse ne serait pas allée bien loin sans les merveilleuses personnes qui m'ont soutenue à travers ces dernières années :

Fahima Nekka, qui m'a acceptée en tant que stagiaire en 2015 et qui m'a guidée sans cesse depuis. Dans le tourbillon d'un doctorat, elle sait toujours trouver les bons mots.

Philippe Robaey, un mentor et collaborateur incroyable qui ajoute non seulement sa touche clinique à ma thèse, mais surtout son brin d'humour inégalable.

Jun Li, dont la soif scientifique n'est jamais étanchée et qui m'a appris à toujours demander « Pourquoi pas ? ».

Amélie Marsot, Philippe Vincent et Roberto Gomeni, qui ont gracieusement accepté de faire partie de mon jury.

Toutes les amitiés qui ont marqué mon quotidien par leurs histoires et anecdotes. En ordre chronologique :

1- Guillaume : le premier à m'accueillir au labo,
2- Mario : qui répond toujours à mes questions NONMEM,
3- Leila : dont j'utilise encore les explications sur Matlab,
4- Steven : qui prenait ses pauses-café à mon bureau,
5- Xiao: who brought so much positive energy,
6- Morgan : qui m'a enseigné les bases des statistiques,
7- Katia : qui m'a encouragée à m'impliquer au CECSP,
8- Soudeh : qui m'a tirée dans le PSWC,
9- Jean-Michel : qui m'a toujours guidée dans les rouages de la faculté,
10- Deniz : qui est toujours ma meilleure cheerleader,
11- Sarah-Jade : qui m'a fait découvrir que j'aimais enseigner la pharmacométrie,

12- Anaëlle et Paul-Antoine : mes poussins préférés,

13- Cassandre : qui a suivi mes conseils sans me connaître,

14- Florence : qui est l'autrice de tant de phrases clés de mon quotidien,

15- Abdullah : who is the big brother I never had,

16- Imad : qui perfectionne encore et toujours mon sens de l'humour libanais,

17- Jeffery : qui est à l'origine du *dress to impress*,

18- Augusto : qui a essayé longtemps de m'expliquer Dune,

19- Vivian : qui a découvert Montréal avant moi,

20- Alexandre : qui m'a supportée pendant tous les TPs,

21- Ibrahim : qui partage mes goûts cinématographiques,

22- Mehdi : qui partage ma philosophie de vie,

23- Miriam, Hamza et Khalil : à qui je laisse la relève des activités sociales du labo.

Finalement, merci à mes parents (et Vanessa, et Joseph). Sans leurs sacrifices, je n'aurais jamais pu être là aujourd'hui. Comme l'a dit Nizar Qabani, لأن حبي لك فوق مستوى الكلام قررت أن اسكت.

Chapitre 1 — Trouble du Déficit de l'Attention avec/sans Hyperactivité

Ce chapitre introduit le trouble du déficit de l'attention avec/sans hyperactivité (TDAH), ce désordre du cerveau étant au cœur de cette étude. Pour tout lecteur motivé, aguerri et avide de lecture, ce chapitre vous présentera les aspects nécessaires pour comprendre le contexte dans lequel s'inscrit cette thèse. Pour tout lecteur démotivé, affaibli et fatigué de lecture (je vous comprends!), consolez-vous par le fait que vous n'avez pas eu à résumer plus d'un siècle de connaissances scientifiques sur le TDAH en quelques pages.

Les premières définitions d'un désordre ressemblant au trouble du déficit de l'attention avec/sans hyperactivité (TDAH) paraissent en 1775 par le médecin allemand Melchior Adam Weikard et en 1798 par le médecin écossais Alexander Crichton (1). Crichton a été l'un des premiers scientifiques à étudier ce trouble. En faisant le tour de plusieurs hôpitaux d'Europe, Crichton a résumé les cas de troubles mentaux qu'il a rencontrés, publiés en trois tomes sous le nom « *An inquiry into the nature and origin of mental derangement: comprehending a concise system of the physiology and pathology of the human mind and a history of the passions and their effects*». Bien qu'on y retrouve une description de patients ayant une «attention changeante», Crichton ne mentionne jamais de symptômes d'hyperactivité (2).

Plus tard, en 1845, Heinrich Hoffmann écrit un livre d'histoires illustrées pour enfant, «*Struwwelpeter*», qui contient le personnage «*Zappelphilipp*» (Philippe l'agité) (2). Ce dernier présente un comportement agité à table. Ceci entraîne un conflit avec son père et le renversement de la nourriture par terre. Ce récit présente donc la notion d'hyperactivité et est encore utilisé pour illustrer le TDAH.

La première définition officielle du TDAH apparaît dans la littérature scientifique en 1902 (3), mais ce n'est qu'en 1937 que Charles Bradley découvre l'efficacité des amphétamines pour traiter les symptômes du TDAH (4). En 1960, l'agence américaine du médicament (*Food and Drug*

Administration - FDA) approuve l'utilisation du méthylphénidate pour les désordres comportementaux chez les enfants.

Prévalence du TDAH

Les statistiques sont nombreuses pour relater la prévalence du TDAH. Cette prévalence est surtout dépendante de deux critères détaillés ci-dessous : le sexe (homme vs femmes) et le groupe d'âge (pédiatrie vs adulte).

En revanche, il est intéressant de rapporter que la prévalence du TDAH ne diffère pas selon les territoires étudiés et qu'elle n'a pas changé depuis les dernières décennies. En effet, une méta-analyse ayant évalué 135 études ne rapporte pas de différence significative entre l'Amérique, l'Europe, l'Asie, l'Afrique ou l'Océanie, et conclut que la prévalence du TDAH n'a pas subi de modification depuis les 30 dernières années (5.9-7.1 %) (5).

Prévalence selon le sexe

Selon une autre méta-analyse ayant inclus plus de 98 000 enfants, il est rapporté que la prévalence du TDAH est trois fois plus grande chez les garçons que chez les filles (6).

Prévalence selon le groupe d'âge

Une méta-analyse qui couvre 55 000 patients a estimé la prévalence du TDAH à 5,9% dans la population pédiatrique (6). Chez les adultes, la prévalence calculée par d'autres méta-analyses (allant de 5300 à 32 000 adultes) est plutôt rapportée entre 2.2 et 2,8% (7,8).

La différence de prévalence entre la population pédiatrique et la population adulte peut être due à plusieurs facteurs. Le premier découle de la disparition des symptômes de TDAH à l'âge adulte ; il se pourrait que ces adultes aient créé de nouvelles synapses et de nouvelles aptitudes qui compensent pour les failles dans le développement de leur cortex préfrontal (9). Ceci a pour conséquence de réduire le bassin d'adultes ayant un TDAH. Le deuxième facteur découle de la difficulté à établir un diagnostic de TDAH à l'âge adulte. En effet, il est parfois ardu de déterminer si les symptômes sont attribuables à un TDAH ou plutôt à une comorbidité (dépression, trouble d'anxiété, trouble de sommeil…) (9).

Étiologie

Bien qu'aucun facteur génétique ou environnemental précis ne soit rapporté être à l'origine du TDAH, il semble qu'une combinaison de divers facteurs semble en augmenter les risques (1).

Facteurs génétiques

Une étude ayant analysé les variantes génétiques de 20 183 patients et 35 191 individus contrôles a conclu qu'une combinaison de plusieurs variantes génétiques est associée au patient TDAH. Plus précisément, certains gènes ont été identifiés comme facteurs de risque du TDAH : *ANKK1, DAT1, LRP5, LRP6, SNAP25, ADGRL3, DRD4, BAIAP2* (10–16). D'ailleurs, les patients ayant un grand risque polygénique ont plus de risque de recevoir un diagnostic de TDAH (17). Il est intéressant de noter que 84–98% des variants associés au TDAH sont également associés à d'autres troubles psychiatriques (18).

Facteurs environnementaux

De nombreux facteurs environnementaux ont été associés au TDAH. Ci-dessous, je détaille les facteurs environnementaux confirmés par plusieurs méta-analyses et sans biais de facteur de confusion. Ces facteurs de risque environnementaux peuvent être classés selon les catégories suivantes :

- **EXPOSITION À DES SUBSTANCES TOXIQUES**
    - **Plombémie** : Plusieurs méta-analyses ont évalué l'impact du taux sanguin de plomb chez des enfants sur l'incidence de TDAH (2 500 à 17 000 jeunes selon l'étude) (19–21). Les patients ayant un haut taux de plombémie ont entre 2 à 4 fois plus de risque d'avoir un TDAH.
    - **Acétaminophène maternel** : L'utilisation d'acétaminophène pendant la grossesse a été associée à une augmentation de 33% de TDAH dans une étude taïwanaise comportant 10 000 naissances (22). Également, une étude norvégienne ayant inclus 113 000 naissances a trouvé un rapport de risque (hazard ratio) allant de 1.07-6.15, selon la durée d'utilisation d'acétaminophène et le trimestre de grossesse (23).

- **Valproate :** Une étude danoise portant sur 913 000 enfants a trouvé une augmentation du risque de TDAH de 50% pour les enfants exposés à une utilisation prénatale de valproate (un médicament antiépileptique) (24).

- **FACTEURS DE RISQUE RELIÉS À LA GROSSESSE OU LA NAISSANCE**
  - **Poids à la naissance** : De nombreuses études rapportent une augmentation de l'incidence de TDAH pour les bébés nés avec un très faible poids ou les bébés très prématurés (25–28). Lorsque le bébé a un faible poids et que la mère souffrait de prééclampsie, le facteur de risque de TDAH augmente à 40% (29).
  - **Trouble d'hypertension maternel** : Une méta-analyse ayant étudié 1,4 million d'individus a noté une augmentation de l'incidence de TDAH de 25% chez les enfants dont la mère souffre d'hypertension pendant la grossesse (30).
  - **Obésité maternelle** : Les enfants nés de femmes obèses ont un risque de TDAH augmenté de 50-60% selon les études (31–33).
- **FACTEURS DE RISQUE SOCIODÉMOGRAPHIQUES**
  - **Violence sexuelle** : Une étude américaine ayant étudié 14 000 volontaires a trouvé que le TDAH avec un sous-type inattentif est associé aux victimes d'agressions sexuelles, même après avoir corrigé pour les facteurs de risque démographiques et socioéconomiques (34).
  - **Revenu familial** : Un revenu familial faible a été associé à une augmentation de l'incidence de TDAH (35,36). Lorsque les parents combinent une situation de pauvreté, de faible niveau d'éducation et de chômage, leurs enfants ont 5% plus de risque de TDAH (37).

Outils de diagnostic du TDAH

Le diagnostic du TDAH est souvent un sujet de discussion dans la culture populaire contemporaine (38). Pour plusieurs, le TDAH est surdiagnostiqué dans la population. Pour certains, la prévalence croissante de TDAH est une conséquence de critères de diagnostic trop permissifs. Pour d'autres, il s'agit plutôt d'une mise à jour de ces critères afin de mieux déceler les patients atteints de TDAH.

Pour la population scientifique (et les lecteurs de cette thèse), nous savons maintenant que la prévalence du TDAH n'a pas changé depuis les dernières décennies (5).

Cette polémique autour du TDAH existe en partie, car son diagnostic n'implique pas des mesures biologiques quantifiables. Il se base plutôt sur des échelles d'évaluation cliniques qui sont établies à la suite de discussions entre cliniciens et patients (ou leurs parents). Ces échelles d'évaluation n'ont pas le mérite d'être aussi objectives que les mesures biologiques, mais bénéficient tout de même d'une validité acceptable en psychiatrie (39).

Le diagnostic du TDAH se fait à l'aide du *Diagnostic and Statistical Manual of Mental Disorders* (DSM). La première version du DSM est écrite en 1980 et représente le premier guide énumérant les critères de diagnostic du TDAH. Le DSM a été mis à jour 5 fois, dont la dernière version datant de 2013 (40,41).

Pour être diagnostiqué de TDAH, le patient doit obligatoirement présenter (i) des symptômes d'hyperactivité, d'impulsivité ou d'inattention qui perdurent depuis plus de 6 mois, (ii) des symptômes qui se manifestent dans différents environnements (par exemple à l'école et à la maison), (iii) des symptômes qui perturbent ses activités quotidiennes et (iv) certains symptômes qui ont apparu pendant l'enfance (1).

Pathophysiologie

Les régions du cerveau touchées dans le TDAH

Grâce aux méthodes d'imagerie médicale, les chercheurs ont identifié de nombreuses différences entre les cerveaux de patients atteints de TDAH et les autres, dont :

- Une altération de la substance blanche dans plusieurs régions du cerveau (42) et une diminution du volume de la matière grise dans les ganglions de la base (responsables des fonctions exécutives) (43),
- Une hypoactivité du cortex préfrontal (44),
- Une hypoactivité des régions du cerveau impliquées dans le contrôle inhibiteur (cortex frontal droit inférieur, ganglions de la base*)* (45–47),
- Une hypoactivité des réseaux d'attention frontostriatal, frontopariétal et ventral (48),
- Une hypoactivité du striatum ventral (processus de récompense) (49).

Ainsi, le TDAH se démarque par un déficit des fonctions cognitives. Ceci se manifeste par des problèmes dans la mémoire de travail, l'attention visuelle et le contrôle de l'inhibition et la planification (41). Les patients souffrant de TDAH préfèrent donc les récompenses immédiates (50) et ne font pas de décisions optimales (51). D'ailleurs, les troubles de contrôle cognitifs, la sensibilité aux récompenses et le temps de processus d'informations manifestés dans un TDAH sont indépendants l'un de l'autre (52,53).

Les neurotransmetteurs du TDAH et leurs transporteurs

Nous présentons ci-dessous les neurotransmetteurs pertinents pour la recherche faite dans le contexte de cette thèse, soient la dopamine et la norépinéphrine. Une décharge équilibrée de ces deux neurotransmetteurs est nécessaire puisqu'elle permet d'activer les bons récepteurs post-synaptiques (D1, alpha-2A, alpha1). L'effet désiré en fonction de la concentration de ces neurotransmetteurs prend donc la forme d'un U inversé, où des concentrations modérées permettent un effet optimal (Figure 1) (9,40). Dans le cas du TDAH, on observe un dérèglement dans l'activation des neurones dopaminergiques et norépinéphrines. Ils sont illustrés à la Figure 2.

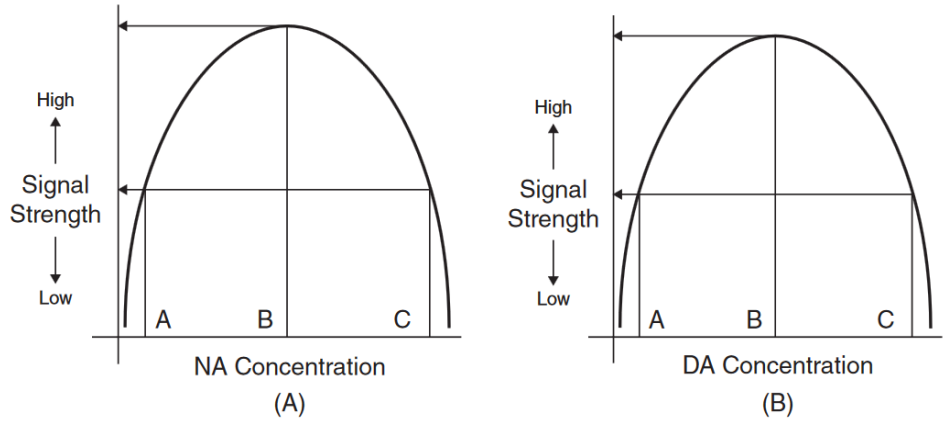

Figure 1. Signal du stimulus en fonction de la norépinéphrine (NA) et de la dopamine (DA) suivant une forme de U inverse. Tiré de (40)

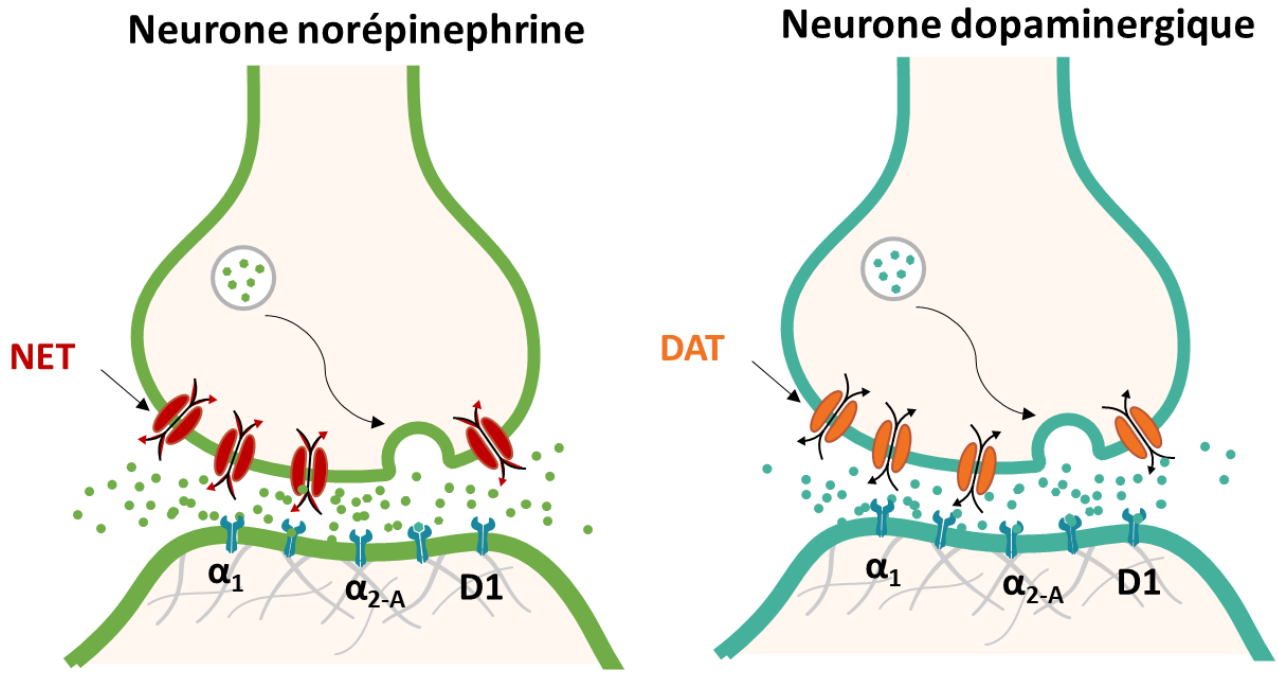

Figure 2. Neurones de norépinéphrine (bleu) et dopaminergiques (vert). La norépinéphrine est désignée par les points bleus et la dopamine par les points verts. Les transporteurs de norépinéphrine (NET) et de dopamine (DAT) sont chargés de recapturer les neurotransmetteurs à partir de la fente synaptique vers le neurone présynaptique.

Norépinéphrine

La norépinéphrine (NE) est synthétisée dans le locus coeruleus (dans les ganglions de la base) (54). Elle est impliquée dans le maintien de la vigilance, le rapport signal/bruit et la réponse à un stimulus urgent (41,55).

Son rôle est bien résumé dans une situation fictive décrite par Robert Hunt, que je me permets de rapporter ici (56). Il demande au lecteur de s'imaginer en prenant une marche dans un bois pendant la nuit. Alors que le son d'une branche qui se brise vous parvient, vos pensées essayent de deviner si la source du bruit représente un danger et quelle est l'action à prendre. Comme la chanson le dit, vous vous demandez *Should I stay or should I go?* Cette vigilance est assurée par la NE. En effet, la NE tonique permet le traitement des informations sensorielles alors que la NE phasique permet de jauger l'importance de ces informations (57). Dans le TDAH, un dérèglement de NE se produit, affectant ainsi la réponse à un stimulus externe (58).

Une fois relâchée dans la fente synaptique, la NE peut être recapturée par les transporteurs de NE (NET) et recyclée à l'intérieur du neurone présynaptique (Figure 2). Pour les patients avec TDAH, certaines études ne rapportent aucune différence dans leur densité du NET (59) alors que d'autres études font état d'une augmentation de l'affinité du NE avec le NET (à cause d'un polymorphisme du NET) (60). Le NET est la cible de plusieurs traitements utilisés dans le TDAH (détaillés à la fin du chapitre).

Dopamine

Bien que la dopamine (DA) était déjà connue des scientifiques, il a fallu attendre les années 1960 pour l'identifier comme un neurotransmetteur. En effet, avant cela, elle était simplement reconnue comme le précurseur de la norépinéphrine (54), un rôle bien réducteur sachant son implication importante dans la neurotransmission.

Les neurones dopaminergiques proviennent de la substance noire ou de l'aire tegmentale ventrale (54). Ils sont impliqués dans plusieurs tâches, dont la réponse motrice et le processus de récompenses (41). Spécifiquement, la voie mésocorticolimbique des neurones dopaminergiques joue un rôle dans l'attention et la mémoire de travail (61). Comme avec la NE, un dérèglement de DA est observé chez les patients TDAH (9).

La DA relâchée dans la fente synaptique peut être recapturée par les transporteurs de la DA (DAT) vers le neurone présynaptique (9) (Figure 2). Il a été démontré que la densité des DAT est plus grande chez les patients atteints de TDAH ayant pris des psychostimulants, suggérant que cette augmentation de la densité des DAT serait un mécanisme compensatoire de l'exposition aux psychostimulants (62).

Il est important de noter que la recapture de la DA peut se faire par DAT et NET. En effet, malgré son nom, le NET a une affinité plus grande pour DA que pour NE (63). C'est donc l'abondance du type de neurone dopaminergique ou noradrénergique qui dicte la recapture de la DA (64). Ceci est démontré dans une étude chez le rat, où la recapture de DA suite au blocage de DAT et NET dans différentes régions du cerveau a été comparée (64). Dans le cortex préfrontal, où le DAT est peu abondant, la DA extracellulaire était éliminée principalement par le NET (64). Dans le *caudate nucleus*, où les DAT sont abondants, la DA extracellulaire était principalement éliminée par le DAT (64).

Métriques utilisées dans les études sur le TDAH

Malgré un siècle de connaissances sur le TDAH, plusieurs questions demeurent sans réponses. Parmi les outils utilisés pour élucider les mystères du TDAH, il existe les méthodes d'imagerie médicale ainsi que les questionnaires cliniques. Chaque méthode décrit le TDAH d'un angle différent et permet de mieux comprendre le trouble et ses mécanismes. Néanmoins, les buts poursuivis sont communs : évaluer la symptomatologie et l'efficacité d'un traitement. Dans cette section, je résume les méthodes pertinentes dans le cadre de ma thèse.

Échelles de résultats cliniques

Les échelles de résultats cliniques sont nombreuses. Chacune cherche à évaluer les symptômes du TDAH tels que définis par le DSM (65). Cependant, au-delà de cette évaluation, il est important de jauger l'impact du TDAH sur la vie sociale, émotionnelle ou scolaire des patients (66,67). Ainsi, allant plus loin que le DSM, chacune de ces échelles cliniques évalue certains aspects supplémentaires.

Ces échelles peuvent donc être utilisées pour évaluer les bénéfices des traitements de TDAH dans des études cliniques ou dans les dossiers de soumission aux agences règlementaires (66). Ci-dessous, je décris brièvement trois échelles cliniques pertinentes au contexte de ma recherche. Deux d'entre elles (SKAMP et ADHD-RS-5) sont les seules qui figurent dans les soumissions à la FDA (66). Par contre, toutes les trois ont fait l'objet de modèles en pharmacométrie pour décrire la pharmacodynamie du méthylphénidate (68–72).

SKAMP

Le nom SKAMP vient des initiales des chercheurs ayant conçu cette échelle clinique (Swanson, Kotkin, Agler, M-Flynn et Pelham). Le questionnaire est effectué dans des salles de classe et permet donc d'évaluer le TDAH dans un contexte scolaire. Il s'agit d'une échelle de 13 questions auxquelles répondent les professeurs. Chaque question quantifie la gravité du symptôme, avec des valeurs allant de 0 (pas de déficience) à 6 points (déficience maximale) (73–75). Ces 13 questions évaluent à la fois l'attention et le comportement des patients par le biais de deux sous-

échelles (SKAMP-attention et SKAMP-comportement). La somme de ces échelles forme le SKAMP-combiné, allant de 0 à 78 points. Plus le score SKAMP-combiné est bas, moins l'enfant présente de symptômes de TDAH.

ADHD-RS-5

L'échelle *ADHD Rating Scale–DSM-5* (ADHD-RS-5) est basée sur le DSM-5 et mesure la fréquence et la gravité des symptômes de TDAH. Cette échelle s'applique à la fois au contexte scolaire et familial. Elle échelonne les symptômes sur 18 questions, chacune de ces questions pouvant être notée par 4 niveaux ordinaux allant de 0 à 3 (jamais/non-problématique à très souvent/sévère) (76). L'ADHD-RS-5 est l'échelle la plus fréquemment utilisée dans les études cliniques pédiatriques (66).

PERMP

Contrairement aux deux échelles précédentes, l'échelle *Permanent Product Measure of Performance* (PERMP) est une échelle objective. Il s'agit d'un test de mathématiques écrit de 10 minutes. Il est présenté aux enfants dans une salle de classe analogique de l'école laboratoire. L'échelle PERMP-A quantifie le nombre d'exercices essayés par l'enfant alors que l'échelle PERMP-C quantifie ceux réussis par l'enfant. Ainsi, plus le score PERMP est élevé, plus l'enfant présente une meilleure attention et concentration (71,73).

Occupation des transporteurs

Dans l'évaluation des traitements du TDAH, l'utilisation d'imagerie médicale est souvent utilisée pour quantifier l'interaction entre la molécule et sa cible (77–80). Ceci se fait par différentes méthodes. La tomographie par émission de positrons (PET) est celle qui est la plus pertinente dans le cadre de ma thèse.

Mesure de l'occupation des transporteurs

Dans le cadre du TDAH, l'imagerie PET permet de quantifier l'occupation des transporteurs impliqués dans la réponse au traitement (DAT et NET). Son caractère non invasif justifie son utilisation chez l'homme pour les médicaments ciblant le système nerveux central (81). L'imagerie

PET utilise un ligand radioactif qui est injecté par voie intraveineuse et dont la radioactivité permet de trianguler sa présence dans le cerveau (82).

Afin de quantifier l'occupation des transporteurs, les études PET font une analyse du cerveau en absence du médicament et une autre après administration du médicament (82). L'occupation des transporteurs est donc calculée par la réduction de la liaison du ligand radioactif au transporteur (*binding potential,* BP*)* après l'administration du médicament tel que décrit ci-bas (82,83).

$$Occupation\ des\ transporteurs = \frac{BP_{placebo} - BP_{médicament}}{BP_{placebo}} * 100$$

Concentration cérébrale du médicament

La microdialyse est une technique invasive où une sonde et un tube semi-perméable sont insérés dans le cerveau d'un animal. Dans le cadre du TDAH, cette technique a été utilisée pour quantifier la libération de neurotransmetteurs ou les concentrations cérébrales de médicament. Elle permet donc de comprendre les échanges entre le médicament et sa cible ou de quantifier le passage du médicament à travers la barrière hématoencéphalique (84–88).

Traitement du TDAH

L'approche courante pour le traitement pharmacologique du TDAH passe par une titration. Les patients débutent avec une faible dose qui sera augmentée jusqu'à atteindre un équilibre entre la réduction des symptômes et les effets indésirables (89–91). Bien que ce processus permette de réduire l'interruption de traitement à cause des effets indésirables, il s'agit tout de même d'un processus lourd pour le patient. Le travail de cette thèse s'inscrit dans cette problématique où on cherche à développer des stratégies d'individualisation des traitements TDAH grâce à des méthodes quantitatives et outils de santé numérique.

Dans cette section, nous ne discuterons pas le traitement du TDAH lorsqu'il y a présence de comorbidités. Nous rappelons que les approches médicamenteuses du TDAH diffèrent selon les diagnostics concomitants (anxiété, tics, bipolarité, abus de substances…) et dépassent le contexte de cette thèse. En effet, ces comorbidités peuvent présenter une pathophysiologie qui s'oppose directement à celle du TDAH et complique davantage les traitements (9). D'ailleurs, chez les

adultes, le TDAH est une des dernières maladies traitées lorsqu'il y a des comorbidités non traitées (abus de substances > trouble d'humeur > trouble d'anxiété > TDAH) (9).

Les traitements du TDAH se séparent en deux catégories : les non-stimulants et les stimulants. Ils sont détaillés ci-dessous.

Non-Stimulants

Atomoxetine

L'atomoxetine est un inhibiteur des NET au niveau du cortex préfrontal (92). Comme le NET participe à la recapture du DA et du NE, l'administration d'atomoxetine aura comme conséquence d'augmenter les DA et NE au niveau du cortex préfrontal (92).

Guanfacine

La guanfacine est un agoniste sélectif des récepteurs alpha-2A. Ces récepteurs se situent partout dans le système nerveux central, et surtout dans le cortex préfrontal et le locus coeruleus. Ce sont les récepteurs post-synaptiques du NE et ils sont impliqués dans l'attention, l'hyperactivité et l'impulsivité. En stimulant les récepteurs alpha-2A, la guanfacine corrige l'acheminement des signaux reliés à la NE (93).

Clonidine

La clonidine est un agoniste non sélectif des récepteurs alpha-2 (alpha-2A, alpha-2B, alpha-2C). Bien que la formulation prolongée de la clonidine soit prescrite pour le TDAH, elle peut occasionner plus d'effets indésirables, car il s'agit d'un agoniste non sélectif (9,93).

Stimulants

Les stimulants sont des principes actifs qui englobent les bloqueurs de la recapture de DA et NE. Les deux principaux stimulants prescrits dans le cadre du TDAH sont les amphétamines et le méthylphénidate (MPH). Certaines méta-analyses ont démontré qu'ils avaient une efficacité similaire (94,95), alors que d'autres indiquent une efficacité supérieure pour les amphétamines (96–98). Leurs effets secondaires sont généralement similaires (99–101).

Amphétamine

Les amphétamines présentent une inhibition compétitive pour DAT et NET et empêchent la recapture de la NE et la DA de la fente synaptique (102–104). À de fortes doses, ils possèdent aussi une inhibition compétitive des transporteurs vésiculaires (VMAT) (104–106). Ceci a pour conséquence de libérer la DA dans la fente synaptique. Le mécanisme d'action sur VMAT est d'ailleurs responsable du sentiment d'euphorie associé à l'abus des amphétamines (9,107).

L'affinité des isomères des amphétamines (d-AMP et l-AMP) diffère selon les transporteurs. Bien que l'isomère d-AMP a plus d'affinité pour les DAT, d-AMP et l-AMP ont une affinité similaire pour les NET (104).

Méthylphénidate

Étant le personnage principal de ce travail, le MPH sera plus amplement détaillé au prochain chapitre.

Chapitre 2 — Méthylphénidate

Il était une fois, un chimiste du nom de Leandro Panizzon, qui travaillait pour la compagnie Ciba (aujourd'hui Novartis) (108). En 1944, il fut le premier à synthétiser le méthylphénidate (MPH) (108,109). Il nomma la nouvelle molécule Ritaline en honneur à sa femme, Marguerite, dont le surnom était Rita (108). Ils vécurent heureux et permirent 80 années de recherche basée sur cette molécule.

Aujourd'hui, le MPH fait partie des traitements pharmacologiques de première ligne pour le TDAH dans plusieurs pays (89,110–112). Sa part du marché des stimulants varie selon le pays. Par exemple, en Europe, les prescriptions de MPH représentent 81,3 à 98,9% du marché (110). En revanche, aux États-Unis, le pourcentage des prescriptions du MPH est beaucoup plus bas, au profit des sels d'amphétamine, avec 52,9% pour le MPH et 42,1% pour les sels d'amphétamine (110).

Ce chapitre vise à résumer la pharmacologie et la pharmacocinétique (PK) du MPH. Il aborde également deux notions importantes dans le contexte clinique du MPH, ainsi qu'en lien avec le sujet de cette thèse : l'effet des faibles doses et la tolérance au MPH.

Pharmacologie

Le MPH existe sous quatre isomères : d-threo-MPH, l-threo-MPH, d-erythro-MPH et l-erythro-MPH (113). Ils sont représentés à la Figure 3. Les isomères threo, en particulier le d-threo-MPH, sont principalement associés à l'effet stimulant du MPH, tandis que les isomères erythro sont plutôt associés aux effets indésirables (113). Par conséquent, les formulations commerciales de MPH ne contiennent que des isomères threo-MPH. En outre, il existe une formulation composée uniquement de d-threo-MPH, soit le Focalin (113).

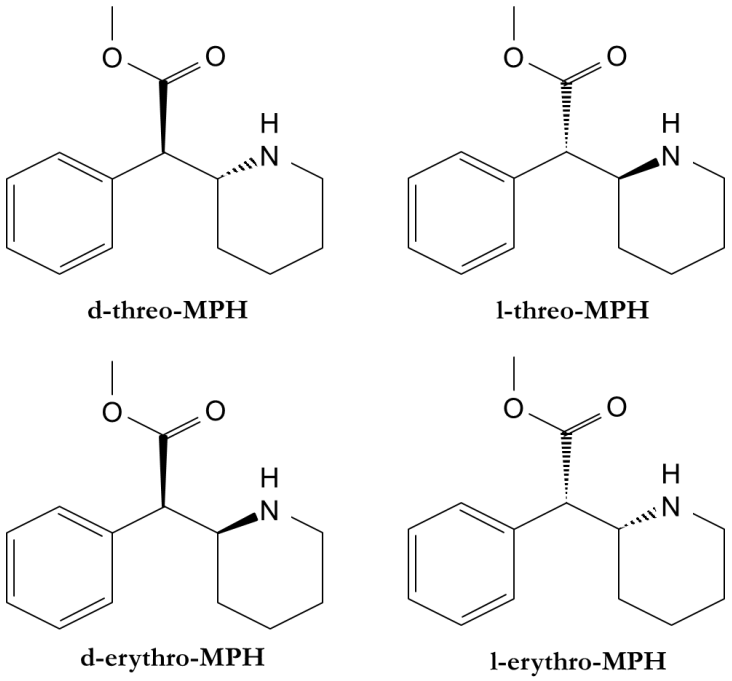

Figure 3. Structures chimiques des isomères de méthylphénidate (MPH)

DAT et NET

Par imagerie PET, il a été démontré que le MPH se lie au DAT (77–80,114,115) et au NET (63). L'action pharmacologique du MPH se résume donc par un blocage allostérique des NET et DAT. En bloquant la recapture de la NE et de la DA, le MPH augmente leur disponibilité dans la fente synaptique et facilite ainsi leur liaison aux récepteurs (104,116–118). Afin d'observer un effet thérapeutique optimal, il est nécessaire que (i) le MPH soit absorbé lentement (ii) qu'un niveau d'occupation des DAT et NET en deçà du niveau de saturation soit atteint et (iii) que l'occupation des transporteurs se maintienne suffisamment dans le temps. Cette combinaison de critères permet une signalisation tonique sans augmenter la signalisation phasique (9).

Il convient de noter que le d-MPH présente une affinité plus élevée pour le DAT que le l-MPH (113,119–124). De plus, l'affinité du MPH pour le DAT (K_i = 193 nmol/L, ED_{50} =0,25 mg/kg) est inférieure à celle pour le NET (K_i = 38 nmol/L, ED_{50} = 0,14 mg/kg) (63,80,125–127).

Autres cibles

Le MPH cible aussi les récepteurs adrénergiques, notamment les récepteurs alpha-2 (128). Comme ces récepteurs sont aussi la cible de la guanfacine et de la clonidine, ce mécanisme d'action pourrait être important pour expliquer l'efficacité du méthylphénidate (129,130). Ce sujet dépasse la portée de cette thèse.

Pharmacocinétique

Le MPH a d'abord été développé sous forme de libération immédiate (ou IR pour *Immediate Release*). À l'époque, les patients devaient prendre jusqu'à trois comprimés par jour pour maintenir un effet thérapeutique soutenu tout au long de la journée (131). Plus tard, des formulations à libération prolongée (ou ER pour *Extended Release*) ont été mises au point. Ces formulations combinent deux vitesses de libération du médicament : une partie immédiate et une autre prolongée, afin d'obtenir un début d'action rapide et une durée d'effet soutenue pendant la journée (113). La proportion de la dose totale qui est libérée de manière immédiate varie entre 20 et 50 % selon le fabricant. Ces formulations ont donc permis aux patients de passer d'un régime avec prise trois fois par jour à un régime avec prise deux fois par jour. (132).

La PK du MPH est linéaire, les concentrations plasmatiques de MPH étant proportionnelles à la dose dans la plage de doses recommandées (133). Également, il a été noté que la PK du MPH est similaire entre les enfants, les adolescents et les adultes (113).

Ci-dessous, nous décrivons la PK du MPH pris sous forme orale. La formulation en timbre transdermique n'est pas abordée dans cette thèse.

Absorption

L'absorption du MPH est très rapide, avec une absorption quasi complète dans le tractus gastro-intestinal. Sa biodisponibilité absolue varie entre 11% et 53% (134,135).

Le temps pour atteindre la concentration maximale (t_{max}) varie selon les formulations. Pour les formulations IR, il est compris entre 1 et 3 heures après administration, avec un début d'effet observé environ 20 minutes post-dose (136). En revanche, pour les formulations à libération prolongée (ER), le t_{max} a une valeur moyenne entre 1,2 à 6,8 heures (113). On remarque que le

t_{max} varie considérablement selon la formulation ER choisie, en raison des différences dans les méthodes de libération utilisées par chaque entreprise, telles que la libération basée sur l'osmose (OROS - *Osmotically Controlled-Release Oral System*) ou l'enrobage entérique à libération retardée (SODAS —*Spheroidal Oral Drug Absorption System* ou DBDS - *Diffucaps Bead-Delivery System*).

Distribution

Le MPH possède une faible liaison aux protéines plasmatiques (15%) et une grande solubilité dans les lipides, ce qui facilite sa distribution rapide dans les tissus (133,135,137). Après une administration intraveineuse, 8% de la dose passe à travers la barrière hématoencéphalique, avec un pic de concentration cérébrale se produisant en moins de 10 minutes (138,139).

Métabolisme

Le MPH est métabolisé par les carboxylesterase 1A1 (CES1A1) en un métabolite inactif, l'acide ritalinique (133). La CES1A1 a une affinité inférieure pour le d-MPH, ce qui entraîne un temps de demi-vie ($t_{1/2}$) plus long pour le d-MPH par rapport au l-MPH. Ce $t_{1/2}$ varie entre 3 et 5 heures, selon les formulations (113).

Élimination

La clairance systémique du MPH est rapide (environ 4,5L/kg/h) (113,140). En revanche, la clairance du cerveau est lente, nécessitant environ 90 minutes pour éliminer la moitié du MPH du cerveau (138).

Le MPH est excrété majoritairement dans l'urine (50% après 8 h post-dose et 90% après 48 h post-dose). Seulement 1-3% sont excrétés dans les fèces et 1-2% sont excrétés sous forme inchangée (133).

Faibles doses vs grandes doses

Plusieurs études ont évalué l'impact de différentes doses de MPH sur son efficacité thérapeutique. Chez le rat, l'effet de la dose sur les fonctions cognitives suit la forme d'un U inversé. Ainsi, une petite dose (2 mg/kg) améliore grandement la mémoire de travail

comparativement à une grande dose (8 mg/kg) (86). Les auteurs de cette étude mentionnent donc l'importance des faibles doses pour le traitement du TDAH (86).

En effet, les faibles doses de MPH augmentent l'efflux de DA et NE dans le cortex préfrontal plutôt que dans d'autres régions subcorticales (86,141,142). Par conséquent, elles améliorent les fonctions cognitives associées au cortex préfrontal (fonctions exécutives) plutôt qu'à d'autres régions (143–146). Étant donné que les DAT ne sont pas abondants dans cette région, la sensibilité du cortex préfrontal aux faibles doses y souligne le rôle du NET dans la recapture de DA. Sachant également que le MPH a une affinité plus élevée pour le NET, on pourrait suggérer que l'optimisation des régimes de MPH pour le traitement du TDAH pourrait être basée sur l'occupation des NET.

Chez l'humain, l'évaluation des faibles doses est présentement investiguée dans le cadre d'une étude clinique (étude clinique NCT02167048 (147)). Les résultats sont publiés dans deux présentations par affiche et semblent supporter l'hypothèse d'une efficacité thérapeutique associée à la moitié des doses habituelles de MPH (143,144).

Tolérance

La relation entre la pharmacodynamie et la PK du MPH est davantage complexifiée par le développement de deux types de tolérance : la tolérance aigüe et la tolérance à long terme (148).

Tolérance aigüe (Tachyphylaxie)

La tolérance aigüe se définit comme une baisse rapide de l'efficacité. Dans le cas du MPH, on observe une diminution de l'efficacité (mesurée à l'aide d'échelles cliniques) en après-midi comparativement aux premières heures post-dose, malgré des concentrations plasmatiques similaires (68,69,71,149,150). En effet, des concentrations constantes pendant la journée sont associées à une diminution de 40% de l'efficacité en après-midi (149).

Cette tolérance aigüe au MPH se développe au cours de la journée, mais il est noté que cela ne perdure pas jusqu'à la dose du lendemain (149). Ces observations ont mené au développement de formulations à libération prolongée de MPH qui permettent une augmentation progressive des concentrations pour compenser la tolérance aigüe qui se développe (151).

L'internalisation des récepteurs dopaminergiques post-synaptiques est l'hypothèse principale expliquant cette tolérance aigüe (152,153). Elle serait donc un mécanisme compensatoire pour la hausse du niveau de dopamine extracellulaire causée par le MPH (152,153).

Bien que la tolérance aigüe ait été observée à l'échelle clinique, elle n'a pas été explicitement étudiée et mesurée au niveau de l'occupation des transporteurs. Par contre, une étude PET qui a mesuré l'occupation des DAT par le MPH mentionne un EC_{50} beaucoup plus bas pour les prélèvements 1 h post-dose (79).

Tolérance à long terme

Le traitement par MPH est aussi complexifié par le développement d'une tolérance à long terme (148). Les études cliniques qui ont évalué la tolérance soutenue suite à la prise du MPH tirent différentes conclusions, selon les critères d'inclusion ou les durées des études. Certaines d'entre elles n'ont pas rapporté de tolérance qui se développe sur le long terme (154–156), tandis que d'autres ont observé une tolérance chez certains patients (après quelques jours ou même un an) (157–159). Outre les changements neuronaux qui pourraient expliquer le développement de la tolérance à long terme, l'évolution naturelle (amélioration ou détérioration) du TDAH semble aussi être un facteur (148,160). Lors d'une baisse d'efficacité du MPH à long terme, il est recommandé de prescrire un autre stimulant ou d'arrêter temporairement le MPH (148).

Modélisation en pharmacocinétique-pharmacodynamie (PKPD)

La PK et la PD du MPH peuvent être décrites par plusieurs méthodes : la modélisation pharmacocinétique basée sur la physiologie (*Physiolocally based pharmacokinetic modeling* - PBPK), la modélisation quantitative des systèmes pharmacologiques (*Quantitative Systems* Pharmacology - QSP) ou la modélisation populationnelle (POP-PKPD) (53,68–72,85,161–166).

La POP-PKPD décrit la PK et/ou la PD en supposant des compartiments fictifs à travers lesquels se distribue le médicament. Étant donné que la POP-PKPD est l'outil utilisé dans cette thèse, nous décrivons ci-dessous les modèles PK et PD spécifiquement utilisés dans le contexte du MPH.

Modélisation populationnelle — pharmacocinétique

Les modèles POP-PK sont des modèles non linéaires à effets mixtes (NLME), qui détaillent un modèle structural (*f*) et un modèle statistique (*g*). Ainsi, pour un sujet *i* au temps *j*, les concentrations plasmatiques sont exprimées par :

$$\boldsymbol{Y}_{ij} = f\left(\boldsymbol{\theta}_i, \boldsymbol{x}_{ij}, \boldsymbol{z}_{\boldsymbol{i}}\right) + g\left(\boldsymbol{\theta}_{\boldsymbol{i}}, \boldsymbol{x}_{ij}, \boldsymbol{z}_{\boldsymbol{i}}\right) \varepsilon_{ij} \ ,$$

où $\boldsymbol{Y}_{ij}$ représente le vecteur des concentrations, $\boldsymbol{\theta}_i$ est un vecteur qui regroupe les paramètres individuels du modèle pour le sujet *i,* $\boldsymbol{x}_{ij}$ sont les variables descriptives (temps, doses) du sujet *i*, $\boldsymbol{z}_{\boldsymbol{i}}$ est le vecteur des covariables (poids, âge, sexe…); ε_{ij} représente les erreurs résiduelles, indépendantes et identiquement distribuées en suivant une loi normale centrée réduite (ε_{ij}~N(0,1)) (167,168).

Modèle structural (*f*)

Dans les modèles POP-PK du MPH, le modèle structural (*f*) décrivant le parcours du MPH à travers le corps est composé d'un ou deux compartiments centraux, selon les sources (68–70,72,85,165,166,169). Son élimination est souvent décrite par un processus de premier ordre. Quant à la modélisation de son absorption, celle-ci varie selon la formulation du MPH. Certaines paramétrisations sont illustrées à la Figure 4. Par exemple, l'absorption des MPH-IR est décrite par un processus de premier ordre. Pour les MPH-ER, l'utilisation de deux processus d'absorption parallèles pour représenter la libération rapide et la libération soutenue du médicament. Certains modèles utilisent une absorption d'ordre zéro pour décrire la libération rapide alors que d'autres utilisent une absorption de premier ordre. La libération lente est décrite par un premier ordre et un délai est ajouté au modèle pour décrire le temps écoulé avant la libération prolongée du MPH (68–70,72,85,165,166,169).

Le modèle structural mentionné ci-dessus permet donc de prédire les concentrations plasmatiques du MPH en fonction du temps. Dans cette thèse, deux processus de premier ordre parallèle avec un délai sont utilisés pour décrire les formulations MPH-ER (Figure 4, B). Les équations suivantes définissent la concentration prédite pour les parties IR et ER, dont la somme permet de prédire les concentrations plasmatiques d'une formulation ER.

$$C_1(\mathrm{t}) = \frac{k_{a1} F\ D}{V(k_{a1} - k_e)}(e^{-k_e t} - e^{k_{a1} t})\ ,$$

$$C_2(\mathrm{t}) = \frac{k_{a2} F\ D}{V(k_{a2} - k_e)}(e^{-k_e(t-\Delta)} - e^{k_{a2}(t-\Delta)})$$

$$C_{IR}(t) = C_1(t)$$

$$C_{ER}(t) = C_1(\mathrm{t}) + C_2(\mathrm{t})$$

où D est la dose administrée, F est la biodisponibilité de la formulation, V est le volume du compartiment central, k_{a1} est la constante d'absorption de premier ordre pour la libération immédiate, k_{a2} est la constante d'absorption de premier ordre pour la libération prolongée, et k_e est la constante d'élimination du compartiment central, t est le temps auquel la concentration est observée, et Δ est le délai avant la relâche de la libération prolongée de MPH.

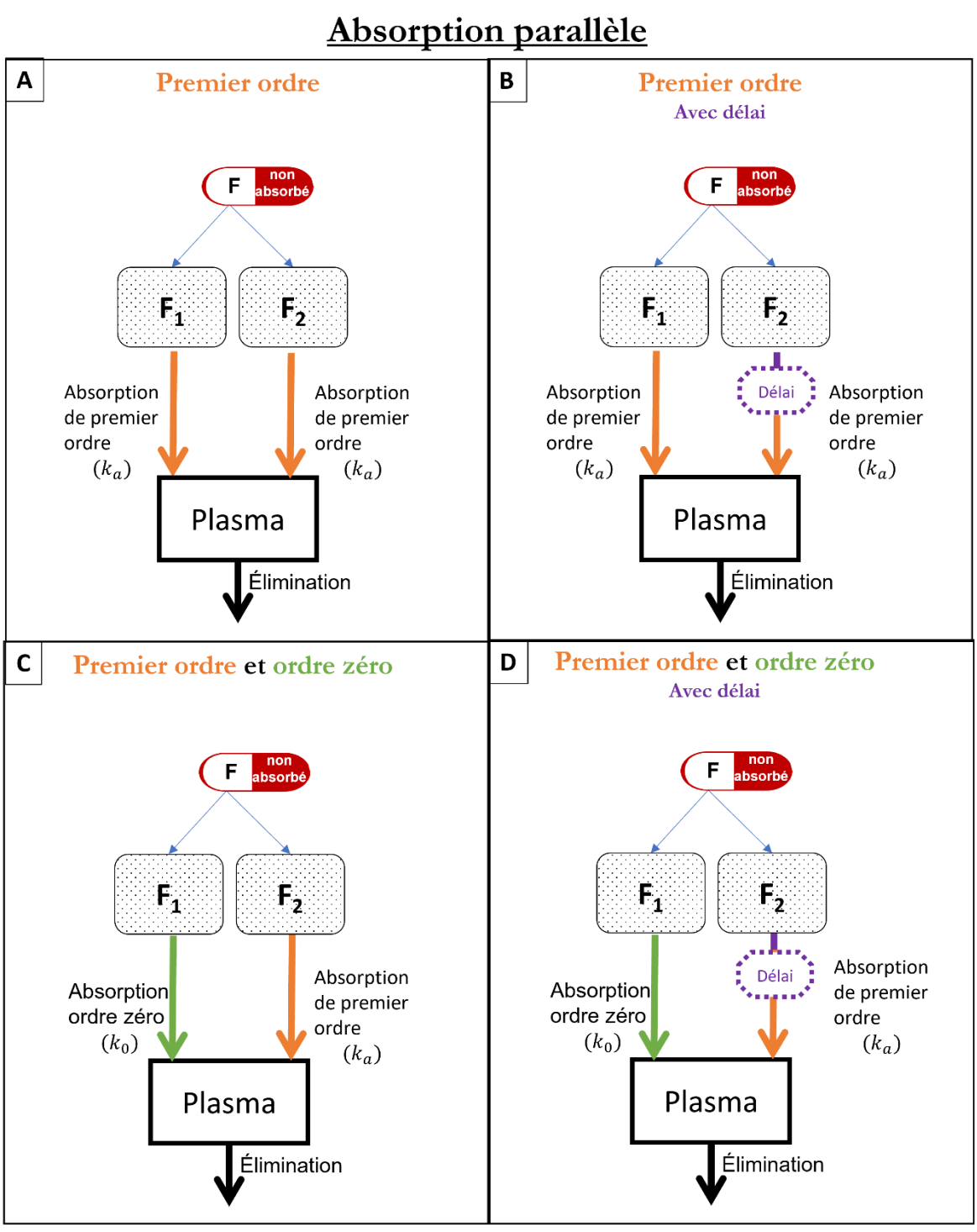

Figure 4. Illustration du modèle structural utilisé pour décrire la pharmacocinétique du méthylphénidate. F : biodisponibilité, F_1 : fraction de la dose en libération immédiate, F_2 : fraction de la dose en libération prolongée.

Modèle de variabilité (*g*)

Dans les modèles POP-PK, il est possible de quantifier la variabilité observée dans une population : la variabilité interindividuelle et la variabilité résiduelle inexpliquée (Figure 5) :

- La <u>variabilité interindividuelle</u> (η_i) est estimée par rapport à $\boldsymbol{\theta}_i$. On suppose qu'elle est distribuée de façon normale, centrée sur 0 avec une variance ω^2 (η_i ~N (0, ω^2)). L'équation la plus fréquemment utilisée est la forme exponentielle, qui suppose une variabilité log normal (167,168,170).

$$\theta_i = \theta_{individu\ typique} * \ e^{\eta_i}$$

- La <u>variabilité résiduelle</u> (ε_i) représente l'erreur entre les concentrations plasmatiques prédites ($C_{pred,i,j}$) et observées ($C_{obs,i,j}$) pour l'individu *i*. Elle suit une distribution ε_i ~N (0, σ^2). L'équation la plus fréquemment utilisée est la forme combinée d'erreur additive et proportionnelle (167,168,170).

$$C_{obs,i,j} = C_{pred,i,j}\left(1 + \varepsilon_{i,j}\right) + \varepsilon_{i,j}$$

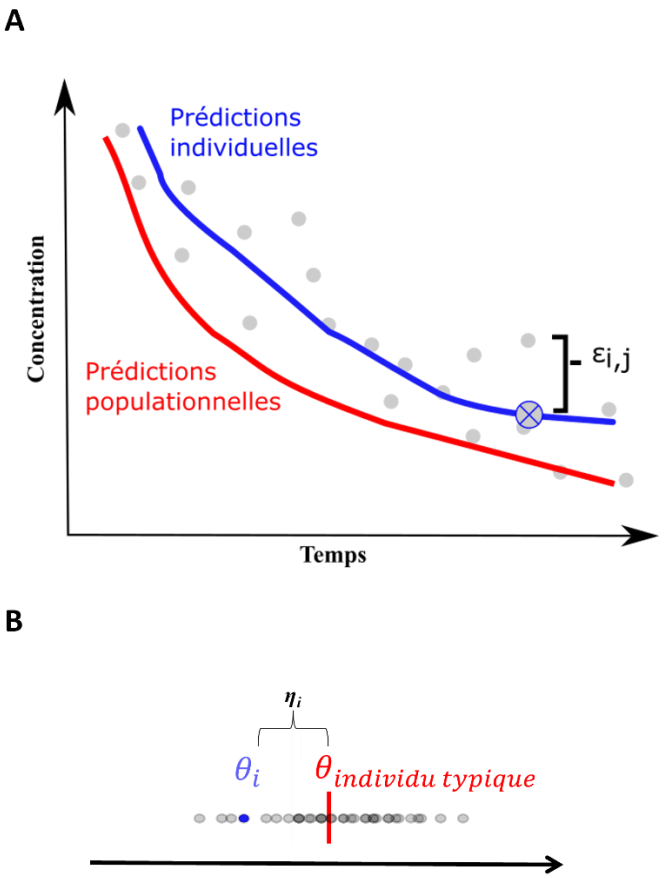

Figure 5. Illustration de la variabilité résiduelle ($\varepsilon_{i,j}$) et de la variabilité interindividuelle (η_i) pour un patient *i*, au temps *j*. A) La courbe de prédiction du patient *i* est en bleu et la courbe de prédiction de l'individu typique est en rouge. B) Le paramètre pharmacocinétique du patient *i* (θ_i) est en bleu et la courbe de prédiction de l'individu typique ($\theta_{individu\ typique}$) est en rouge. Adapté de (171).

Modélisation populationnelle — pharmacodynamie

Outre la PK, les modèles POP-PKPD permettent également une estimation de la PD du médicament en prédisant l'effet du médicament à partir des concentrations plasmatiques, de la dose ou de métriques relatant la PK (ex. l'aire sous la courbe ou la concentration maximale).

En partant des cinétiques enzymatiques (médicament + récepteur ⇄ complexe), il est possible de dériver une équation pour décrire la PD en utilisant l'équation de Hill, qui est également connue sous le nom de courbe E_{max} (172–174). La relation entre la concentration plasmatique et la réponse suit une courbe sigmoïde qui croît jusqu'à l'atteinte d'un plateau (illustré à la Figure 6 A). La sigmoïdicité de la courbe est déterminée par le coefficient γ. Elle est décrite par l'équation :

$$E = \frac{E_{max}\, C^{\gamma}}{EC_{50}^{\gamma} + C^{\gamma}}$$

où E_{max} est l'effet maximal, C sont les concentrations du médicament et EC_{50} est la concentration nécessaire pour atteindre 50% de l'effet.

Lorsque γ=1, l'équation de Hill se simplifie (172–174). Cette équation, dénommée Michaelis-Menten, est illustrée à la Figure 6 B. Elle s'écrit :

$$E = \frac{E_{max}\, C}{EC_{50} + C}$$

Il est possible d'adapter les équations de Hill et Michaelis-Menten pour inclure la tolérance aigüe observée suite à l'administration d'un médicament (70,71,175). Spécifiquement pour le MPH, la tolérance aigüe est décrite dans la littérature par un EC_{50} dépendant du temps (70,71), tel que :

$$EC_{50}(t) = EC_{50,start} * \left(1 + \frac{t^{\gamma}}{t_{50}^{\gamma} + t^{\gamma}}\right) \qquad (5)$$

, où t est le temps post-dose, $EC_{50,start}$ est le EC_{50} à t=0 ($EC_{50}(t=0)$), t_{50} est le temps nécessaire pour observer la moitié de la hausse de EC_{50} à partir du point de départ $EC_{50,start}$, et γ est le coefficient de sigmoïdicité représentant le changement de $EC_{50}(t)$.

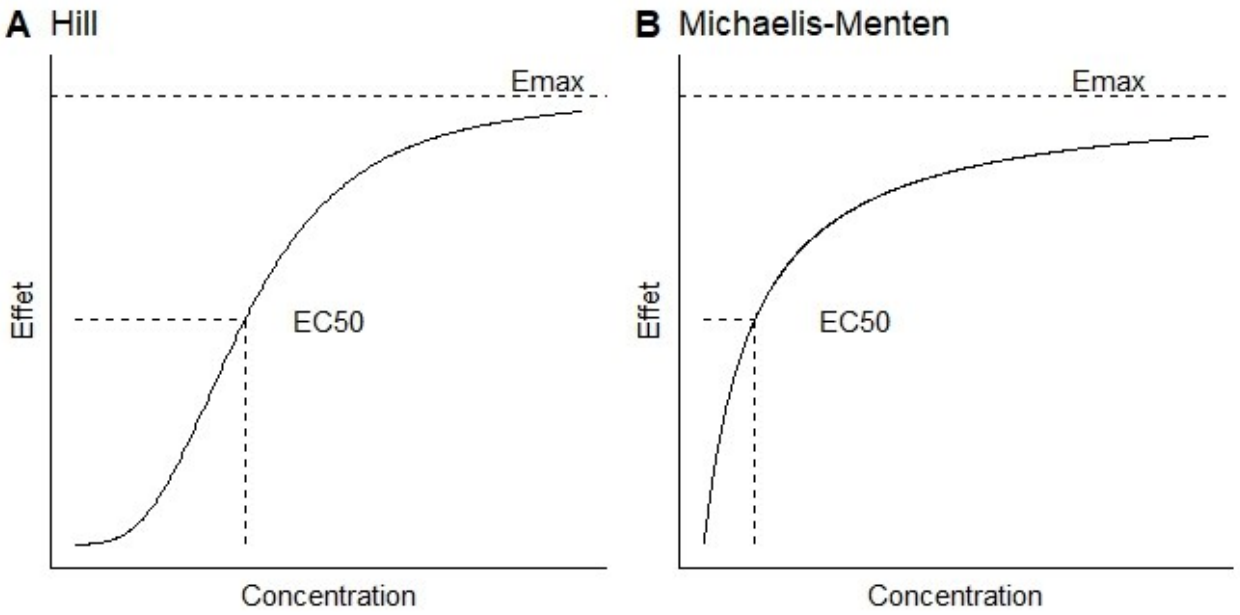

Figure 6. Illustration des courbes de l'effet en fonction des concentrations plasmatiques par les équations de Michaelis-Menten (A) et Hill (B). EC50 : Concentration nécessaire pour atteindre 50% de l'effet maximal, Emax : Effet maximal.

Cette relation entre la concentration et l'effet est décrite par deux grandes catégories de modèles : les modèles directs et les modèles indirects. Un modèle direct suppose que l'effet est directement relié aux concentrations plasmatiques. Ainsi, les concentrations plasmatiques sont utilisées dans les équations de Hill et Michaelis-Menten pour calculer l'effet (174).

En revanche, lorsqu'un délai entre l'effet et les concentrations plasmatiques est observé, un modèle indirect est utilisé. Ce délai est généralement dû au temps nécessaire pour atteindre l'équilibre au site d'action du médicament, à la présence de métabolites ou à la régulation à la hausse des récepteurs par exemple (174). Il est modélisé par un compartiment à effet, dont les concentrations d'une substance biologique (fictive ou réelle) proviennent des concentrations plasmatiques. La synthèse de cette molécule se fait par une constante de vitesse k_{e0} (Figure 7A). Dans les modèles indirects, ce sont les concentrations du compartiment à effet qui sont utilisées dans les équations de Hill et Michaelis-Menten (174).

Lorsque les courbes de concentrations plasmatiques-effet se présentent sous forme d'une hystérèse horaire, la tolérance aigüe est modélisée par l'ajout d'un compartiment de tolérance (Figure 7B). Une molécule inhibitrice de l'effet est synthétisée à une constante de vitesse k_{t0}. L'effet net du médicament est donc la somme du compartiment à effet et du compartiment de tolérance (174).

D'autres modèles structuraux PD sont aussi utilisés dans la littérature, mais ils ne font pas partie du cadre de cette thèse.

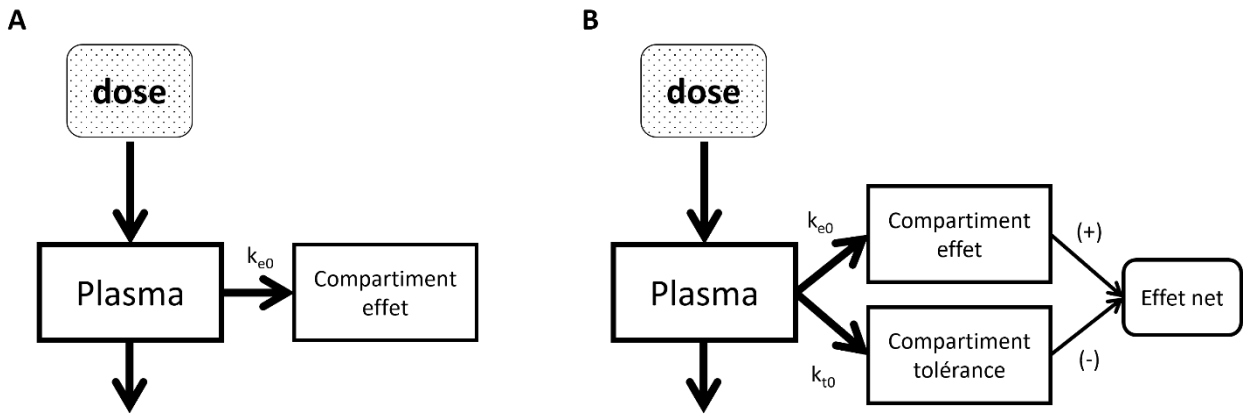

Figure 7. Modèles pharmacocinétique-pharmacodynamique indirects. A) L'effet est causé par la synthèse d'une substance dans un compartiment à effet, à une constante k_{e0}. B) L'effet est causé par la synthèse d'une substance dans un compartiment à effet, à une constante k_{e0}, et il est diminué par la synthèse d'une substance dans un compartiment de tolérance, à une constante k_{t0}. Adapté de (174).

Chapitre 3 — Bioéquivalence

Dans une longue quête d'humour reliée à la bioéquivalence, je suis revenue bredouille. Néanmoins, l'intelligence artificielle (ChatGPT) est venue à ma rescousse et a réussi l'impossible :

Q : Qu'a dit le médicament bioéquivalent à son ami ?

R : Nous devons être les mêmes à l'intérieur !

La bioéquivalence est une étude où l'on cherche à comparer deux produits pharmaceutiques : un produit générique (ou médicament test) doit démontrer qu'il présente une équivalence thérapeutique à un produit novateur (ou médicament de référence) déjà commercialisé. L'équivalence thérapeutique stipule que ces deux produits possèdent une équivalence dans leur efficacité et toxicité (176). Les études de bioéquivalence visent donc à démontrer que la quantité de principe actif disponible atteignant la circulation sanguine et la vitesse à laquelle celui-ci atteint la circulation sanguine sont identiques pour les deux formulations. Ainsi, toutes deux se comportent de la même manière dans l'organisme en termes d'absorption, de distribution et d'élimination.

L'objectif des études de bioéquivalence n'est donc pas de démontrer l'efficacité clinique ni la sécurité de cet ingrédient actif, car ces études ont déjà été faites pour le produit novateur (177). Également, comme ces deux produits partagent le même ingrédient actif et que seulement les caractéristiques reliées à leur formulation diffèrent, le générique et le produit novateur se distinguent essentiellement sur leur phase d'absorption.

Les études de bioéquivalence peuvent être réalisées *in vitro, in vivo* ou *in silico*. Dans cette thèse, nous nous concentrons uniquement sur les études *in vivo* puisque ce sont les plus répandues pour les ANDA. Ces études sont effectuées sur des volontaires sains (sauf en cas de problèmes éthiques) et peuvent être réalisées en design parallèle, chassé-croisé, répliqué ou non.

Nous nous limitons également à la définition la plus répandue des études de bioéquivalence : celles effectuées en développement du médicament pour une soumission abrégée d'une nouvelle formulation (*Abbreviated New Drug Submission* au Canada ou *Abbreviated New Drug Application* - ANDA aux États-Unis) (177).

Ces soumissions concernent un nouveau produit pharmaceutique ayant les propriétés suivantes identiques à celles d'un autre produit pharmaceutique déjà approuvé par les agences règlementaires (178) :

- Principe actif
- Critères de pureté
- Critères d'uniformité
- Temps de désintégration ou de dissolution

Métriques de bioéquivalence

L'objectif des études de bioéquivalence est d'estimer la vitesse et l'étendue de l'absorption du médicament test et référence (177). Ces caractéristiques du médicament sont quantifiées à l'aide de métriques PK. Elles sont illustrées à la Figure 8.

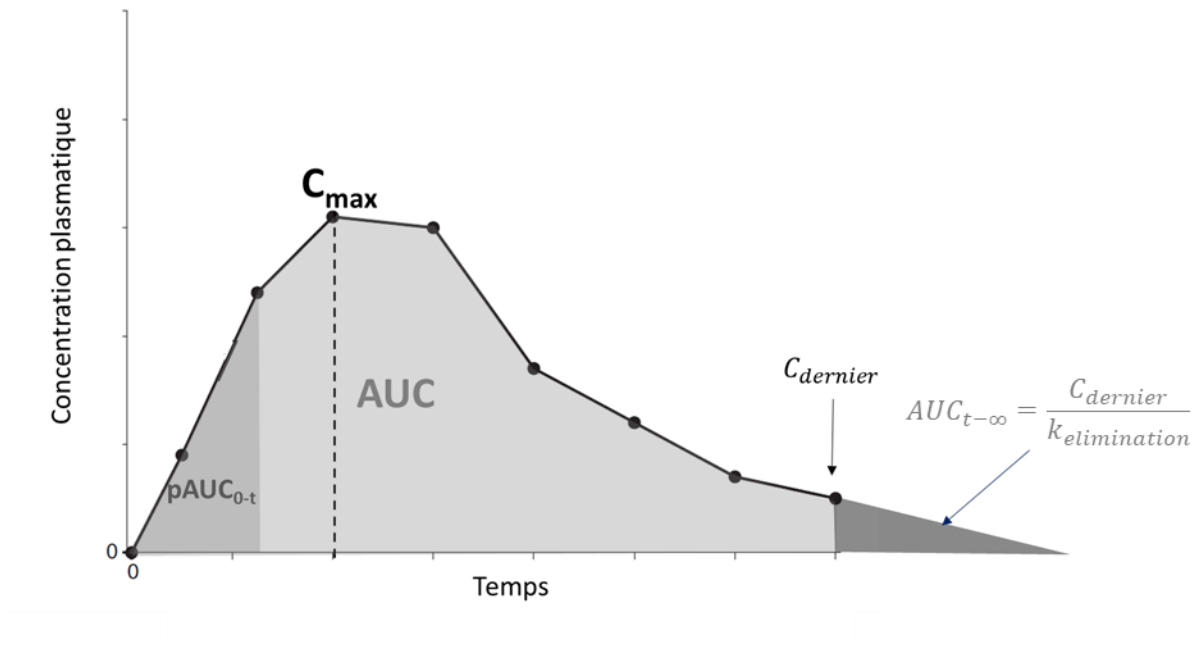

Figure 8. Illustration des métriques utilisées en bioéquivalence : la concentration maximale (C_{max}), l'aire sous la courbe (AUC), l'aire sous la courbe partielle entre 0 et un temps t ($pAUC_{0-t}$) et l'aire extrapolée à l'infini par la division de la dernière concentration mesurée ($C_{dernier}$) et la constante d'élimination obtenue sur la dernière portion de la courbe en semi-log ($k_{élimination}$)

Aire sous la courbe

L'aire sous la courbe PK (*area under the curve* - AUC) est utilisée pour quantifier l'étendue de l'absorption.

L'AUC calculée du temps initial à l'infini ($AUC_{0-\infty}$) permet d'estimer l'étendue de l'absorption. Son utilisation est justifiée par la relation suivante entre la biodisponibilité (F) et l'AUC (177) :

$$F * dose = clairance * AUC_{0-\infty}$$

Comme l'ingrédient actif est identique pour le médicament test et référence, il est possible de réécrire l'équation ci-haut en supposant une PK linéaire :

$$\frac{\frac{AUC_{0-\infty,T}}{dose_T}}{\frac{AUC_{0-\infty,R}}{dose_R}} = \frac{F_T}{F_R}$$

L'AUC est communément calculée par la méthode des trapèzes pour l'AUC jusqu'au dernier temps de prélèvement (AUC_{0-t}) et elle est extrapolée jusqu'à l'infini par le ratio de la constante d'élimination ($k_{elimination}$) et de la concentration au dernier temps de prélèvement ($C_{dernier}$) (177):

$$AUC_{0-\infty} = AUC_{0-t} + \frac{C_{dernier}}{k_{elimination}}$$

L'aire extrapolée ne doit pas dépasser 20% de $AUC_{0-\infty}$ (177).

Pour des profils PK complexes, notamment les formulations ER de MPH, l'AUC ne permet plus de comparer adéquatement l'absorption (179). À titre d'exemple, deux formulations différentes de MPH sont illustrées à la Figure 9 (180). Selon l'AUC et C_{max}, ces deux formulations sont jugées bioéquivalentes. Par contre, il est facile de distinguer que le profil PK est différent.

Ainsi, l'aire sous la courbe partielle (pAUC) a été proposée pour tenir compte de l'absorption aux premiers temps de prélèvement post-dose (181). En calculant l'AUC sur une période spécifique, il est possible de distinguer des formulations ayant des profils de libération différents (182).

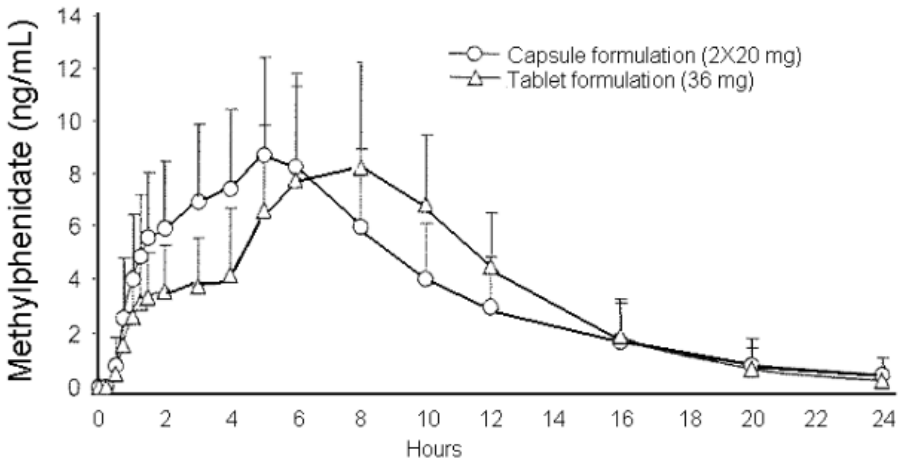

Figure 9. Concentrations plasmatiques du Metadate (*capsule*) et du Concerta (*tablet*) en fonction du temps. Tiré de (180)

Un guide spécifique pour les formulations ER du MPH a été publié par la FDA, où les seuils de coupure dans le temps sont définis (182). Ces seuils varient selon la prise concomitante de nourriture. À jeun, la pAUC est calculée pour les temps post-dose suivants : 0 à 3 h, 3 à 7 h et 7 à 12 h (182). Lorsque le MPH est pris avec nourriture, les temps sont plutôt : 0 à 4 h, 4 à 8 h, 8 à 12 h (182).

Concentration maximale

La métrique utilisée dans les études de bioéquivalence pour refléter la vitesse d'absorption d'un médicament est la concentration maximale (C_{max}). Cependant, comme elle est une mesure de concentration plutôt qu'une mesure de vitesse, la C_{max} est donc mesure indirecte de la vitesse d'absorption (183–193). Bien que la C_{max} puisse être quantifiée par une simple analyse non compartimentale, elle possède plusieurs autres limites importantes en bioéquivalence (194).Son utilisation est donc souvent controversée.

D'abord, l'estimation de C_{max} est dépendante des temps de prélèvements (Figure 8) (194). Effectivement, si les prélèvements sanguins dévient du t_{max}, la valeur estimée de C_{max} sera biaisée. Également, la C_{max} ne peut être raisonnablement utilisée pour comparer des profils PK complexes (177,194). Par exemple, deux profils ER biphasiques pourraient avoir une C_{max} identique à deux différents t_{max} (Figure 9) (180).

Afin de contourner les limites de l'utilisation de C_{max}, plusieurs autres métriques ont été proposées. Bien qu'aucune ne soit décrite dans les guides des agences règlementaires, il est intéressant de mentionner le ratio $\frac{C_{max}}{AUC}$ (187,188). Il a été proposé en 1991 et longuement étudié depuis. Il a été démontré qu'il est plus sensible que C_{max} pour détecter des différences dans la vitesse d'absorption lorsqu'il y a en a une (189). Un autre article ayant analysé 20 études de bioéquivalence a démontré que $\frac{C_{max}}{AUC}$ est plus sensible que C_{max} pour distinguer la vitesse d'absorption des médicaments à courte demi-vie (moins de 5 h) (195).

Alors que C_{max} est une mesure indirecte de la vitesse d'absorption, la constante d'absorption du médicament (décrite à la page 51) en est une mesure directe (196). Elle reflète purement la

vitesse d'absorption et n'est pas influencée par les autres phases PK. Cependant, celle-ci nécessite une modélisation mathématique pour être estimée. Son utilisation en bioéquivalence est d'actualité et la modélisation PK compartimentale fait ses premiers pas dans les guides règlementaires en bioéquivalence (196–198).

Méthodes de bioéquivalence proposées par les agences règlementaires

La bioéquivalence, tout comme Rome, ne s'est pas faite en un jour. Plusieurs méthodes statistiques ont été proposées pour démontrer l'équivalence thérapeutique de deux médicaments. La plus répandue est la bioéquivalence moyenne (*Average bioequivalence* – ABE), qui compare la moyenne des métriques PK entre deux médicaments (199). En 1997, la FDA s'est penchée sur l'interchangeabilité des médicaments (échanger entre un médicament test et référence pour des patients jamais traités ou en cours de traitement) (200). L'ABE ne peut pas garantir cette interchangeabilité. Ainsi, un panel d'experts a proposé deux autres méthodes de bioéquivalence qui tiendraient compte de cette problématique : la bioéquivalence de population (PBE) et la bioéquivalence individuelle (IBE) (199,201,202). Ces trois méthodes, figurant dans les guides de bioéquivalence de la FDA, sont résumées dans cette section. Elles sont aussi illustrées à la Figure 10 (203).

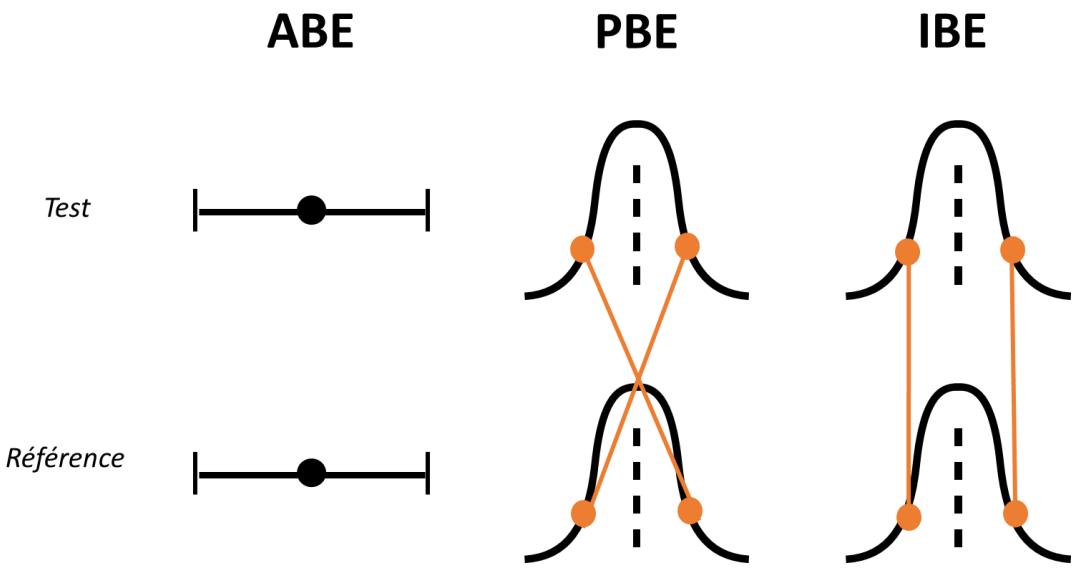

Figure 10. Illustration de la bioéquivalence moyenne (*Average bioequivalence* – ABE), la bioéquivalence de population (PBE) et la bioéquivalence individuelle (IBE). Inspiré de (203,204)

ABE

La ABE traite la différence entre la moyenne des métriques pour le médicament test et le médicament de référence. Elle se base sur les tests d'hypothèse suivants, où $\mu_T \; et \; \mu_R$ sont les moyennes des métriques de bioéquivalence sur l'échelle logarithmique pour le médicament test et le médicament de référence, respectivement (177,199):

$$H_{01}: \mu_T - \mu_R \leq \ln(0.8) \quad H_{11}: \mu_T - \mu_R > \ln(0.8)$$

$$H_{02}: \mu_T - \mu_R \geq \ln(1.25) \; H_{12}: \mu_T - \mu_R < \ln(1.25)$$

Afin de démontrer une bioéquivalence par ABE, l'intervalle de confiance à 90% pour $\mu_T - \mu_R$ doit se situer entre $\ln(0.8)$ et $\ln(1.25)$. Ces limites sont définies par les agences règlementaires. Spécifiquement pour les médicaments à intervalle thérapeutique étroit, une limite plus sévère est imposée.

Pour toutes les méthodes de bioéquivalence, les erreurs de type 1 (rejeter H_0 alors que H_0 est vraie) et type 2 (ne pas rejeter H_0 alors que H_0 est fausse) sont donc le risque du consommateur et le risque du fabricant, respectivement. Généralement, l'erreur de type 1 est fixée à 5% (177).

PBE

Alors que la ABE repose sur une comparaison de ratios non transformés, la bioéquivalence de population (PBE) repose plutôt sur un critère agrégé qui combine la différence entre les moyennes ($\mu_T - \mu_R$) et la différence entre les variances du médicament test et du médicament de référence ($\sigma_T \; et \; \sigma_R$, respectivement). Ainsi, la PBE permet de comparer toute la distribution des métriques de bioéquivalence pour les deux médicaments. Elle se fait par les tests d'hypothèses suivants (177,199):

$$H_0: \frac{(\mu_T - \mu_R)^2 + \sigma_T^2 - \sigma_R^2}{\max(\sigma_R^2, 0.04)} \geq \frac{\ln(1.25)^2 + 0.02}{0.04}$$

$$H_1: \frac{(\mu_T - \mu_R)^2 + \sigma_T^2 - \sigma_R^2}{\max(\sigma_R^2, 0.04)} < \frac{\ln(1.25)^2 + 0.02}{0.04}$$

Afin de démontrer une bioéquivalence par PBE, la limite supérieure de l'intervalle de confiance à 95% du critère agrégé ci-haut est plus basse que $\frac{\ln(1.25)^2+0.02}{0.04}$.

IBE

La bioéquivalence individuelle (IBE) ajoute une considération pour (i) l'interaction entre la métrique de bioéquivalence de chaque sujet et la formulation administrée (σ_D^2) et (ii) la variance de la variabilité intrasujet pour le médicament test et référence (σ_{WT}^2 et σ_{WR}^2, respectivement). Ainsi, un design d'étude répliqué est nécessaire pour estimer l'IBE. Elle est calculée par les tests d'hypothèses suivants (177,199):

$$H_0: \frac{(\mu_T - \mu_R)^2 + \sigma_D^2 + \sigma_{WT}^2 - \sigma_{WR}^2}{\max(\sigma_R^2, 0.04)} \geq \frac{\ln(1.25)^2 + 0.05}{0.04}$$

$$H_1: \frac{(\mu_T - \mu_R)^2 + \sigma_D^2 + \sigma_{WT}^2 - \sigma_{WR}^2}{\max(\sigma_R^2, 0.04)} < \frac{\ln(1.25)^2 + 0.05}{0.04}$$

Afin de démontrer une bioéquivalence par IBE, la limite supérieure de l'intervalle de confiance à 95% du critère agrégé ci-haut est plus basse que $\frac{\ln(1.25)^2+0.05}{0.04}$.

Limites de ces méthodes

La communauté scientifique ayant travaillé sur la bioéquivalence a longtemps débattu sur la méthode la plus appropriée en bioéquivalence. En effet, chacune des méthodes décrites ci-haut possède des limites (205–208).

L'ABE ne garantit pas l'interchangeabilité des médicaments test et référence puisqu'elle ne compare que la moyenne des métriques de bioéquivalence (C_{max} ou AUC) (209–211). Ainsi, elle ne permet pas de tenir compte de la forme de la distribution de ces métriques (voir Figure 10).

La PBE et la IBE sont d'abord critiquées, car elles ne peuvent pas être traduites sur une échelle normale. Contrairement à ABE, où une transformation sur l'échelle logarithmique peut être retransformée sur l'échelle normale, les valeurs de PBE et IBE ne peuvent être interprétées sur l'échelle originale des C_{max} ou AUC (211,212).

La PBE et la IBE sont également critiquées pour le compromis qu'elles introduisent entre la différence de moyenne et la différence de variances des médicaments test et référence (205–208,213,214). En effet, comme elles agrègent ces deux considérations dans une même équation, il est possible de déclarer une bioéquivalence par PBE (ou IBE) sans avoir une bioéquivalence par ABE. En d'autres mots, une grande différence $\mu_T - \mu_R$ peut être compensée par une réduction entre σ_T^2 et σ_R^2. Ainsi, $\mu_T - \mu_R$ peut dépasser les limites établies de $\ln(0.8) - \ln(1.25)$ et introduire un problème de hiérarchie, où IBE ne signifie pas une PBE ni une ABE.

Plusieurs autres méthodes ont été proposées pour corriger les limites de ABE, PBE et IBE. Certaines proposent des équations désagrégées, qui règlent ainsi le problème de hiérarchie (215). D'autres passent par des équations agrégées plus complexes qui ne posent pas de problème de hiérarchie ni de transposition d'échelle. La méthode de la divergence de Kullback-Leibler est l'une d'entre elles (216).

Cette méthode statistique permet de comparer deux distributions de probabilité. Appliquée à la bioéquivalence, elle permet ainsi de quantifier la distance entre les distributions du médicament test et référence ($f_T$et f_R) (216). En supposant des distributions normales et en considérant la variabilité interindividuelle, elle s'écrit :

$$d(f_T, f_R) = \frac{1}{2}\{(\mu_T - \mu_R)^2 + \sigma_T^2 + \sigma_R^2\}\left(\frac{1}{\sigma_T^2} - \frac{1}{\sigma_R^2}\right) - 2$$

Il a été démontré que l'utilisation de la méthode de Kullback-Leibler respecte la hiérarchie (IBE signifie PBE, qui signifie aussi ABE) et peut se transposer entre l'échelle logarithmique et l'échelle normale (216).

Finalement, la communauté scientifique s'est mise d'accord sur le fait qu'il n'y ait pas de cas démontrant que ABE puisse mener à l'échec clinique d'une formulation (217). Ainsi, PBE et IBE ne seraient utilisés que dans des situations jugées nécessaires par les agences règlementaires (199).

Chapitre 4 – Trapezoid bioequivalence: A rational bioavailability evaluation approach on account of the pharmaceutical- driven balance of population average and variability

Sara Soufsaf, M.Sc.[1], Fahima Nekka, Ph.D.[1], Jun Li, Ph.D.[1]

[1] Université de Montréal, Montréal, Québec, Canada

Préambule

Le premier travail de cette thèse s'inscrit dans l'oasis scientifique de la bioéquivalence et tente de proposer une méthode qui résolve les limites de ABE et PBE sans introduire de nouvelles limites. Nous y proposons la bioéquivalence trapézoïdale (TBE). Celle-ci permet une comparaison de la distribution des métriques de bioéquivalence (moyenne et variance) avec des pondérations flexibles et adaptées aux médicaments. Nous montrons que la TBE peut être efficacement appliquée pour comparer les formulations et respecter la hiérarchie avec ABE. La TBE pourrait être mise en œuvre dans les études de bioéquivalence lorsque la variabilité interindividuelle d'un médicament constitue un facteur limitant dans son interchangeabilité entre le test et la référence.

Cet article a été publié dans le journal « Clinical Pharmacology and Therapeutics : Pharmacometrics and Systems Pharmacology » (218).

Abstract

Among the current approaches for the analysis of bioequivalence, the average bioequivalence (ABE) is limited only to the mean bioavailability while the population bioequivalence (PBE)

criterion aggregates both mean and variance in a general comparison formula. However, a rational bioequivalence criterion capable of judging specific drug considerations is still preferred.

As an alternative approach, we introduce an aggregate criterion, namely the trapezoid bioequivalence (TBE), which includes the consideration of both mean and variance of the bioavailability and adapted weighting of a drug's therapeutic properties. We first applied our method to specific simulated scenarios to compare the strengths and weaknesses of current bioequivalence approaches and demonstrate the improvements brought by TBE. As well, the impact of sample size and variability on ABE, PBE and TBE are assessed using a population pharmacokinetic model of methylphenidate.

Our results indicate that TBE inherits the advantages of both ABE and PBE while greatly reducing their inadequacies. Through simulations with population pharmacokinetic models of specific scenarios, we confirm that 1) TBE does not encounter the overly permissiveness issue of PBE; 2) TBE respects the hierarchy to ABE (TBE => ABE); 3) TBE assesses bioequivalence with restriction on $\sigma_T^2 - \sigma_R^2$ without an increase to type 2 errors.

The clinically inspired simulations demonstrate TBE's superiority in a realistic context and its potential usefulness in practice. Moreover, the parameter choice in TBE may be adapted according to the specific context of a drug's pharmacological and pharmacodynamic properties.

Key words: *Bioequivalence, methylphenidate, variability, population*

Study highlights

- ***What is the current knowledge on the topic?***

Average and Population bioequivalence (ABE and PBE) are the current statistical analyses of bioequivalence. ABE does not consider the variability of bioavailability. PBE is an aggregate criterion which considers variability but poses hierarchy problems with ABE.

- ***What question did this study address?***

Can we propose an aggregate bioequivalence criterion which addresses the flaws of ABE and PBE without adding limitations of its own?

- ***What does this study add to our knowledge?***

We propose the Trapezoid bioequivalence (TBE) as a criterion which considers the mean and variance of bioavailability with flexible and drug-specific weights. We show that TBE can effectively be applied to compare formulations and respect hierarchy with ABE.

- ***How might this change drug discovery, development, and/or therapeutics?***

TBE might be implemented in bioequivalence studies as a flexible approach when a drug's interindividual variability is a limiting factor in prescribability and switchability.

Introduction

When the patent of an innovative drug expires, a generic can be approved with an abbreviated new drug application (ANDA), which states that the generic is bioequivalent to the brand name formulation in terms of efficacy and safety (1). Indeed, only the absorption process might differ, and it must be assessed through the bioavailability (2). The bioavailability is measured by the rate and extent of drug absorption, represented by the maximum concentration (C_{max}) and the area under the curve (AUC) of the plasma concentrations, respectively. Statistical analyses have been proposed to determine the therapeutical equivalence between the test and reference formulations (2).

Among the aggregate approaches, the US Food and Drug Administration (FDA) proposes three levels of bioequivalence: average bioequivalence (ABE), population bioequivalence (PBE) and individual bioequivalence (IBE) (2). Since IBE is less used, we focus our work on ABE and PBE.

ABE applies to the **averages of bioavailability metrics** on the logarithmic scale for the test and reference formulations (μ_T and μ_R, respectively). ABE states that the test may be a substitute for the reference formulation if the difference between μ_R and μ_T is within 20%. Since ABE is a simple comparison of averages, the declared bioequivalent event can be challenged by largely different

variances of two formulations. Consequently, ABE has been questioned for its limited applicability (3–5). To correct the situation, an additional consideration was proposed by Sheiner (3) and Hauck &Anderson (4), for example. These authors pointed out that the variability in bioavailability evidently translates to a low precision in predicting the efficacy, which led to the introduction of the PBE criterion (2–4,6–8).

PBE considers the drug variability by accounting for the **distribution of bioavailability metrics**. Compared to ABE, it aggregates the mean and variance (σ_T^2 and σ_R^2) into a one-step comparison by simultaneously considering σ_T^2 - σ_R^2 and $\mu_T - \mu_R$ (2,3). PBE finds its use when addressing the issue of drug prescribability, which is defined as the substitutability of a test drug to a reference drug for treatment of naïve patients (4).

Nonetheless, PBE does not automatically imply ABE, which leads to overly permissive and contradictory results (9–12). The non-respect of hierarchy is a fundamental issue when combining two elements into one criterion. In fact, if σ_T^2 is smaller than σ_R^2, a larger difference between μ_R and μ_T is accepted with PBE (9–11), offsetting thus the benefit of adding the variance in the evaluation. Hence, a better criterion is needed for a fair trade-off between average and variance to respect the natural hierarchical property (8,13). Indeed, several adaptations were proposed in the literature, with some questioning the idea that PBE gives equal importance to μ and σ^2 in the assessment of bioequivalence (7,12,14–17). As a solution, Hauck and Midha proposed to add a weight to σ^2 (13,18) that can be modified to alter the acceptable threshold of bioequivalence.

The objective of our work is to propose a new bioequivalence criterion, named trapezoid bioequivalence (TBE), which simultaneously takes into account the average (μ) and variance (σ^2) of bioavailability by addressing the flaws of ABE and PBE without adding new limitations. Moreover, the goalpost of the new criterion for establishing bioequivalence should not become more permissive as the within-subject variability of the test drug is reduced, contrarily to PBE whose performance deteriorates in these cases. Finally, we add a trade-off between mean and variance that can be adjusted according to specific drug properties.

As a concrete drug example, we will show how we can directly apply our proposed approach to methylphenidate (MPH), the main drug for Attention Deficit Hyperactivity Disorder (ADHD). Since

the interindividual variability (IIV) is very large for MPH, the dose individualization is especially difficult (19,20). By adopting TBE, we show how we can effectively establish bioequivalence between various formulations while reducing uncertainty related to substitutability. For an objective evaluation of bioequivalence, we have also used enriched clinical trial data for specific scenarios by incorporating population pharmacokinetic (Pop-PK) modelling and simulation in our investigation (21,22).

Methods

The detailed ABE and PBE approaches are described in Supplementary Material 1.

Trapezoid bioequivalence (TBE)

Trapezoid bioequivalence (TBE) is our proposed strategy to address the role of average and variance in bioequivalence evaluation, and most importantly the trade-off between both. Contrary to ABE or PBE, which use a single metric, TBE includes a trapezoid zone of acceptance outlined by two distinct sets of inequalities. This zone is expressed as:

Equation 1. .

$$zone_{TBE} = \left\{(x,y)\middle| \begin{matrix} -\sigma_R^2 \leq x < \alpha_1 \; and \; 0 \leq y < \theta^{TBE}; \\ or \\ \alpha_1 \leq x < \alpha_2 \; and \; 0 \leq y < -\lambda_1 x + \lambda_2 \end{matrix} \right\}$$

The explanation for each variable of TBE is given below, while the specific values chosen for these variables will be detailed in the Scenario-based Simulations section in the Methods.

For the purpose of bioequivalence, we specifically define $x = \sigma_T^2 - \sigma_R^2$ and $y = (\mu_T - \mu_R)^2$. θ^{TBE} is the maximal squared difference of μ allowed for bioequivalence; α_1 is the therapeutically acceptable difference of σ^2 where TBE can be judged solely based on the difference in μ, and α_2 is the therapeutically unacceptable difference of σ^2 beyond which TBE will directly fail. α_1 and α_2

are used to control the trade-off between μ and σ^2. Given these parameters, λ_1 and λ_2 are weights which regulate the trade-off between mean and variance and are computed as follows:

$$\lambda_1 = \frac{\theta^{TBE}}{\alpha_2 - \alpha_1} \qquad \text{Equation 2.}$$

$$\lambda_2 = \lambda_1 \alpha_2 \qquad \text{Equation 3.}$$

Specific values for $\theta^{TBE}, \alpha_1, \alpha_2$ are to be defined by regulatory agencies according to the drug's pharmacological properties and its tolerance for IIV. In this work, we assigned values that would respect general clinical significance and would allow an agreement with ABE and PBE. Each of these values is explained in the Scenario-Based Simulations section in the Methods.

To facilitate the hypothesis test, Equation 1 can be transformed as:

- $(\mu_T - \mu_R)^2 - \theta^{TBE} < 0$, when $-\sigma_R^2 \leq \sigma_T^2 - \sigma_R^2 < \alpha_1$
- $(\mu_T - \mu_R)^2 + \lambda_1 (\sigma_T^2 - \sigma_R^2) - \lambda_2 < 0$, when $\alpha_1 \leq \sigma_T^2 - \sigma_R^2 < \alpha_2$

TBE can be dynamically accessed in https://mphss.shinyapps.io/SoufsafTrapezoidBE/.

TBE conclusions are drawn based on the upper 90% confidence interval (CI_{90}) of the previous inequalities. The bootstrap procedure was used to compute the confidence interval (CI) and 2000 replicates were used for the bootstrap (2). As in PBE, TBE is declared if this value falls below 0. Otherwise, TBE will not be concluded. The TBE acceptance zone ($zone_{TBE}$) is illustrated in Figure 1 (a) and a flowchart of TBE computation and decision is presented in Figure 1 (b).

Similar to PBE and in accordance with Equation 1, $zone_{TBE}$ is defined by limits in terms of $(\mu_T - \mu_R)^2$ and $\sigma_T^2 - \sigma_R^2$. When $\sigma_T^2 - \sigma_R^2 > 0$, $zone_{TBE}$ corrects the drawback of ABE and adds a consideration of variability to bioequivalence. As well, when $\sigma_T^2 - \sigma_R^2 < 0$, $zone_{TBE}$ corrects the drawback of PBE and imposes a limit to $(\mu_T - \mu_R)^2$.

As defined in Equation 1, TBE possesses multiple favourable properties. First, its limits are defined with a clinical significance for each parameter (θ^{TBE} and α_1, α_2). Indeed, θ^{TBE} may be set in accordance with current ABE criteria and α_1, α_2 may be set in accordance with clinically acceptable limits of variability. Second, it can be shown that TBE is reduced to ABE assuming $\sigma_T^2 = \sigma_R^2$ and fixing $\theta^{TBE} = \ln^2(1.25)$. Third, TBE respects the hierarchy with ABE. Indeed, TBE introduces θ^{TBE} to prevent widening the acceptable limits of $(\mu_T - \mu_R)^2$ when σ_T^2 is reduced with respect to σ_R^2. Finally, TBE allows a flexible trade-off between mean and variance with the weights λ_1 and λ_2. Indeed, TBE permits a control on the weight and importance given to $(\mu_T - \mu_R)^2$ and $\sigma_T^2 - \sigma_R^2$. These favourable properties are examined in this work.

ABE, PBE and TBE were applied in three ways. First, we computed statistical methods of bioequivalence to broad scenario-based simulations applicable to all drugs. Second, we used MPH as a specific drug to exemplify our work. Third, we computed the type 1 and 2 errors.

(a) Bioequivalence zones

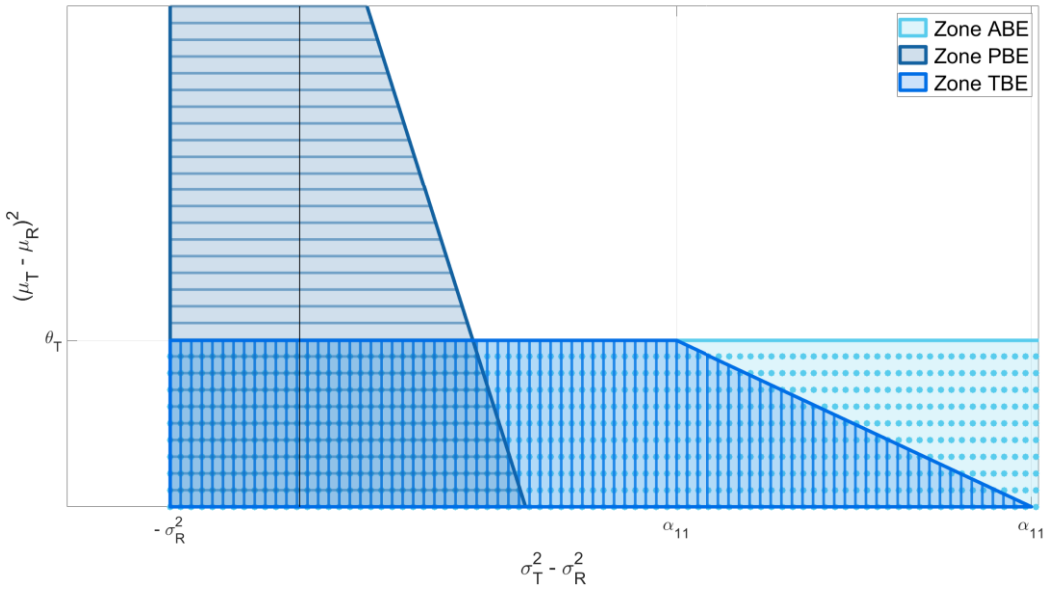

(b) Flowchart of Trapezoid Bioequivalence

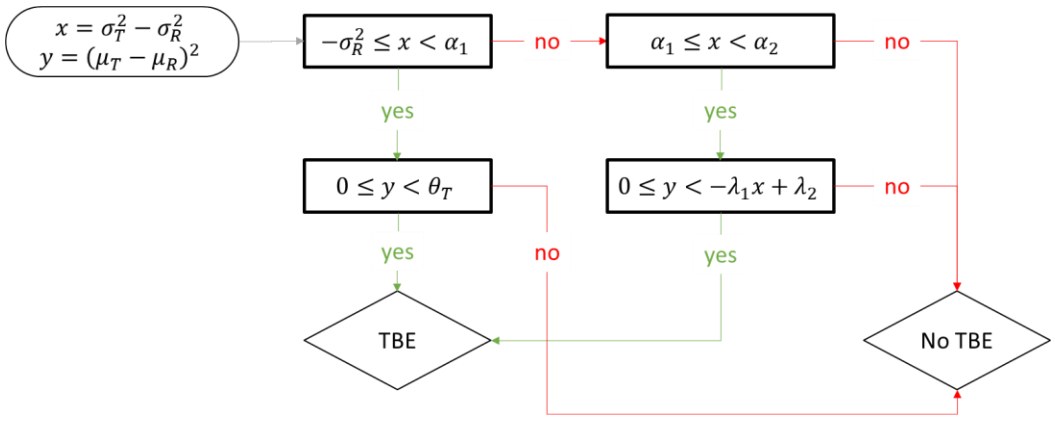

Figure 1. The top panel (a) illustrates the zones of acceptance of bioequivalence for average bioequivalence (ABE), population bioequivalence (PBE) and trapezoid bioequivalence (TBE) as shaded areas. μ_T and μ_R are the averages of bioavailability metrics on the logarithmic scale for the test and reference formulations respectively; σ_T^2 and σ_R^2 are the variances of bioavailability metrics on the logarithmic scale for the test and reference formulations respectively; θ^{TBE} is the maximal squared difference of μ allowed for bioequivalence; α_1 is the therapeutically acceptable difference of σ^2 ; α_2 is the

therapeutically unacceptable difference of σ^2; λ_1 and λ_2 are weights applied to control the trade-off between μ and σ^2. The bottom panel (b) is a flowchart of bioequivalence decisions with TBE.

Scenario-Based Simulations

The scenarios chosen for simulation are combinations of the following situations: a relatively small variability for the test formulation ($\sigma_T^2 - \sigma_R^2 < 0$); a large mean difference between the test and reference formulations ($(\mu_T - \mu_R)^2 > \theta^{TBE^2}$); a therapeutically tolerable difference of variability ($\alpha_1 \leq \sigma_T^2 - \sigma_R^2 < \alpha_2$); non- substitutable test and reference formulations ($\sigma_T^2 - \sigma_R^2 > \alpha_2$). The first and second situations identify failures of PBE while the third and fourth situations identify failures of ABE.

For each patient, the bioavailability metric values (AUC or C_{max}) of test (or reference) formulations are drawn from normal distributions with means μ_T (or μ_R) and variances σ_{T}^2 (or σ_{R}^2). The fixed values of μ_R, μ_T, σ_R^2 and σ_T^2 as reported in Table 1.

For each scenario, 40 subjects are used. Thus, 80 AUC measurements (2 per subject) are simulated for a crossover and non-replicated clinical trial. ABE, PBE and TBE results are then computed for each scenario as described in the previous section. For the sake of respecting the desirable properties of bioequivalence criterion, we fixed TBE parameters in accordance with ABE's and PBE's FDA goalposts.

$\underline{\theta^{TBE}}$:By fixing $\theta^{TBE} = \ln^2(1.25)$, we respect ABE's acceptable ±20% mean difference on the log scale (or 80–125% on the original scale).

$\underline{\alpha_1}$:We fix ±30% as the tolerable difference of σ2 on the log scale as suggested (23). Clinically, this is a range of variance between 70–143% on the original scale.

Using Equation 2 and Equation 3, we have λ_1=0.1480 and λ_2=0.1026.

We repeated each sampling scenario 100 times.

Table 1. Results for the Scenario-Based Simulations

Scenario	$(\mu_T - \mu_R)^2$	$\sigma_T^2 - \sigma_R^2$	σ_R^2	ABE		PBE		TBE	
				90% CI	Probability of passing bioequivalence (%)	Mean $upper$ 90% CI (CV %)	Probability of passing bioequivalence (%)	Mean $upper$ 90% CI (CV %)	Probability of passing bioequivalence (%)
1	0.0111	0.3	0.0225	0.9529 - 1.2977	1	0.4070 (12.86)	0	**-0.0271 (-18.67)**	**100**
2	0.0900	0.3	0.0225	1.1572 - 1.5751	0	0.5069 (9.86)	0	0.1317 (29.40)	0
3	0.0225	0.8	0.0225	0.9174 - 1.4834	0	1.1530 (11.68)	0	0.0953 (11.34)	0
4	0.0900	-0.01	0.0225	1.2894 - 1.4217	0	0.1918 (12.17)	0	0.1347 (22.30)	0
5	0.0111	-0.01	0.0225	**1.0574 - 1.1651**	**100**	0.0142 (74.343)	10	**-0.0278 (-17.69)**	**100**
6	0.0111	0.3	0.1225	0.9188 - 1.3461	0	0.3605 (15.42)	0	**-0.0270 (-18.803)**	**100**
7	0.0900	0.3	0.1225	1.1146 - 1.6374	0	0.4330 (15.28)	0	0.1327 (33.158)	0
8	0.0225	0.8	0.1225	0.8885 - 1.5235	0	1.1009 (14.67)	0	0.0948 (15.63)	0

9	0.0900	-0.1	0.1225	1.2287 - 1.5012	0	**-0.0476 (-80.4)**	**85**	0.1388 (26.29)	0
10	0.0111	-0.1	0.1225	**1.0059 - 1.2293**	**86**	**-0.1827 (-12.45)**	**100**	**-0.0271 (-18.67)**	**100**

Values in **bold** signify that the approach passes bioequivalence.

ABE: average bioequivalence; PBE: population bioequivalence; TBE: trapezoid bioequivalence; μ_T and μ_R : averages of bioavailability metrics on the logarithmic scale for the test and reference formulations respectively; σ_T^2 and σ_R^2: variances of bioavailability metrics on the logarithmic scale for the test and reference formulations respectively; CI_{90}: mean 90% CI across all replications; CV: coefficient of variation across all replications.

Methylphenidate Model-Based Simulations

In addition to the scenario-based simulations, we apply the described bioequivalence methods to the specific context of MPH. Indeed, as a drug with a higher IIV, it exemplifies the added value of using TBE instead of ABE or PBE.

The bioequivalence methods were applied to two types of data. First, it was applied to the analysis of a randomized clinical trial (Supplementary Material 2). Second, as the available clinical trial data were limited, we used model-based simulations to explore additional considerations pertinent to bioequivalence: IIV and sample size.

Interindividual Variability

To explore the impact of IIV on the bioequivalence methods, we used the published MPH Pop-PK model to simulate databases which incorporate inter- and intra-individual variability (19). Each simulated pair of test and reference formulation is chosen with a random variance of IIV (ω2) listed in Table 2, while the fixed effects and residual variability remained unchanged. Consequently, the σ_R^2 and σ_T^2 evaluated by PBE and TBE still depend on inter and intra-individual variability. However, as total IIV is the only difference between the reference and test databases, only the impact of IIV on ABE, PBE and TBE is evaluated. The magnitude of IIV on each parameter was chosen according to a reasonable scale observed in Pop-PK models. In staying true to the original Pop-PK model, we did not explore any IIV on lag and fixed it for all simulations.

Sample Size

Subsequently, we explored the impact of sample size on ABE, PBE and TBE. The same methods as above were applied with 40 and 100 subjects in each simulation. These numbers were chosen to investigate a realistic range observed in clinical trials.

TBE parameters used in the MPH model-based simulations were chosen exactly as in the Scenario-based Simulations of Section 0.

Table 2. Results for MPH model-based simulations

Number of patients in clinical study	**Sum of IIV* for the reference formulation**	**Sum of IIV* for the test formulation**	**Results of bioequivalence**		
			ABE	**PBE**	**TBE**
40	$IIV_T = IIV_R$				
	0.1	0.1	**YES**	**YES**	**YES**
	1	1	**YES**	**YES**	**YES**
	1.5	1.5	**YES**	**YES**	**YES**
	$IIV_T > IIV_R$				
	0.1	1	**YES**	NO	**YES**
	0.1	1.5	*NO*	NO	**YES**
	$IIV_T < IIV_R$				

	1	0.1	**YES**	**YES**	**YES**
	1.5	0.1	*NO*	**YES**	**YES**
100	$IIV_T = IIV_R$				
	0.1	0.1	**YES**	**YES**	**YES**
	1	1	**YES**	**YES**	**YES**
	1.5	1.5	**YES**	**YES**	**YES**
	$IIV_T > IIV_R$				
	0.1	1	**YES**	NO	**YES**
	0.1	1.5	***YES***	NO	**YES**
	$IIV_T < IIV_R$				
	1	0.1	**YES**	**YES**	**YES**
	1.5	0.1	***YES***	**YES**	**YES**

Bold signifies that the approach passes bioequivalence. Italic and underline signify a result that changes according to the number of patients in the clinical study

Abbreviations: ABE, average bioequivalence; IIV_T and IIV_R, interindividual variability for the test and reference formulations, respectively; MPH, methylphenidate; PBE: population bioequivalence; TBE: trapezoid bioequivalence.

*Interindividual variability (IIV) Expressed as the sum of variance (ω^2) on ka_1 (first absorption constant); ka_2 (first absorption constant); F_1 (immediate release fraction of MPH) , where ω^2 is the variance of the normally distributed IIV $\eta \sim N(0, \omega^2)$ and $\omega^2_{ka1} \in \{0.05, 0.15, 0.35, 0.5\}$; $\omega^2_{ka2} \in \{0.05, 0.15, 0.35, 0.5\}$; $\omega^2_{F1} \in \{0.001, 0.3, 0.5, 0.7\}$; $\omega^2_{lag} = 0$.

Type 1 and Type 2 Errors

The type 1 and type 2 errors of ABE, PBE and TBE were evaluated through simulations of 1000 trials with a crossover and non-replicated design. To evaluate the impact of sample size, the type 1 and type 2 errors were computed separately with sample sizes of 10, 20, 40, 60, 80 and 100.

First, we computed the type 1 error for simulated trials which follow the null hypothesis of bioinequivalence. Specifically, we chose to simulate PK measures from distributions where $(\mu_T - \mu_R)^2 = 0.0498$. In keeping with the scenario-based simulations and the range observed in bioequivalence studies in Nakal et al (9), the value of σ_R^2 was fixed to 0.0225. The type 1 error was computed as the proportion of the simulated trials which reject the bioinequivalence.

Second, we computed the type 2 error for simulated trials which follow the alternative hypothesis of bioequivalence where $(\mu_T - \mu_R)^2 = 0$, $\sigma_T^2 = \sigma_R^2 = 0.0225$. The type 2 error was computed as the proportion of the simulated trials which accept the bioinequivalence. Additionally, we computed power curves by simulating trials with varying levels of $(\mu_T - \mu_R)^2 \in \{0,\ 0.01,\ 0.04,\ 0.0498,\ 0.09\}$ with $\sigma_T^2 = \sigma_R^2 = 0.0225$.

Results

Scenario-Based Simulations

For the three bioequivalence methods, five specific scenarios are chosen and tested as reported in Table 1. Each scenario is applied to a small variability ($\boldsymbol{\sigma_R^2 = 0.0225}$) and a large variability ($\boldsymbol{\sigma_R^2 = 0.1225}$). Thus, we have ten scenarios. To have more reliable conclusions, all scenarios were repeated 100 times. The results are also illustrated in Figure 2.

In Table 1, the results of ABE, PBE and TBE are presented pertaining to the CI and the percentage of all replications which conclude bioequivalence. Specifically, we report the average $90\%\ CI$ across all replications for ABE analysis, and the average upper limit of the linearized $90\%\ CI$ across all replications for PBE and TBE analysis. As well, to account for the results of each

replication, we report the probability of passing bioequivalence as the percentage of all replications which conclude bioequivalence.

The results are summarized as follows while the details are displayed in Figure 2.

- As expected, the scenarios where the **clinically acceptable limits of $(\boldsymbol{\mu_T - \mu_R})^2$ and $\boldsymbol{\sigma_T^2 - \sigma_R^2}$ are exceeded** never conclude bioequivalence (scenarios #2 and #7).
- The scenarios where **solely the acceptable limits of $\boldsymbol{\sigma_T^2 - \sigma_R^2}$ are exceeded** show cases where ABE has been criticized (scenarios #3 and #8). Indeed, ABE only considers the mean μ and does not take into account the variability σ^2. By implementing α_1 in Equation 1, TBE corrects these situations. However, although these scenarios are found in zone_{ABE}, the probability of concluding bioequivalence with ABE is null. This contradiction stems from its $90\%\ CI$'s sensitivity to sample size (Equation S2). When the sample size is large enough, $90\%\ CI$ tightens and ABE can conclude bioequivalence. Larger sample size and their results are discussed further in the next section.
- A scenario where **the limits of ABE, PBE and TBE are all respected** concludes to bioequivalence for all methods (scenario #10) with $\underline{\sigma_R^2 = 0.1225}$. With $\underline{\sigma_R^2 = 0.0225,}$ we can identify the first drawback of PBE. Indeed, due to its reference-scaled Equation S4, PBE's permissiveness depends on σ_R^2 (9). Thus, the criterion PBE is expected to be stricter when σ_R^2 is decreased. In fact, PBE's probability of concluding bioequivalence drops from 100% to 6% (scenario #10 vs #5). TBE corrects this drawback as its probability of concluding bioequivalence remains at 100% for either scenario.
- For scenarios where **the clinically acceptable limits of $(\boldsymbol{\mu_T - \mu_R})^2$ and $\boldsymbol{\sigma_T^2 - \sigma_R^2}$ are respected** (scenarios #1 and #6), we highlight cases where TBE accepts bioequivalence while ABE and PBE do not. Indeed, these scenarios do not fall inside zone_{PBE} and the null probability of passing bioequivalence with PBE is expected. Additionally, similarly to the scenarios #3 and #8, ABE does not pass bioequivalence due to a small sample size. Nonetheless, TBE still successfully concludes bioequivalence.

- For scenarios where **solely the acceptable limits of $(\boldsymbol{\mu_T - \mu_R})^2$ are exceeded**, we show the second drawback of PBE. In fact, these are cases where PBE has been criticized and deemed too permissive compared to ABE (9–11). It is clearly shown that, with $\underline{\sigma_R^2 = 0.1225}$ and $\underline{(\mu_T - \mu_R)^2 > \theta^{ABE}}$ (scenario #9), PBE is the only approach which concludes bioequivalence. Conversely, if σ_R^2 is reduced to $\underline{\sigma_R^2 = 0.0225}$ (scenario #4), PBE no longer concludes bioequivalence. TBE corrects this contradiction through θ^{TBE} and its probability of concluding bioequivalence is the same as ABE's regardless of σ_R^2.

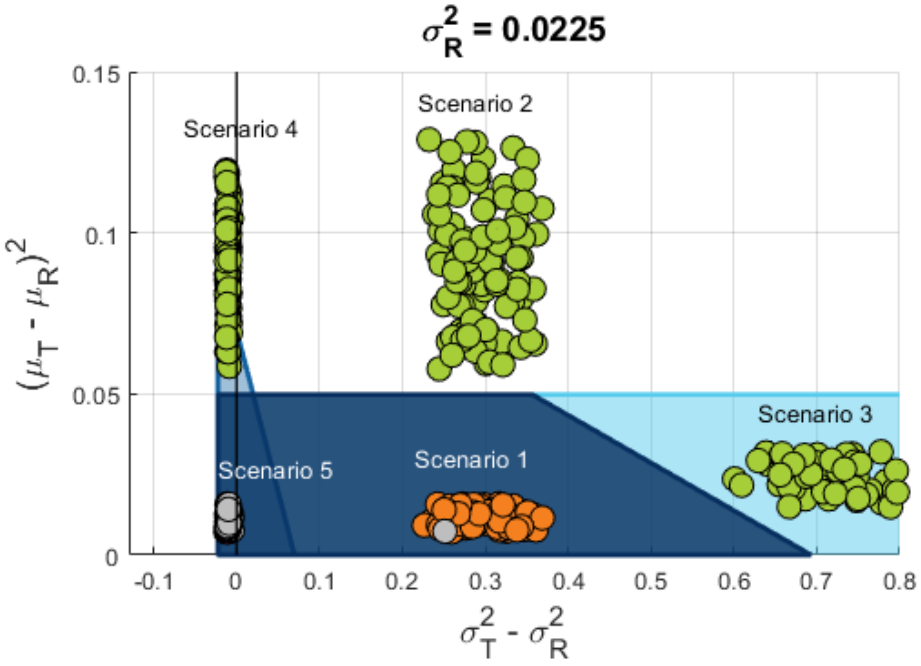
$\sigma_R^2 = 0.0225$
Scenario 4
Scenario 2
Scenario 3
Scenario 5
Scenario 1
$(\mu_T - \mu_R)^2$
$\sigma_T^2 - \sigma_R^2$

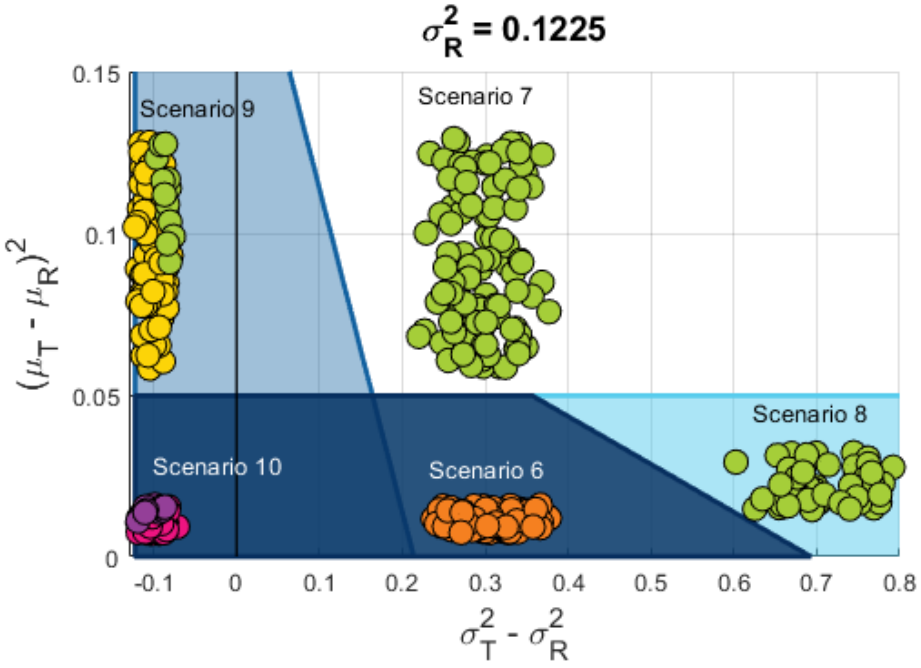
$\sigma_R^2 = 0.1225$
Scenario 9
Scenario 7
Scenario 8
Scenario 10
Scenario 6
$(\mu_T - \mu_R)^2$
$\sigma_T^2 - \sigma_R^2$

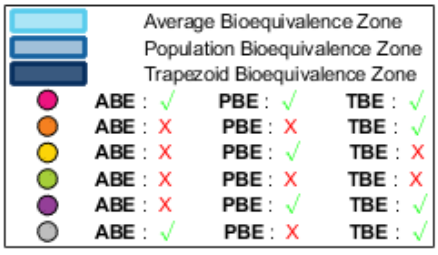
Average Bioequivalence Zone
Population Bioequivalence Zone
Trapezoid Bioequivalence Zone
ABE : √ PBE : √ TBE : √
ABE : X PBE : X TBE : √
ABE : X PBE : √ TBE : X
ABE : X PBE : X TBE : X
ABE : X PBE : √ TBE : √
ABE : √ PBE : X TBE : √

Figure 2. The conclusion of bioequivalence for average bioequivalence (ABE), population bioequivalence (PBE) and trapezoid bioequivalence (TBE) are represented as a scatter and the bioequivalence zones are illustrated as shaded areas. Each cluster is identified with a textbox referring to the scenario number in Table 1. μ_T and μ_R are the averages of bioavailability metrics on the logarithmic scale for the test and reference formulations respectively; σ_T^2 and σ_R^2 are the variances of bioavailability metrics on the logarithmic scale for the test and reference formulations respectively; √: the approach passes bioequivalence; X: the approach fails to demonstrate bioequivalence. The top panel illustrates scenarios for $\sigma_R^2 = 0.0225$ and the bottom panel illustrates scenarios for $\sigma_R^2 = 0.1225$.

Table 3. Type 1 and Type 2 error

TYPE 1 ERROR* (%)			
SAMPLE SIZE	**ABE**	**PBE**	**TBE**
10	5.4	2.3	15.6
20	4.3	0.3	7.1
40	4.8	0	2.3
60	5.4	0	0.5
80	4	0	0.1
100	4	0	0
TYPE 2 ERROR** (%)			
SAMPLE SIZE	**ABE**	**PBE**	**TBE**
10	15.2	55.1	1.2
20	0	23.1	0
40	0	7.3	0
60	0	2.2	0
80	0	0.7	0
100	0	0.6	0

*The type 1 error was computed from simulations with $(\mu_T - \mu_R)^2 = 0.0498$ and $\sigma_T^2 = \sigma_R^2 = 0.0225$.

**The type 2 error was computed from simulations with $(\mu_T - \mu_R)^2 = 0$ and $\sigma_T^2 = \sigma_R^2 = 0.0225$.

ABE: average bioequivalence; PBE: population bioequivalence; TBE: trapezoid bioequivalence; μ_T and μ_R : averages of bioavailability metrics on the logarithmic scale for the test and reference formulations respectively; σ_T^2 and σ_R^2: variances of bioavailability metrics on the logarithmic scale for the test and reference formulations respectively

Methylphenidate Model-Based Simulations

To complement the results obtained from the clinical trial data (Supplementary Material 2), we used the model-based simulations to examine various levels of IIV, which were not observed in the MPH clinical trial data. The IIV was modified for 3 pharmacokinetic parameters: the first and second absorption (ka_1 and ka_2, respectively), and the release of the external MPH fraction (F_1).

Since the typical values for all parameters did not change, the mean pharmacokinetic profile was the same for all MPH model-based simulations. Thus, this section demonstrates differences between ABE, PBE, and TBE solely when the IIV is involved. Two sample sizes were tested to represent realistic numbers of patients enrolled in the MPH clinical trial and general bioequivalence studies (11).

The total IIV for ka_1, ka_2 and F_1 and the bioequivalence results for ABE, PBE and TBE are presented in Table 2. As expected, ABE, PBE and TBE always conclude to bioequivalence when the IIV is unchanged between the test and reference formulations ($IIV_T = IIV_R$) regardless of sample size.

When $IIV_T > IIV_R$, PBE does not conclude bioequivalence in either of the two examples given in Table 2 ($IIV_T = 1$; $IIV_R = 1.5$). In fact, this situation precisely represents the restrictiveness of PBE and its lack of drug-specific flexibility. On the other hand, ABE passes bioequivalence only if $IIV_T = 1$ which can be explained with ABE's sensitivity to sample size (this property is mentioned in the Scenario-Based Simulations section in the Results). In fact, when the sample size is increased to 100 and $IIV_T = 1$, ABE passes bioequivalence. By contrast, TBE concludes to bioequivalence for both examples and both sample sizes because the IIV values respect the chosen TBE parameter used for MPH: $\theta^{TBE} = \ln^2(1.25), \alpha_1 = \ln 1.4286,\ \alpha_2 = \ln 2\ , \lambda_1 = 0.1480$ and $\lambda_2 = 0.1026$. Nonetheless, these parameter values may be changed by regulatory agencies to restrict the tolerated IIV.

Finally, when $IIV_T < IIV_R$, ABE draws once again different conclusions depending on IIV_T and sample size. If $IIV_T = 1$, ABE concludes to bioequivalence. Contrarily, if $IIV_T = 1.5$, ABE does not conclude to bioequivalence for a small sample size. However, when the sample size is increased to 100, ABE can conclude to bioequivalence. PBE and TBE always conclude to bioequivalence regardless of sample size.

Type 1 and Type 2 errors

Table 3 provides the type 1 and type 2 error for all the tested sample sizes.

When the sample size is 10, the type 1 error exceeds 5% for ABE and TBE. It is 5.4%, 2.3% and 15.6% for ABE, PBE and TBE respectively. We also note that the type 1 error with TBE is greater when the sample size is small (10 and 20 patients). For all other sample sizes, the type 1 error is below the acceptable 5% threshold and shows a satisfactory level of rejection of the null hypothesis. The type 1 error was also computed for cases where $\sigma_T^2 - \sigma_R^2 \in \{0.3, 0.7\}$ and was evaluated at 0% for all tested sample sizes (results not shown).

The Type 2 error presented in Table 3 shows that the power of TBE is greater than that of ABE and PBE for all sample sizes. Specifically, we note that the type 2 error of TBE is very low for all the sample sizes analyzed. Notably, the type 2 error with TBE is 1.2% for a sample size of 10, while it is 15.2% with ABE and 55.1% with PBE. When the sample sizes are greater than 10, the type 2 error is null for ABE and TBE while those for PBE are higher.

Figure 3 provides the power curves of ABE, PBE and TBE, explicitly the probability of concluding bioequivalence for different values of $(\mu_T - \mu_R)^2$ and samples. Amongst all simulations and sample sizes, TBE's power was higher or similar to ABE's and PBE's. Specifically, the minimal sample sizes which allow a power larger than 80% are 20, 40 and 10, respectively for ABE, PBE and TBE. We note that the power for larger sample sizes decreased as $(\mu_T - \mu_R)^2$ approaches its maximum threshold. In other words, larger sample sizes allow a more precise and accurate assessment of true BIE.

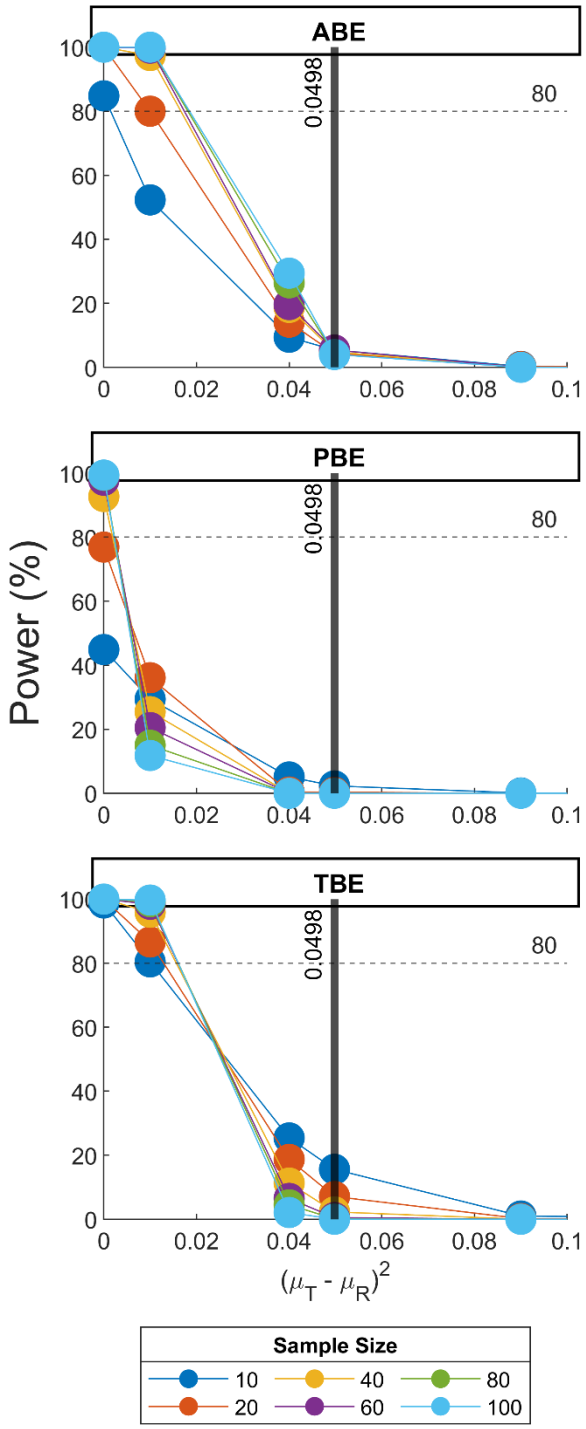

Figure 3. Power curve for $(\mu_T - \mu_R)^2 = \{0, 0.01, 0.04, 0.0498, 0.09\}$ applied to average bioequivalence (ABE), population bioequivalence (PBE) and trapezoid bioequivalence (TBE). The power of ABE, PBE and TBE were evaluated through simulations of 1000 trials with a

crossover and non-replicated design. Each simulation was applied to a sample size of 10, 20, 40, 60, 80 and 100. μ_T and μ_R are the averages of bioavailability metrics on the logarithmic scale for the test and reference formulations respectively

Discussion

Several bioequivalence methods have been proposed to solve the issues of ABE and PBE (13,18,24). As an alternative bioequivalence method, we propose the aggregate bioequivalence criterion TBE that encompasses ABE and PBE. TBE can balance the similarity in both formulations' average (μ) and variance (σ^2) of bioavailability at the same time. Moreover, this balance can be adapted to specific pharmacological characteristic through weights applied in TBE. For example, the weight of the difference of variance may be chosen larger for drugs with large IIV to ensure the best substitutability for a patient.

Table 4 summarizes TBE's appealing properties as observed from the scenario-based simulations and the MPH case studies. For the former, each scenario was chosen to demonstrate TBE's properties in various clinical settings and to compare them to ABE and PBE. We analyzed small and large σ_R^2, large mean difference between the test and reference formulation, substitutable and non- substitutable formulations according to a therapeutically defined tolerance of variability. These scenarios allowed us to identify inadequacies of ABE and PBE and to confirm TBE's strengths. Namely, we first showed that an increase in σ_R^2 did not change TBE's acceptable limits of bioequivalence. Indeed, TBE's probability of passing bioequivalence was identical whether $\sigma_R^2 = 0.0225$ or $\sigma_R^2 = 0.1225$. This was not the case for PBE, where comparable levels of $(\mu_T - \mu_R)^2$ and $(\sigma_T^2 - \sigma_R^2)$ resulted in opposite conclusions of bioequivalence depending on σ_R^2. Additionally, we showed that TBE is not overly permissive compared to ABE when $\sigma_T^2 - \sigma_R^2 < 0$, contrary to PBE. On the other hand, when $\sigma_T^2 - \sigma_R^2 > 0$, we define TBE to differ from ABE by imposing a clinically defined threshold on $\sigma_T^2 - \sigma_R^2$ and proportionally reducing the threshold on $(\mu_T - \mu_R)^2$. This property was only observed when the sample size was high enough for ABE to lead to bioequivalence (results not shown with scenario-based simulations).

We explored additional conditions of variability and sample size through a Pop-PK model of extended release MPH (19). By varying the IIV on absorption parameters and testing a larger sample size, we simulated $IIV_T = IIV_R$; $IIV_T > IIV_R$; and $IIV_T < IIV_R$ when the sample size is 40 or 100 subjects. All results concurred with the scenario-based method. We observed again PBE's increased permissiveness as we reduce IIV_T. Furthermore, as the sample size increased, we observed an agreement between results from ABE and TBE. These results complemented the scenario-based simulations and confirmed that TBE's permissiveness was only apparent and dependent on the study sample size.

An interesting feature of TBE was demonstrated in the type 2 error computations. Indeed, higher or similar power may be achieved with TBE across all sample sizes compared to ABE and PBE. Thus, while ABE supposes that there is no difference in variance between both drugs, TBE imposes an explicit restriction to $\sigma_T^2 - \sigma_R^2$ without additional cost to the type 2 errors. We note that the use of $90\%\ CI$ reduces the fixed maximum threshold of $(\mu_T - \mu_R)^2$. Namely, we find that only simulations where the sample $(\mu_T - \mu_R)^2 < 0.0365, (\mu_T - \mu_R)^2 < 0.0055\ or\ (\mu_T - \mu_R)^2 < 0.025$ were declared bioequivalent with ABE, PBE and TBE respectively. Since the $(\mu_T - \mu_R)^2$ limit of TBE is further removed from its theoretical value than in the case of ABE, future work should improve TBE's computation of $90\%\ CI$ and replace the current use of the bootstrap.

Additionally, the type 1 error is dependent upon sample size for TBE, which is contrary to statistical definitions of the type 1 error. We hypothesize that it is due to the nonparametric bootstrap in TBE's CI, which transfers its dependance on sample size to the type 1 error (25-27). The authors chose a nonparametric bootstrap to compute the TBE's CI as it does not rely on any assumptions, and it is the most accessible.

We acknowledge that the application of TBE is limited to cases where the variability has a significant impact on treatment. The example we chose in our work is MPH, whose dose individualization is challenging due to its large IIV. As well, it is known that MPH's therapeutic effect closely follows its pharmacokinetics. Thus, it is our hypothesis that controlling for variability between test and reference formulations will reduce the titration period by increasing drug substitutability.

In conclusion, the clinically inspired simulations showed TBE's superiority in a reasonable context and its potential usefulness in practice. Indeed, TBE is mathematically accessible, and its statistical analysis is not more complex than PBE. As well, a standard 2x2 crossover design is sufficient to estimate TBE. Furthermore, TBE's parameters (θ^{TBE} and α_1, α_2) permit a highly flexible approach. Although these parameters were specifically fixed to values justified for MPH in this work, they can be modified to reflect any drug's pharmacological and pharmacodynamic characteristics. For example, stricter limits can be established by regulatory agencies for narrow therapeutic drugs that require close titration (insulin, blood thinners, anticonvulsants, …). Further work on TBE should involve work on the calculation of the CI, and estimation of optimal sample size must be applied to complete work on TBE.

Table 4. Desirable properties of ABE, PBE and TBE

Properties	**ABE**	**PBE**	**TBE**
Sensitive to μ and σ^2	X	√	√
Interpreted on the normal scale	√	X	X
Stable results with different n	X	√	√
Stable results with different σ_R^2	X[a]	X[b]	√
Stable results when $\sigma_T^2 < \sigma_R^2$	√	X	√

[a] If σ_R^2 is large, bioequivalence is less permissive

[b] If σ_R^2 is large, bioequivalence is more permissive

Note: √ Signifies that the property applies to the bioequivalence method and X signifies that the property does not apply to the bioequivalence method.

Abbreviations: ABE, average bioequivalence; PBE, population bioequivalence; TBE, trapezoid bioequivalence; μ, average of the bioavailability metrics on the logarithmic scale; σ, variance of the bioavailability metrics on the logarithmic scale; σ_T^2 and σ_R^2, the variances of the bioavailability metrics on the logarithmic scale for the test and reference formulations, respectively.

References

1. U.S. Food and Drug Administration. Abbreviated New Drug Application (ANDA) [Internet]. FDA. FDA; 2019 [cited 2021 May 21]. Available from: https://www.fda.gov/drugs/types-applications/abbreviated-new-drug-application-anda

2. U.S. Food and Drug Administration. Guidance for industry. Statistical Approaches to Establishing Bioequivalence [Internet]. FDA: Rockville, MD; 2001 [cited 2020 Oct 22]. Available from: https://www.fda.gov/regulatory-information/search-fda-guidance-documents/statistical-approaches-establishing-bioequivalence

3. Sheiner LB. Bioequivalence revisited. Stat Med. 1992 Sep 30;11 (13):1777–88.

4. Hauck WW, Anderson S. Measuring switchability and prescribability: when is average bioequivalence sufficient? J Pharmacokinet Biopharm. 1994 Dec;22 (6):551–64.

5. Steinijans VW. Some Conceptual Issues in the Evaluation of Average, Population, and Individual Bioequivalence. Therapeutic Innovation & Regulatory Science. 2001;35 (3):893–9.

6. Hyslop T, Hsuan F, Holder DJ. A small sample confidence interval approach to assess individual bioequivalence. 2000;13.

7. Schall R. Assessment of Individual and Population Bioequivalence Using the Probability That Bioavailabilities are Similar. Biometrics. 1995;51 (2):615–26.

8. Endrenyi L, Hao Y. Asymmetry of the mean-variability trade-off raises questions about the model in investigations of individual bioequivalence. Int J Clin Pharmacol Ther. 1998 Aug;36 (8):450–7.

9. Nakai K, Fujita M, Tomita M. Comparison of average and population bioequivalence approach. Int J Clin Pharmacol Ther. 2002 Sep;40 (9):431–8.

10. Barrett JS, Batra V, Chow A, Cook J, Gould AL, Heller AH, et al. PhRMA perspective on population and individual bioequivalence. J Clin Pharmacol. 2000 Jun;40 (6):561–70.

11. Zariffa NM, Patterson SD. Population and individual bioequivalence: lessons from real data and simulation studies. J Clin Pharmacol. 2001 Aug;41 (8):811–22.

12. Dragalin V, Fedorov V, Patterson S, Jones B. Kullback–Leibler divergence for evaluating bioequivalence. Statistics in Medicine. 2003;22 (6):913–30.

13. Hauck WW, Chen ML, Hyslop T, Patnaik R, Schuirmann D, Williams R. Mean difference vs. variability reduction: trade-offs in aggregate measures for individual bioequivalence. FDA Individual Bioequivalence Working Group. Int J Clin Pharmacol Ther. 1996 Dec;34 (12):535–41.

14. Karalis V, Symillides M, Macheras P. Novel methods to assess bioequivalence. Expert Opinion on Drug Metabolism & Toxicology. 2011 Jan 1;7 (1):79–88.

15. Pereira LM. Bioequivalence testing by statistical shape analysis. J Pharmacokinet Pharmacodyn. 2007;34.

16. Polli JE, McLean AM. Novel Direct Curve Comparison Metrics for Bioequivalence. Pharm Res. 2001 Jun 1;18 (6):734–41.

17. Marston SA, Polli JE. Evaluation of direct curve comparison metrics applied to pharmacokinetic profiles and relative bioavailability and bioequivalence. Pharm Res. 1997 Oct;14 (10):1363–9.

18. Midha KK. Individual and Average Bioequivalence of Highly Variable Drugs and Drug Products. 1997;86 (11):5.

19. Soufsaf S, Robaey P, Bonnefois G, Nekka F, Li J. A Quantitative Comparison Approach for Methylphenidate Drug Regimens in Attention-Deficit/Hyperactivity Disorder Treatment. J Child Adolesc Psychopharmacol. 2019 Feb 4.

20. Ermer JC, Adeyi BA, Pucci ML. Pharmacokinetic variability of long-acting stimulants in the treatment of children and adults with attention-deficit hyperactivity disorder. CNS Drugs. 2010 Dec;24 (12):1009–25.

21. Yue CS, Ozdin D, Selber-Hnatiw S, Ducharme MP. Opportunities and Challenges Related to the Implementation of Model-- Based Bioequivalence Criteria. CLINICAL PHARMACOLOGY. 2019;105 (2):13.

22. Dubois A, Gsteiger S, Pigeolet E, Mentré F. Bioequivalence Tests Based on Individual Estimates Using Non-compartmental or Model-Based Analyses: Evaluation of Estimates of Sample Means and Type I Error for Different Designs.:13.

23. Mould DR, Upton RN. Basic concepts in population modelling, simulation, and model-based drug development-part 2: introduction to pharmacokinetic modelling methods. CPT Pharmacometrics Syst Pharmacol. 2013 Apr 17;2:e38.

24. Wellek S. On a reasonable disaggregate criterion of population bioequivalence admitting of resampling-free testing procedures. Stat Med. 2000 Oct 30;19 (20):2755–67.

25. Chernick MR. Bootstrap methods : a guide for practitioners and researchers. 2nd ed. Wiley-Interscience; 2008.

26. Hesterberg TC. What Teachers Should Know About the Bootstrap: Resampling in the Undergraduate Statistics Curriculum. null. 2015 Oct 2;69(4):371–86.

27. Efron Bradley, Tibshirani RJ. An introduction to the bootstrap. Chapman and Hall; 1993. Monographs on statistics and applied probability; vol 57

Supplementary material 1

Average Bioequivalence (ABE)

The ABE procedure is described in the FDA's 2001 guidance (2). The treatment effect is assessed with an ANOVA analysis (26) assuming the following linear additive mixed-effect model

$$Y_{ijkl} = \mu_k + \gamma_{ikl} + \delta_{ijk} + \varepsilon_{ijkl} \qquad \text{Equation S1.}$$

for the logarithmic transformed BE parameter $\boldsymbol{Y_{ijkl}}$ in the sequence *i* of the subject j with formulation k (R: reference; T: test) and period *l*; $\boldsymbol{\mu_k}$ is the formulation effect; $\boldsymbol{\gamma_{ikl}}$ is the fixed replicate effect; $\boldsymbol{\delta_{ijk}}$ is the random subject effect; and $\boldsymbol{\varepsilon_{ijkl}}$ is the random error term. $\boldsymbol{\varepsilon_{ijkl}}$ are assumed normally distributed : $\boldsymbol{\varepsilon_{ijkl}} \sim \boldsymbol{N}(\mathbf{0}, \boldsymbol{\sigma^2_{Wk}})$, where $\boldsymbol{\sigma^2_{Wk}}$is the within-subject variance.

First, the 90% confidence interval (CI_{90}) of the formulation difference is computed as

$$CI_{90} = \mu_T - \mu_R \pm t_{1-\alpha,n_1+n_2-2}\, \hat{\sigma}_W \sqrt{\frac{1}{2}\left(\frac{1}{n_1}+\frac{1}{n_2}\right)} \qquad \text{Equation S2.}$$

$$\hat{\sigma}_W = \sqrt{MS_{within}}$$

Where n_1 and n_2 are the number of subjects for each sequence and $MS_{within}$is the mean square error obtained from the ANOVA.

Then, CI_{90} is back transformed to its original scale and ABE is declared if the original-scaled CI_{90} is fully included within 0.8 and 1.25. Otherwise, no conclusion of ABE is established. Mathematical condition for ABE can be formulated as:

$$(\mu_T - \mu_R)^2 < (\theta^{ABE})^2 \qquad \text{Equation S3.}$$

where $\theta^{ABE} = \ln(1.25)$.

The ABE acceptance zone ($zone_{ABE}$) is illustrated in Figure 1 (a). Within $zone_{ABE}$, the test and reference formulations will be declared bioequivalent. As expected, $zone_{ABE}$ does not change with respect to $\sigma_T^2 - \sigma_R^2$ and its upper limit is fixed as $(\theta^{ABE})^2$.

Population Bioequivalence (PBE)

PBE is defined in the 2001 Guide *Statistical Approaches to Establishing Bioequivalence* as follows (2):

$$\frac{(\mu_T - \mu_R)^2 + \sigma_T^2 - \sigma_R^2}{\max\{\sigma_0^2, \sigma_R^2\}} < \theta_{moment-based}^{PBE} \qquad \text{Equation S4.}$$

where $\boldsymbol{\mu_T}$ and $\boldsymbol{\mu_R}$ are the averages, $\boldsymbol{\sigma_T^2}$ and $\boldsymbol{\sigma_R^2}$ are the associated total variability of the analyzed bioavailability metric for the test (T) and reference (R) formulations, respectively; $\boldsymbol{\sigma_0^2}$ is a constant term in variance that bounds from above the scaling factor of total variance of R (fixed as 0.04 by the FDA); and $\boldsymbol{\theta_{moment-based}^{PBE}}$ is the moment-based BE limit defined by the regulatory agency (fixed as ~1.744 by the FDA).

A simple manipulation can transform Equation S4 into:

$$(\mu_T - \mu_R)^2 + \sigma_T^2 - \sigma_R^2 - \theta_{moment-based}^{PBE} \max\{\sigma_0^2, \sigma_R^2\} < 0 \qquad \text{Equation S5.}$$

The 90% confidence interval CI_{90} of the left term of Equation S5 can be computed using the formulas specified in the FDA guidance (2). The upper limit of CI_{90} must fall below 0 to conclude PBE for the test and reference formulations. Otherwise, they cannot be deemed bioequivalent with PBE.

In accordance with Equation S4, PBE is defined by limits in $(\mu_T - \mu_R)^2$ and σ_T^2-σ_R^2. The overly permissive results from PBE arise when σ_T^2 is significantly smaller than σ_R^2. Indeed, as we define $d = \theta_{moment-based}^{PBE} \max\{\sigma_0^2, \sigma_R^2\}$, PBE passes bioequivalence when $(\mu_T - \mu_R)^2 < d - (\sigma_T^2 - \sigma_R^2)$. Thus, as $\sigma_T^2 < \sigma_R^2$, it allows a larger difference between μ_R and μ_T to conclude bioequivalence with PBE. The PBE acceptance zone ($zone_{PBE}$) is illustrated in Figure 1 (a). Within $zone_{PBE}$, the test and reference formulations will be declared bioequivalent with PBE. PBE's permissiveness is observed in Figure 1 (a) where $zone_{PBE}$ exceeds $zone_{ABE}$ when $\sigma_T^2 - \sigma_R^2 < 0$.

Supplementary References

1. U.S. Food and Drug Administration. Guidance for industry. Statistical Approaches to Establishing Bioequivalence [Internet]. FDA: Rockville, MD; 2001 [cited 2020 Oct 22]. Available from: https://www.fda.gov/regulatory-information/search-fda-guidance-documents/statistical-approaches-establishing-bioequivalence

2. Hauschke D, Steinijans V, Pigeot I. Bioequivalence studies in drug development : methods and applications [Internet]. Chichester, England ; Hoboken, NJ: Wiley,; 2007. 1 online resource (xi, 311 pages). (Statistics in practice). Available from: http://onlinelibrary.wiley.com/book/10.1002/9780470094778 Accès réservé UdeM Conditions d'utilisation: https://bib.umontreal.ca/public/bib/conditions-utilisation/conditions-utilisation-fiche_006.pdf

Supplementary Material 2

Methods: Methylphenidate Clinical Trial Data

In our previous work, concentration-time datasets of an immediate release (IR) and an extended release (ER) oral MPH formulation were presented (167). Herein, we add generics IR and ER. For the IR formulations, a randomized, double-blind, crossover study enrolled 44 adult participants aged between 18 and 35 years who were given single IR doses of 20 mg. The PK of these formulations was assessed for each patient following a single dose on Day 1, with blood samples collected at times specified in Table S1.

Table S1 - Patients demographics and clinical trial summary in methylphenidate clinical study

Subject Characteristics	**IR Dataset (N = 44)**	**ER Dataset (N = 39)**
Age (years)	25.58	28 (18 – 40)
Weight (kg)	77.40	79.7 (70.3 – 95.5)
Body Mass Index (kg/m^2)		25.9 (21.7 – 28.9)
Height (cm)	175.92	177 (162 - 198)
Sex (N, %)		
Male	44	39 (100.0)
Female	-	0 (0.0)
Race (N, %)	NA	
White	-	32 (82)
Black	-	6 (15.4)
Other	-	1 (2.6)
Concomitant Food Intake (N, %)	NA	
No (Fasting condition)	-	19 (49.7)
Yes (Fed condition)	-	20 (51.3)
Smoking status	NA	
No	-	24 (61.5)
Yes	-	15 (38.5)
Sample time	0, 0.5, 1, 1.33, 1.66, 2, 2.5, 3, 4, 6, 8, 10, 12- and 14-hours post-dose	Fasted: 0, 1, 2, 3, 4, 4.5, 5, 5.5, 6, 6.5, 7, 7.5, 8, 8.5, 9, 10, 12, 14, 16, and 24 hours post-dose Fed: 0, 1, 2, 3, 4, 5, 5.5, 6, 6.5, 7, 7.5, 8, 8.5, 9, 9.5, 10, 10.5, 12, 14, 16, and 24 hours post-dose
Bioavailability metrics	C_{max} and AUC_{inf}	Fasted : C_{max}, AUC_{inf}, AUC_{0-3}, AUC_{3-7} and AUC_{7-12} Fed : C_{max}, AUC_{inf}, AUC_{0-4}, AUC_{4-8} and AUC_{8-12} (2)

IR: Immediate Release; ER: Extended Release; C_{max}: maximum plasma concentration; AUC_{inf}: area under the curve 0-inf; AUC_{i-j} : area under the curve *i-j* hours.

In parallel to the IR formulations, we were able to analyze the concentration-time datasets of ER oral formulations. A randomized, double-blind, crossover study enrolled 39 adult patients aged between 18 and 40 years. Each patient was given single ER oral doses of 54 mg. During the 24 hours post-dose, two sets of blood sampling times were used according to concomitant food intake. The sampling times and population demographic data are summarized in Table S1. The concentration-time profiles for all formulations are illustrated in Figure S1.

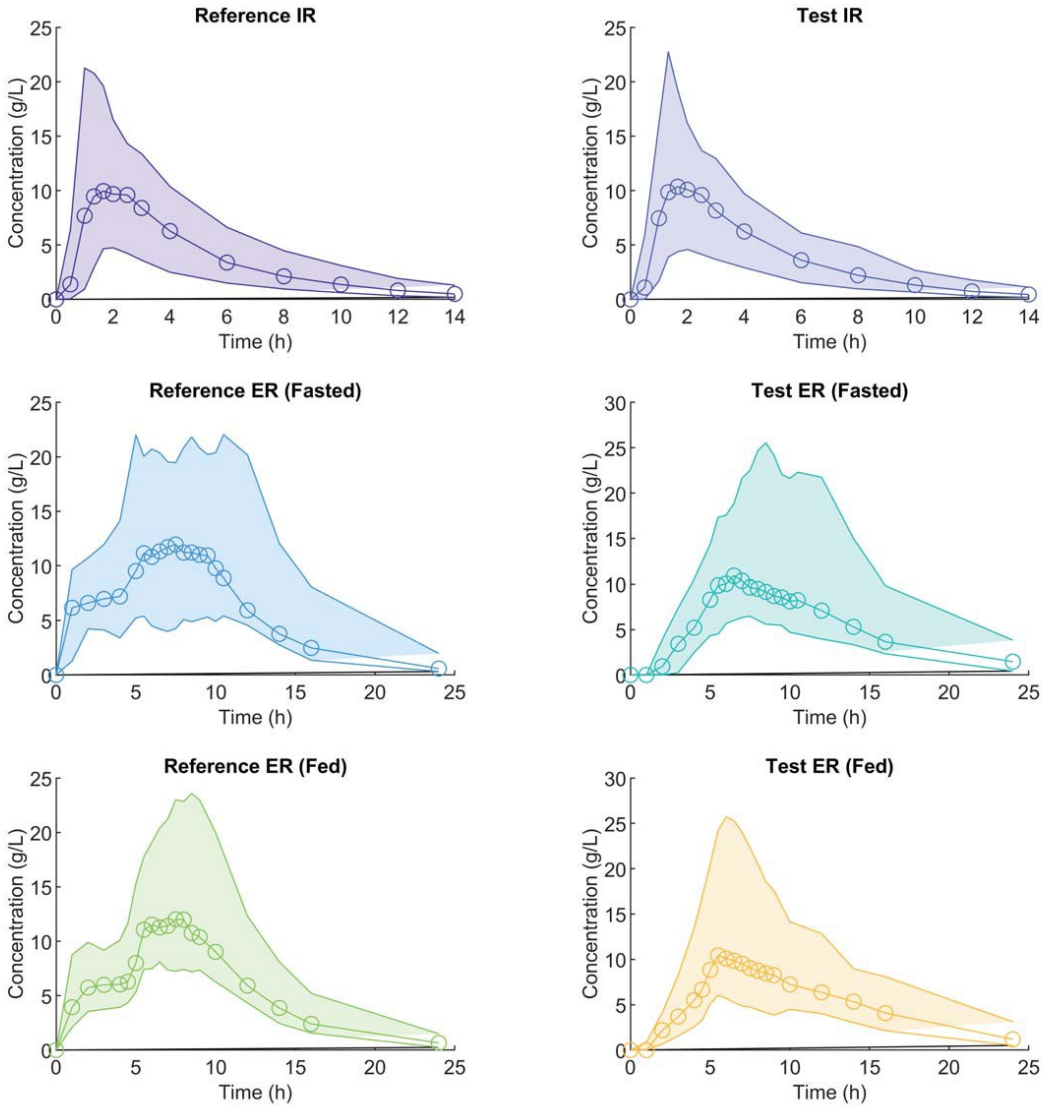

Figure S1 - Concentration-time profiles for 4 methylphenidate formulations. The scatter represents the median concentrations for each sample time. The shaded area is delimited by the minimum and maximum concentrations for each sample time. IR: Immediate Release; ER: Extended Release.

The IR and ER formulations are currently sold and commercialized as bioequivalent according to Health Canada's ABE criteria: the IC_{90} of AUC_{inf} ratios and the point estimate of C_{max} ratios fall between 0.8 and 1.25.

The statistical analysis was performed using the bioavailability metrics chosen in accordance with FDA's draft guidance on MPH (180). Specifically, bioequivalence of IR formulations are applied to C_{max} and AUC_{inf}, while ER formulations require an evaluation of C_{max}, AUC_{inf}, $AUC_{0\text{-}T1}$, $AUC_{T1\text{-}T2}$ and $AUC_{T2\text{-}T3}$ (180). When ER MPH is taken with a concomitant food intake (fed), T1=4h, T2=8h and T3=12h. Otherwise (fasted), T1=3h, T2=7h and T3=12h.

TBE parameters were chosen just as in the Scenario-Based Simulations section in the Methods.

Results: Methylphenidate Clinical Trial Data

ABE, PBE and TBE results applied to MPH clinical trial data (IR and ER formulations) are presented in Table S2.

As projected, all formulations are shown to be bioequivalent with all three methods for AUC_{inf} and C_{max}. Thus, both IR formulations are concluded to be bioequivalent.

The ER results vary according to the BE metric and concomitant food intake. When patients have taken the ER formulations with food, $AUC_{0\text{-}3}$ is the only BE metric that is not similar between

the two formulations. These results are supported by the PK profiles in Figure S1. Indeed, there is a notable difference in the shape of the curve in the first hour post-dose.

When the ER formulations are taken fasting, the PK profiles differ from 0-4h as well as 8-12h post-dose, and at C_{max}, as observed in Figure S1. Thus, ABE, PBE and TBE agree and do not conclude to bioequivalence with AUC_{0-4}, AUC_{8-12} and C_{max}.

The results for AUC_{4-8} of the fasted ER formulations are the only ones where ABE, PBE and TBE draw different conclusions. Indeed, PBE does not conclude bioequivalence and it is in contradiction with ABE and TBE. This situation shows that all BE methods can conclude differently on real data as well as scenario-based simulations. However, as the MPH data are limited, it is not possible to observe other contradictions between ABE, PBE and TBE. Therefore, it is necessary to explore simulations based on this clinical trial data. The results of these MPH simulations are presented in section 3.3 of the paper.

Table S2 - Results for The Methylphenidate Clinical Trial Data

MPH formulation	*BE metric*	ABE	PBE	TBE
		CI_{90}	$upper\ CI_{90}$	$upper\ CI_{90}$
Immediate Release	C_{max}	**96.5-105.2**	**-0.0497**	**-0.0497**
	AUC_{inf}	**96.8-101.9**	**-0.1098**	**-0.0497**
Extended Release (Fed)	C_{max}	**90.0-104.2**	**-0.1918**	**-0.0487**
	AUC_{inf}	**96.7-105.5**	**-0.1555**	**-0.0497**

	AUC_{0-3}	25.1-37.6	1.4994	1.7404
	AUC_{3-7}	**85.4-104.1**	**-0.2115**	**-0.0431**
	AUC_{7-12}	**87.6-99.1**	**-0.1655**	**-0.0403**
Extended Release (Fasted)	C_{max}	76.7-92.4	0.2563	0.0084
	AUC_{inf}	**91.2-99.7**	**-0.0048**	**-0.0455**
	AUC_{0-4}	26.5-37.3	4.3141	1.7046
	AUC_{4-8}	**81.4-100.4**	0.1606	**-0.0299**
	AUC_{8-12}	73.9-87.6	0.2785	0.0396

Values in **bold** signify that the approach passes bioequivalence.

ABE: average bioequivalence; PBE: population bioequivalence; TBE: trapezoid bioequivalence; CI_{90}: 90% confidence interval; C_{max}: maximum plasma concentration; AUC_{inf}: area under the curve 0-inf; AUC_{i-j} : area under the curve *i-j* hours.

Supplementary References: Methylphenidate Clinical Trial Data

1. Soufsaf S, Robaey P, Bonnefois G, Nekka F, Li J. A Quantitative Comparison Approach for Methylphenidate Drug Regimens in Attention-Deficit/Hyperactivity Disorder Treatment. J Child Adolesc Psychopharmacol. 2019 Feb 4;

2. U.S. Food and Drug Administration. Draft Guidance on Methylphenidate [Internet]. 2018. Available from: https://www.accessdata.fda.gov/drugsatfda_docs/psg/Methylphenidate_draft_Orally%20disintegrating%20tab%20ER_RLD%20205489_RC07-18.pdf

Chapitre 5 — An exploratory analysis of the performance of methylphenidate regimens based on a PKPD model of dopamine and norepinephrine transporter occupancy

Sara Soufsaf, M.Sc.[1], Philippe Robaey,M.D., Ph.D.[2], Fahima Nekka, Ph.D.[1]

[1] Université de Montréal, Montréal, Québec, Canada

[2]University of Ottawa, Ottawa, Ontario, Canada

Préambule

Le travail du chapitre précédent se concentre sur les médicaments ayant une grande variabilité interindividuelle en PK, comme le MPH qui a été utilisé comme exemple pour concrétiser la méthode proposée. Le travail précédent se limite donc à la PK du MPH. Or, selon plusieurs études, la PK et la PD du MPH ne semble pas être reliées par une relation directe puisqu'une tolérance aigüe se développe au courant de la journée. Cette relation a été modélisée dans plusieurs modèles de population où la PD du MPH est mesurée par les échelles de résultats cliniques et la tolérance aigüe est intégrée par l'usage d'un EC_{50} dépendant du temps.

D'autres études ont quantifié la PD du MPH par l'occupation de transporteurs, mesurée grâce à l'imagerie PET. Ces études ont analysé l'occupation des DAT en fonction de la concentration plasmatique du MPH alors qu'une seule étude a quantifié l'occupation des NET par le MPH. Parmi toutes ces études, aucune n'a exploré la présence de tolérance aigüe observée au niveau des transporteurs.

Ainsi, l'objectif de ce chapitre est de présenter un modèle rassemblant la PK et la PD du MPH en considérant l'occupation des DAT et NET. Ce modèle a ensuite été utilisé pour calculer la performance de différents régimes de MPH. Les résultats pointent vers la présence d'une tolérance aigüe observée dans les DAT. Elle est manifestée par un taux d'occupation des DAT qui diminue en après-midi, malgré des niveaux de concentrations plasmatiques similaires.

Cet article a été publié dans le journal «Journal of Pharmacokinetics and Pharmacodynamics» (219).

Graphical Abstract

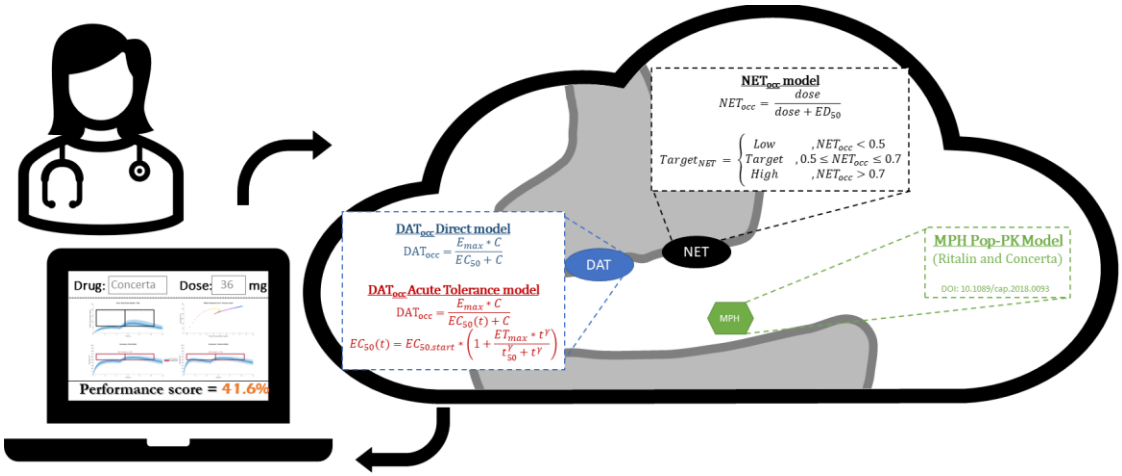

Abstract

Methylphenidate (MPH) is a psychostimulant which inhibits the uptake of dopamine and norepinephrine transporters, DAT and NET, and is mostly used to treat Attention Deficit/Hyperactivity Disorder. The current dose optimization is done through titration, a cumbersome approach for patients.

To assess the therapeutic performance of MPH regimens, we introduce an *in silico* framework composed of (i) a population pharmacokinetic model of MPH, (ii) a pharmacodynamic (PD) model of DAT and NET occupancy, (iii) a therapeutic box delimited by time and DAT occupancy, and (iv) a performance score computation. DAT occupancy data was digitized (n=152) and described with Emax models. NET occupancy was described with a KPD model. We used this integrative framework to simulate the performance of extended-release (18-99mg) and *tid* MPH regimens (25-40mg).

Early blood samples of MPH seem to lead to higher DAT occupancy, consistent with an acute tolerance observed in clinical rating scales. An Emax model with a time-dependent tolerance was fitted to available data to assess the observed clockwise hysteresis. Peak performance is observed at 63mg.

While our analysis does not deny the existence of an acute tolerance, data precision in terms of formulation and sampling times does not allow a definite confirmation of this phenomenon. This work justifies the need for a more systematic collection of DAT and NET occupancy data to further investigate the presence of acute tolerance and assess the impact of low MPH doses on its efficacy.

Keywords: methylphenidate, DAT occupancy, NET occupancy, acute tolerance

Introduction

Methylphenidate (MPH) is a psychostimulant commonly used for the treatment of Attention-Deficit/Hyperactivity Disorder (ADHD) symptoms [1–4]. While MPH has been proven to be both efficacious and safe for patients with ADHD [5–8], much work is still needed for its dosing optimization. The currently recommended approach to find a patient's optimal dose is to increase the doses by steps of 1-2 weeks until no more improvement is observed or adverse events occur, whichever comes first [9–11].

This process proves to be cumbersome to the patients and a proposed solution is the use of predictor-based algorithms to aid in dose individualization. In a previous work, we have developed endpoints based on pharmacokinetic (PK) to compare the efficacy of various MPH treatments [12, 13]. This algorithm was based on the supposition that the efficacy of some MPH regimens is closely correlated to its PK [14]. This allowed us to use the MPH PK as a surrogate for its effect.

Yet, it was observed that stable concentrations of MPH throughout the day were associated with lower efficacy compared to increasing concentrations of MPH [14–18]. Indeed, an acute tolerance

to MPH has been proposed to explain that there is a lower efficacy of MPH in the afternoon compared to the early hours post-dose, despite similar levels of plasma concentration [15–18].

It is believed that this acute tolerance is developed to counter the increase of extracellular dopamine (DA) levels [19, 20] caused by MPH's inhibition of DA and norepinephrine transporters (DAT and NET) [1]. The acute tolerance to MPH may be caused by the internalization of these transporters [15, 21], which further complicates the relationship between the PK and pharmacodynamic (PD) of MPH.

Previous PKPD studies of patients' behavioral manifestation of ADHD have accounted for this observed acute tolerance, using clinical rating scales [16, 18, 22–24]. However, to our knowledge, relating this acute tolerance to neurotransmitter-related endpoints and MPH's mechanism of action was never assessed before. The subject is however still a highly topical issue, with a recent review addressing acute and chronic tolerance to stimulant medication in ADHD [25]. It is important to work upstream and consider PD endpoints that characterize the time course of MPH effect and quantify its target binding (i.e. to DAT and NET). Indeed, this mechanistic approach allows an exploration of (i) each transporter's involvement in the efficacy of MPH and (ii) an objective and mechanistic rationale for the acute tolerance to MPH upstream of behavioral effects which may be further confounded by environmental factors.

Several DA-related changes were monitored and assessed in MPH studies to be used as objective PD endpoints. These include extracellular levels of DA in the striatum or prefrontal cortex [26], DA uptake and DAT levels [27], or DAT and D2 receptor binding in the rat striatum [28]. Considering that ADHD pathophysiology and MPH's mechanism of action mainly revolve around the blockade of DAT and NET, we here choose to focus on DAT occupancy (DATocc) and NET occupancy (NETocc).

While many studies have assessed the relationship between DATocc and MPH doses [29–35], only one published PKPD model has presented a mathematical model for its quantification [36]. This study measured extracellular DA levels in rats following an intraperitoneal administration of MPH and the authors calculated DATocc using their PKPD model. Although this model accounted both for plasma and effect site concentrations (cerebrospinal fluid), DATocc was not a measured

outcome. Moreover, the model parameters stem from an analysis of non-human data. Thus, a PKPD model based on DATocc measured in humans is needed.

Furthermore, the studies mentioned above do not take into account the NETocc despite the reported MPH's higher affinity for NET than DAT [37, 38]. To our knowledge, no PKPD model involving NETocc is available in the literature nor is there a framework that guides dosing of MPH based on NETocc. As the cognitive functions associated with DA can be differentiated from those associated with NE, it is important to consider both transporters when assessing the performance of MPH regimens. Low doses of MPH increase dopamine (DA) and norepinephrine (NE) in the prefrontal cortex more than in subcortical regions [38–40] and preferentially improve cognitive processing in the prefrontal cortex, such as executive functions, compared to other functions subtended by other structures, such as motor learning [41–44]. This increase in prefrontal cortex sensitivity to stimulants probably implies a role for NET in DA reuptake in the prefrontal cortex where DAT is scarcer. With MPH's higher affinity for NET, one could argue that a consideration for NETocc would allow the tailoring of MPH dosage according to the ADHD deficits.

Thus, we propose a quantitative evaluation of the therapeutic performance of MPH regimen based on a PKPD framework composed of (i) population PK (Pop-PK) models of MPH, (ii) PD models of DATocc and NETocc, (iii) a therapeutic box delimited by time and DATocc, and (iv) a performance score computation based on therapeutic indicators. In addition, here we perform an exploratory study of the acute tolerance of DATocc. Finally, we test whether currently available data are sufficient to base therapeutic performance indices on DAT and NET occupancy and make recommendations for future research.

Methods

Each element of our PKPD framework is described in further sections. The Pop-PK models of MPH used in this work were previously published in [12]. The PK models used for Ritalin and Concerta are one-compartment models with first-order input and first-order elimination [12]. Specifically, for Concerta, two parallel first-order absorptions are used [12]. Only the Concerta model involves a covariate (concomitant food on the second first-order absorption) [12]. In this work, we

simulated PK profiles at a fasted state for simplification. We refer the reader to the original manuscript for a description of the PK models.

PKPD Model

Data

Data of DAT_{occ} and dexmethylphenidate (d-MPH) plasma concentrations following an oral dose of MPH were extracted using WebPlotDigitizer from [30, 33, 34, 35]. The data is shown in Figure 1. This dataset contains 152 sample points with immediate release (IR) or extended release (ER) doses ranging from 5mg to 90mg (Table 1). In total, 58 healthy adults were included in these studies.

While we were able to digitally extract the DAT_{occ} and the plasma concentration, it was not possible to obtain precise information regarding all sample times. If a concentration-time graphic was published, it was estimated graphically. Otherwise, the sample time was estimated through an appropriate PK model according to the MPH formulation (IR or ER; single or dual first-order absorption). Among the 152 samples, there were 45 samples from [34] where the sample time could not be estimated due to insufficient precision. As well, data from [30] was excluded from the analysis of acute tolerance since we could not precisely distinguish the sampling times with sufficient accuracy. Indeed, these sampling times fall within a key interval for the estimation of the acute tolerance model parameters (1-3h post-dose). Even with this exclusion, the dataset still contained IR data points from [33], so that the analysis still benefited from two formulations (IR and ER). The final dataset contained 95 samples.

In all studies, the DAT_{occ} was measured with positron emission tomography (PET) imaging and computed using the binding potential (BP) following an administration of MPH (BP_{MPH}) and an administration of placebo ($BP_{placebo}$), as shown in (Equation 1). The DAT_{occ} is thus computed as a difference from placebo.

$$DAT_{Occupancy} = \frac{BP_{placebo} - BP_{MPH}}{BP_{placebo}} * 100 \qquad (1)$$

As DAT occupancy following MPH administration has been extensively studied, the extracted data was rich enough to fit a PKPD model describing DAT_{occ} as a function of MPH plasma concentration using NONMEM VII (VERSION 7.4.2, ICON, Dublin).

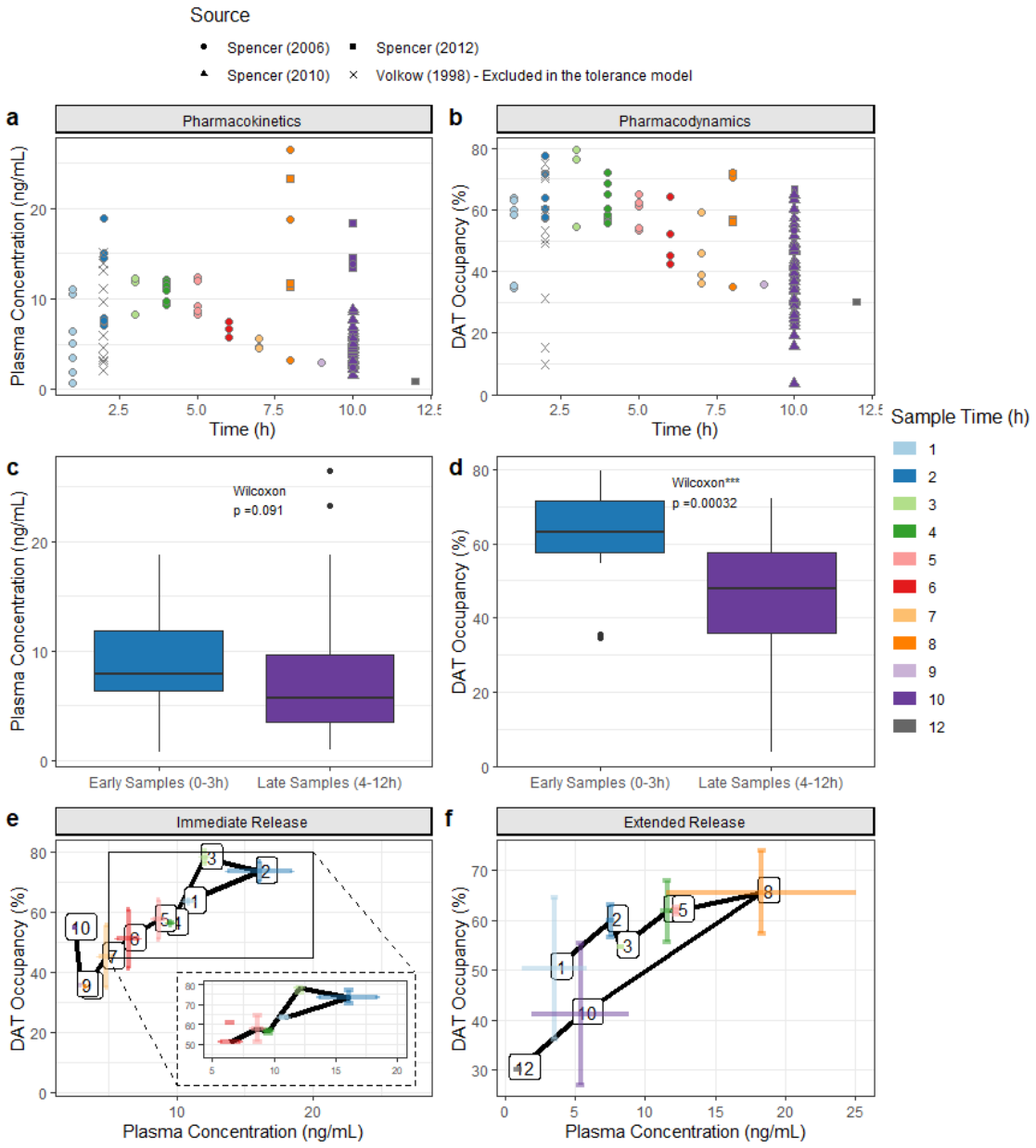

Figure 1. d-MPH plasma concentration and DAT occupancy of the digitally extracted data from [33, 30, 34, 35]. Each color in the scatter corresponds to a different sample time and each shape of the scatter represents the reference. Panels A and B show the plasma concentration and DAT_{occ} as a function of time, respectively. Panels C and D show the plasma concentration and DAT_{occ} as a function of early and late sample times, respectively. Panels E and F show the DAT_{occ} as a function of plasma concentration for immediate-release and extended-release, respectively. The black line connects the average DAT_{occ} for each

nominal sample time, which is written in boxes along the curve. In panels E and F, each sample time is drawn with error bars (± standard deviation) for the DAT_{occ} and plasma concentration. The data from [30] was not considered in the computation of the average black curve

Table 1. Source of the DAT_{occ} extracted data and description of each study. IR: Immediate release, ER: Extended release, DBDS: Diffucaps bead-delivery system, OROS: osmotically controlled-release oral delivery system, SODAS: osmotically controlled-release oral delivery system.

Dose	Formulation of MPH	Sample Time for PK (h)	Sample Time for PET (h)	Study Sample Size	Number of Data Points Extracted	Source
5mg, 10mg, 20mg, 40mg and 60mg	IR (assumed[a])	1,2,3h post-dose	2h post-dose	7	12	[30]
40mg (IR) and 90mg (ER)	IR and ER	hourly from 0-10h post-dose	1,3,5,7h post-dose	12	46	[33]
40mg (DBDS) and 36mg (OROS)	ER	9,10,11h post-dose	10h post-dose	21	42	[35]
20mg, 30mg and 40mg	SODAS	1 hour prior to scanning, at the hour of scanning and at the completion of the scan (the scan lasted 1h)	1,8,10,12h post-dose (20 mg and 30 mg), or 1,8,10,14h (40 mg) post-dose	18	52	[34]

[a]The formulation is not precisely mentioned in the paper. We assumed it is an immediate release based on the date of publication.

DAT_{occ} Direct PKPD Model

Based on an exploratory data analysis, we fitted two direct PKPD models: Michaelis-Menten (MM) and a Hill curve, represented by Equation 2 and Equation 3, respectively. Data assembly and plotting in this work was done with R (version 4.1.2, R Core Team, Vienna). The models were compared based on multiple factors: the estimates and the standard error of parameter estimates, AIC, and residuals plots. The models were also internally validated using a visual

predictive check (VPC) and a bootstrap analysis using Perl-speaks-NONMEM (version 4.9.0, Karlsson et al, Uppsala). The bootstrap analysis was done with 1000 samples with replacement and without stratification.

$$DAT_{occupancy,Michaelis-Menten} = \frac{E_{max} C_{plasma}}{EC_{50} + C_{plasma}} \qquad (2)$$

$$DAT_{occupancy,Hill} = \frac{E_{max} C_{plasma}^{\gamma}}{EC_{50}^{\gamma} + C_{plasma}^{\gamma}} \qquad (3)$$

whereE_{max} is the maximal DAT_{occ}, C_{plasma} is the plasma concentration of the drug, EC_{50} is the concentration producing half of E_{max}, and γ is the Hill coefficient.

DAT_{occ} Tolerance PKPD Model

Several tolerance models are used in the literature to characterize time-dependent attenuation of drug effect, depending on the intended purpose and the data in hand. For example, to model acute tolerance to nicotine, Porchet proposed a PKPD model composed of both an effect compartment and a tolerance compartment [45]. In the context of MPH, another tolerance model was proposed to describe the acute tolerance observed in clinical rating scales after MPH oral administration [24, 46]. This tolerance model assesses the clinical rating scales in terms of MPH plasma concentrations and assumes a time-dependent acute tolerance through a change of EC_{50} in function of time. This type of model is most appropriate for drugs where the hypothesized mechanistic underlying the acute tolerance is the internalization of transporters [15,21,53]. We adopt this tolerance model and apply it to DAT_{occ} instead, as the following:

$$DAT_{occ} = \frac{E_{max} * C_{plasma}}{EC_{50}(t) + C_{plasma}} \qquad (4)$$

$$EC_{50}(t) = EC_{50,start} * \left(1 + \frac{ET_{max} * t^{\gamma}}{t_{50}^{\gamma} + t^{\gamma}}\right) \qquad (5)$$

, whereE_{max} is the maximal DAT_{occ}, C_{plasma} is the plasma concentration of the drug, t is the time post-dose, $EC_{50}(t)$ is the concentration producing half of E_{max} as a function of t, $EC_{50,start}$ is the estimated EC_{50} at t=0 ($EC_{50}(t = 0)$), ET_{max} is fixed to 1 [24], t_{50} is the time observed for half of

the increase in EC_{50}, and γ is the steepness parameter representing the rate of change in $EC_{50}(t)$.

NET_{occ} KPD Model

Due to limited imaging studies for NET, only a published KPD equation could be used to predict NET_{occ} [37]. In this study, 11 healthy subjects received oral doses of MPH ranging from 2.5 to 40mg. The NET_{occ} was measured by PET imaging 75 min and 195 min post-dose and was computed using the BP. The authors computed the average NET_{occ} over these sample times and presented only a static outcome. It is expressed as in (Equation 6), where the dose at which 50% of NET are occupied (ED_{50}) was estimated to be 0.14mg/kg. In this paper, the NET_{occ} will be scaled from 0.0-1.0 rather than a percentage. This will avoid confusion with DAT_{occ} and its performance score, which are both expressed as a percentage (0-100%).

$$NET_{Occ} = \frac{dose}{dose + ED_{50}} \qquad (6)$$

Performance Score

Drug Regimen Performance Applied to DAT_{occ}

A numerical score of performance for a given MPH regimen was computed using therapeutic indicators and a time-DAT_{occ} plane defining a therapeutic box (TB). The TB was adapted from [13]. In a previous work, different concentration zones were set up in reference to values that indicate the minimum effective concentration and the maximum tolerated concentration. This window was further delimited by time intervals corresponding to specific daily activities, defining thus a TB. To relay a performance based on PD endpoints, we here substitute the MPH concentration by a DAT_{occ}. Keeping with the original work, we translate the lower and upper concentration bounds to their DAT_{occ} counterparts. Hence, 50% and 70% DAT_{occ} were used to refer to the corresponding plasma concentrations previously adopted [13, 30]. In terms of temporal information that accounts for time, school/work activities, we define a time period that is between 8:00 am and 6:00 pm, during which the maximum benefit of MPH's therapeutic effect is expected. A further

division of time can be done (at 1:00 pm here) to allow a separate evaluation of the results between the morning and afternoon.

The performance score is computed with three therapeutic indicators (TI), namely time-based and DAT_{occ}-based, in a similar way to what we previously introduced [13]. To make the current paper self-contained, we here give a brief summary of each TI:

- **TI_{Eff}** is the mean percentage of time spent by the DAT_{occ} profiles within a TB.
- **TI_{R}** is the proportion of simulated subjects classified as responders (R), i.e. if 80% of the DAT_{occ} profile remains within the TB.
- **TI_{RCE}** is computed as the mean of the relative differences between the local maximum peak concentrations and the trough concentrations that precede the next dose compared to these peaks. It takes into account the waxing and waning of peaks and troughs following each administration of MPH, dubbed the Roller Coaster Effect (RCE) in [13]. For a fair comparison between *qd* doses of ER formulations and *tid* regimens, we chose to adapt the definition of TI_{RCE}. In this paper, we compute TI_{RCE} for all regimens rather than only for regimens involving multiple administrations.

The performance score of a given dosing regimen is computed as in (Equation 7), where each TI is affected an importance through a weight chosen by the clinician ($0\% < w_j < 100\%$).

$$PerformanceScore(Regimen) = \sum_{i \in I} w_i \begin{cases} \dfrac{\max\left(TI_i(.)\right) - TI_i(\text{ Regimen })}{\max\left(TI_i(.)\right) - \min\left(TI_i(.)\right)} & \text{for minimisation} \\ \dfrac{\text{TI}_\text{i}(\text{Regimen}) - \min\left(TI_i(.)\right)}{\max\left(TI_i(.)\right) - \min\left(TI_i(.)\right)} & \text{for maximisation} \end{cases} \quad (7)$$

where TI is the therapeutic indicator, i refers to the TI, and w_i is the weight attributed to TI_i based on a practitioner's experience, with $\sum w_i = 1$ [13]. For all DAT_{occ} profiles, $\max\left(TI_i(.)\right)$ is the maximal value of TI_i and $\min\left(TI_i(.)\right)$ is the minimal value of TI_i. Among the above-mentioned TIs, TI_{Eff} and TI_R are to be maximized while TI_{RCE} is to be minimized. In this work, $w_{Eff}=w_R=w_{RCE}=1/3$.

Drug Regimen Performance Applied to NETocc

To describe the performance of MPH in terms of NET_{occ}, we use the same occupancy limits as the TB defined in the previous section for DAT_{occ}, namely a lower target of 0.5 and an upper target of 0.7. While DAT_{occ} benefits from a PKPD model and can be simulated as a time-varying endpoint, the NET_{occ} is simulated as a static endpoint from the KPD equation [37]. Namely, each total daily dose of MPH is associated with a unique NET_{occ}. Therefore, we define NET_{occ} performance by a qualitative categorical indicator (i) if the NET_{occ} is below 0.5, $Performance_{NET} = Low$, (ii) if it falls between 0.5-0.7, $Performance_{NET} = Target$, (iii) if it is higher than 0.7, $Performance_{NET} = High$.

Simulations

To illustrate our performance evaluation methodology, we will consider several aspects of the proposed PKPD model and the corresponding performance scores.

First, *qd* doses of Concerta (MPH ER) (18-99mg) were simulated to compare the PK performance, the PD performance with the direct model and the PD performance with the tolerance model. This investigation also allowed specifically the assessment of low doses of MPH per the studies of [41–44], and the exploration of the low doses' differentiated impact on NET_{occ} vs DAT_{occ}. Each dose of Concerta is given at 7:30 am, in accordance with the first timing mentioned in [13] (7:30 am, 9:30 am and 12:30 pm).

Second, the acute tolerance was illustrated with *tid* regimen simulations of Ritalin (MPH IR). The timing of each dose was taken from the NIMH Collaborative Multisite Multimodal Treatment study of Children with ADHD (MTA study) [10] (7:00 am, 11:00 am, 3:00 pm) and from the optimal dosing for a *tid* MPH regimen in [13] (7:30 am, 9:30 am and 12:30 pm). Moreover, the doses for each administration were chosen to reflect therapeutic total daily doses taken by adult patients. Thus, we simulated total daily doses (TDD) ranging from 25-40mg, where the third dose was augmented by 5mg increments to illustrate the impact of acute tolerance on DAT_{occ}. Indeed, an increase in the afternoon dose should impact the PD performance simulated with the tolerance model as it is the only model which allows a decrease in DAT_{occ} with time.

Each simulation was based on 1000 adult patients of 70kg. We did not assume an impact of food intake on PK and only inter-individual variability in PK was taken into account. The residual variability in PD was ignored because it was indistinguishable from the inter-individual variability (due to the limitations of the data explained above). The variability in performance scores is consequently purely reflective of PK inter-individual variability.

Results

DAT_{occ} Direct and Tolerance Models

Figure 1 depicts the PK and PD of MPH. Panels A and B show the digitally extracted MPH plasma concentration and DAT_{occ} as a function of time. We note that samples at 10h post-dose span across a large range of plasma concentration and DAT_{occ}. Indeed, despite samples times reported from 9-11h in [35] (Table 1), it was not possible to distinguish the data from each sample time separately. Thus, it was fixed as 10h post-dose and this explains the large span of values for this sample time.

In Figure 1, panels C and D depict, respectively, MPH plasma concentration and DAT_{occ} for early and late sample times. We note that, while plasma concentrations are similar between early samples (0-3h post-dose) and late samples (4-12h post-dose), the DAT_{occ} is statistically different for these time frames (Wilcoxon rank sum test, $p<0.001$). These results suggest the presence of an acute tolerance that may develop during the day.

Panels E and F of Figure 1 show DAT_{occ} in terms of MPH plasma concentration for the IR and ER MPH. The IR plot seems to illustrate a counter-clockwise hysteresis. However, it must be noted that the hysteresis is only based on 7 samples. Thus, we cannot justify considering it in our analysis.

In panel F of Figure 1, we notice that for similar plasma concentrations, DAT_{occ} is higher for early sample times compared to late sample times, in accordance with the boxplots in panels C and D of Figure 1. This is in line with observational studies that report existence of hysteresis associated with an acute tolerance (tachyphylaxis) in DAT_{occ} [15–17].

Although some ER formulations are manufactured with increasing concentrations throughout the day to compensate for acute tolerance to MPH, the average PK profiles of the ER drugs used in our analysis instead appear to have constant concentrations between 6-11h post-dose (data not shown here; see source articles [30, 33–35]). This explains why acute tolerance can be detected despite the fact that 76% of the data analyzed are from ER. With regards to the results above, we considered both a direct and a tolerance PKPD model for DAT_{occ}.

Based on standard error of parameter estimates, AIC, plots of residuals and keeping with the principle of parsimony, the direct MM model provided a better fit to the data compared to the direct Hill model. Its parameter estimates are presented in Table 2. The extracted data and model fits are shown in panel A of Figure 2 and the model output files are presented in the supplementary information S3.

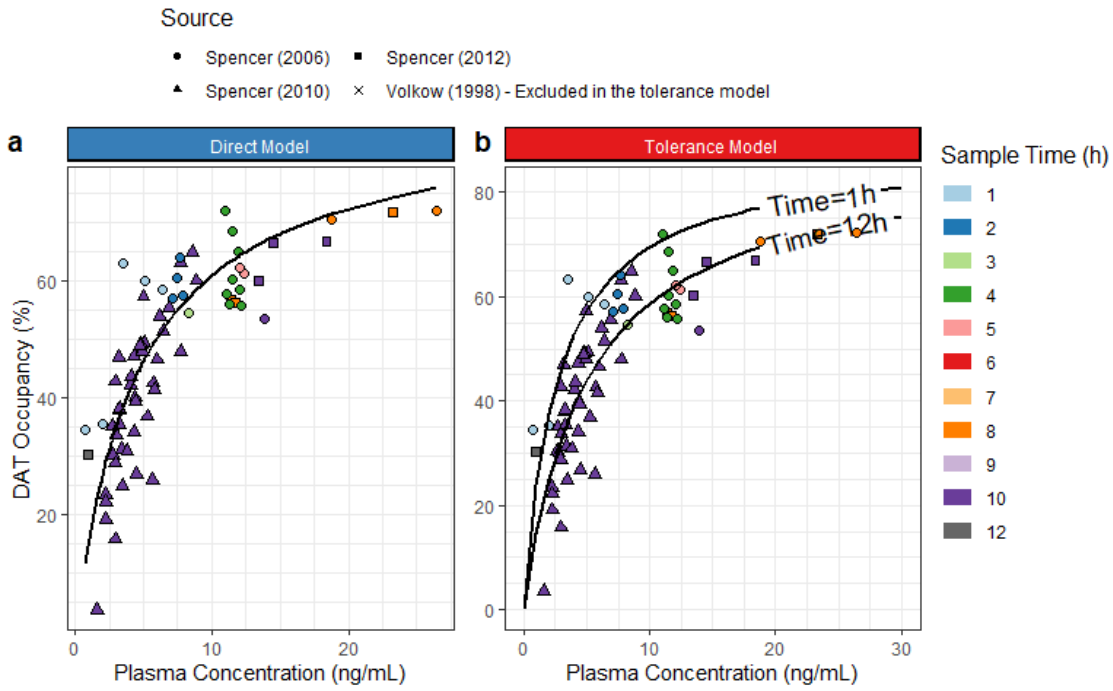

Figure 2. DAT occupancy and d-MPH plasma concentration of the digitally extracted data from [30, 33, 34, 35]. Each color in the scatter corresponds to a different sample time. The direct model is the MM model. The black lines show the model predictions. Due to the dependance of EC_{50} on time for the tolerance model, model predictions are shown for two examples of sample times (at 1h and 12h post-dose)

The parameter estimates of the tolerance model are also presented in Table 2. In accordance with [24] and for a better fit, ET_{max} was not estimated and fixed to 1. As well, gamma was estimated with very low precision and was also fixed to 1. We note that E_{max} is slightly lower for the tolerance model and that it would take approximately 13 hours for the EC_{50} of the tolerance model to be equal to the EC_{50} from the direct model.

Additive and proportional error models were tested, but the additive error model performed best. It is presented in Table 2. The residual error for both models is very large, which is expected as the inter-individual variability is not estimated.

Table 2. Parameter Estimates of the direct and tolerance DAT_{occ} models. RSE: Residual Standard Error

	Direct Model		Tolerance Model	
	Estimated Parameter Value	RSE (%)	Estimated Parameter Value	RSE (%)
Emax	89.39	3.4	85.08	2.9
EC50	4.67	10.2	-	-
EC50,start	-	-	2.68	9.7
ETmax	-	-	1	-
t50	-	-	4.56	8.1
gamma	-	-	1	-
Additive Residual Error	90	11.2	68.22	12

As seen in Figure 3, the residuals of the direct model show an underestimation of early samples, mainly at 1-3h post-dose. These results are in agreement with the hypothesis of an observed tachyphylaxis associated with MPH. The tolerance model slightly reduces the residuals associated with 1-2h post-dose samples, with the median residuals much closer to 0.

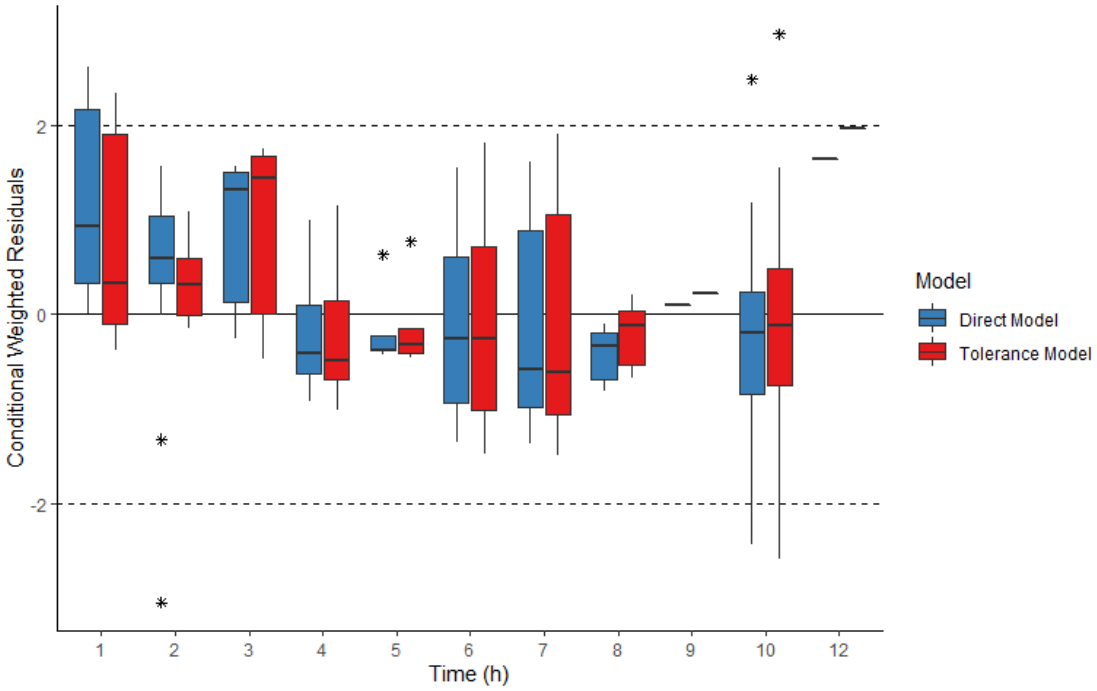

Figure 3. Residuals computed from the direct and tolerance DAT_{occ} models as a function of sample time. Horizontal lines represent sample times where only one data point was available. Outliers are represented as asterisks

An internal validation was explored for the direct and tolerance model. The VPC and bootstrap results are presented in the supplementary information S1 and S2. Both internal validations show that the models developed are appropriate to describe the observed DAT_{occ} data of MPH as a function of plasma concentrations.

The mean absolute prediction error (MAPE) and the root mean square error (RMSE) were computed to assess the predictive performance of both models (Equations 8 and 9).

$$\mathrm{RMSE} = \sqrt{\frac{1}{\mathrm{N}}\sum_{\mathrm{j}=1}^{\mathrm{N}}\left(\mathrm{pred_j} - \mathrm{obs_j}\right)^2} \quad (8)$$

$$\mathrm{MAPE} = \frac{1}{\mathrm{N}} \sum_{\mathrm{j}=1}^{\mathrm{N}} \left[\left(\frac{\left| \mathrm{pred_j} - \mathrm{obs_j} \right|}{\mathrm{obs_j}} \right) \times 100 \right] (9)$$

where $\mathrm{pred_j}$ is the jth predicted value, $\mathrm{obs_j}$ is the jth observed value.

Both the direct and tolerance models yield similar low precision. The MAPE of the direct and tolerance model are 10.72% and 10.39%, respectively. The RMSE of the direct and tolerance model are 9.49% and 8.68%, respectively.

Tolerance and Drug Regimens

The performance score based on the PK curves, the DAT_{occ} simulated with the direct PKPD model ($Perf_{DAT,direct}$), the performance score based on the DAT_{occ} simulated with the tolerance PKPD model ($Perf_{DAT,tolerance}$), the NET target and NET_{occ} are presented in Table 3 and illustrated in Figure 4 and Figure 5.

Table 3. Performance scores for MPH regimen. The total daily dose of Concerta is increased in 9mg increments, which is the smallest increase that can be achieved by combining the existing dosages (18,27,36,54mg). The optimized timing refers to 7:30 am, 9:30 am and 12:30 pm [13] and the NIMH Collaborative Multisite Multimodal Treatment study of Children with ADHD (MTA) timing refers to 7:00 am, 11:00 am, 3:00 pm [10]. The NET target is classified as: Below minimum target of 0.5 (Low), Achieving target of 0.5-0.7 (Target), Above maximum target of 0.7 (High)

Dose	Performance Score			NET	
	PK[a]	DAT			
	$Perf_{PK}$ (%)	$Perf_{DAT,direct}$ (%)	$Perf_{DAT,tolerance}$ (%)	Target	Occupancy (0-1)
Concerta					
18	22	22.7	19.8	Target	0.6

Dose	Performance Score			NET	
	PK[a]	DAT			
	$Perf_{PK}$ (%)	$Perf_{DAT,direct}$ (%)	$Perf_{DAT,tolerance}$ (%)	Target	Occupancy (0-1)
27	29.3	31.3	23.7	High	0.7
36	48.9	50.1	41.6	High	0.8
45	61.8	63	69.4	High	0.8
54	76.9	79.3	83.7	High	0.8
63	82	79.7	85.1	High	0.9
72	80.6	71.8	83.4	High	0.9
81	75.2	62.1	77.7	High	0.9
90	62.8	56.9	62.1	High	0.9
99	62.4	56.4	53.4	High	0.9
Ritalin tid, optimized timing					
10,10,05mg	34.6	39.9	51.3	High	0.7
10,10,10mg	43.9	48	59.3	High	0.8
10,10,15mg	44.3	50	60.7	High	0.8
10,10,20mg	52.3	55.5	65.1	High	0.8
Ritalin tid, MTA timing					
10,10,05mmg	31.7	34.3	34.4	High	0.7
10,10,10mmg	41.6	44.9	42.9	High	0.8
10,10,15mmg	45	48.9	46.9	High	0.8
10,10,20mmg	46.8	49.1	47.4	High	0.8

[a] It is important to explain a disparity between the $Perf_{PK}$ reported in this work and in [12, 13]. Firstly, the Pop-PK models in [13] are different from the ones used in this paper. The simulated plasma concentrations in this manuscript are lower and less variable than in [13]. Secondly, the performance score computations in [12] were based only on TI_{Eff}, TI_{Tox} and TI_{RCE}. Contrastingly, in this paper, TI_{Tox} is replaced by TI_R and TI_{RCE} is applied to ER simulations.

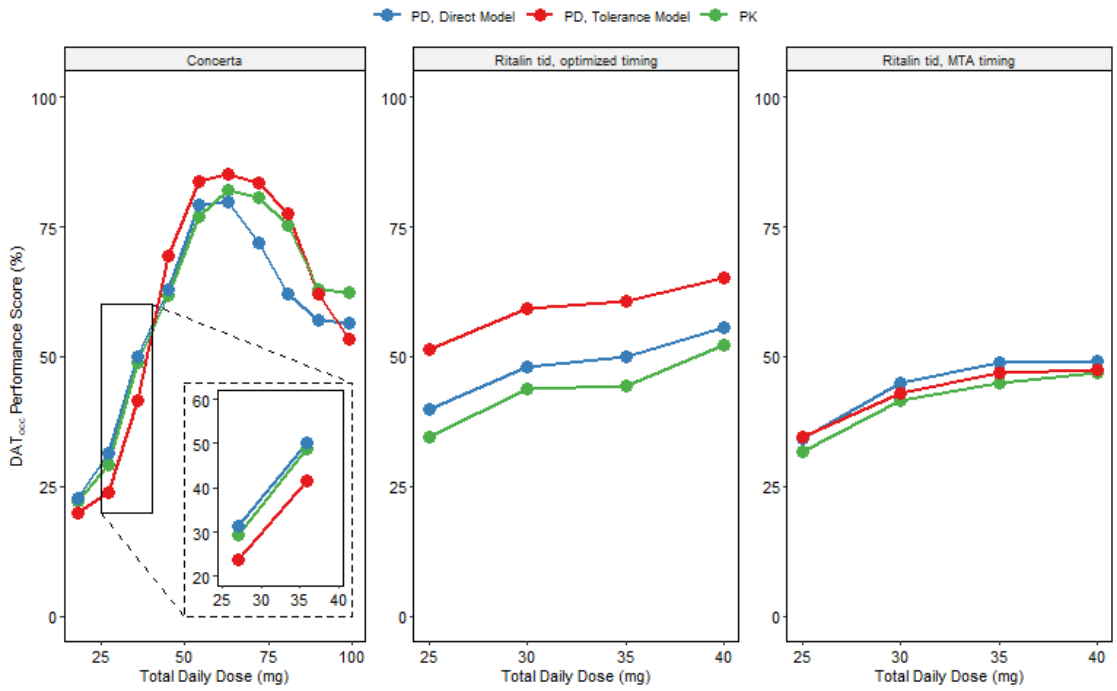

Figure 4. Dopamine transporter occupancy (DAT_{occ}) performance scores for MPH regimen as a function of the total daily dose. The optimized timing refers 7:30 am, 9:30 am and 12:30 pm and the NIMH CollaborativeMultisite Multimodal Treatment study of Children with ADHD (MTA) timing refer to 7:00 am, 11:00 am, 3:00 pm

In Table 3 and Figure 4, we notice that the *qd* 63mg doses of Concerta dose yields the peak of performance for $Perf_{PK}$, $Perf_{DAT,direct}$, and $Perf_{DAT,tolerance}$. Higher doses of MPH are associated with PK or DAT_{occ} curves which exceed the TB, which explains the decrease in performance scores. Additionally, we note that $Perf_{DAT,tolerance}$ is larger than $Perf_{DAT,direct}$ for higher doses. Indeed, the DAT_{occ} simulated with the direct model at these doses are higher than those simulated with the tolerance model (which lowers DAT_{occ} because it accounts for tachyphylaxis). Thus, the DAT_{occ} curves from the direct model exceed the TB's target (50-70%) while the DAT_{occ} from the tolerance model fall within the TB's target.

In comparing $Perf_{PK}$, $Perf_{DAT,direct}$, and $Perf_{DAT,tolerance}$ following *qd* doses of Concerta, we note that they vary greatly depending on the TDD (Table 3 and Figure 4). Specifically, at doses lower than 36mg, $Perf_{DAT,tolerance}$ is lower than $Perf_{PK}$ and $Perf_{DAT,direct}$. Conversely, when the dose is between 45mg and 81mg, $Perf_{DAT,tolerance}$ surpasses the other performance scores. As mentioned above,

this is because the PK and the DAT_{occ} curves from the direct model exceed the TB's target while the DAT_{occ} from the tolerance model fall within the TB's target. Consequently, $Perf_{DAT,tolerance}$ is higher since the performance score computation takes into account the percentage of time spent in the TB by the DAT_{occ} curves (TI_{eff}).

We observe that the smallest commercially available dose of Concerta is the only one which leads to a NET_{occ} within the desired range despite very poor performance regarding DAT_{occ} ($Perf_{PK} = 22\%$, $Perf_{DAT,direct} = 22.7\%$, and $Perf_{DAT,tolerance} = 19.8\%$). Larger MPH doses are associated with a higher DAT_{occ}, while their NET_{occ} exceeds the 0.7 maximum limit. This is due to the higher affinity of MPH for NET than DAT.

The *tid* regimens illustrate more clearly the impact of tolerance. Indeed, we notice that all performance scores increase when the last dose is increased (Table 3). In order to examine precisely the difference between the morning and afternoon performances, we present the TI_{Eff} and TI_R for each division of the TB (AM and PM) in Figure 5. It can be seen that the TI computed with the tolerance model decrease in the afternoon for all the regimens, accounting for the tachyphylaxis. This drop in performance between AM and PM is counteracted when the last dose increases.

Furthermore, we note that TIs related to the PK model and the direct PD model are almost identical (Figure 5). This observation is accordance with the direct (albeit non-linear) relationship between the PK and PD curves in the direct model.

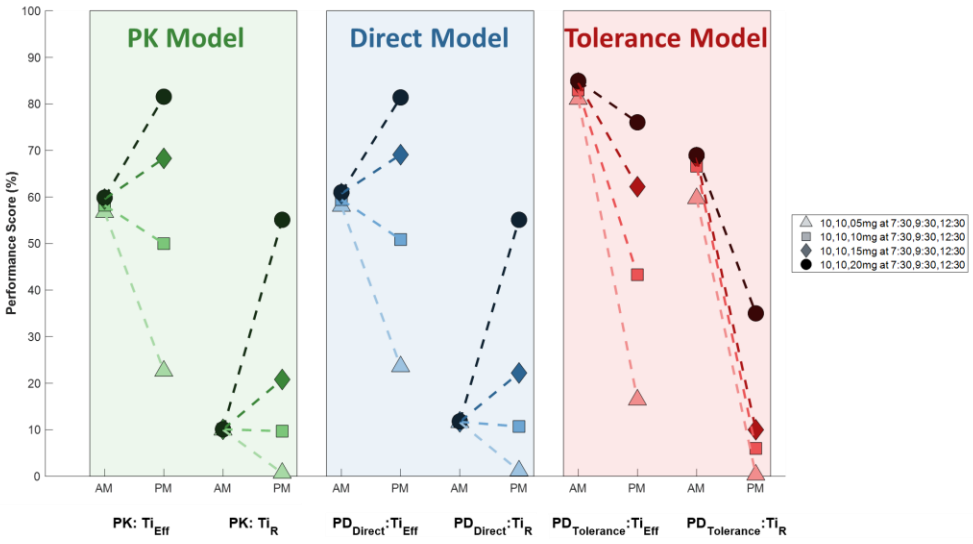

Figure 5. Performance Scores and TiEff of four tid regimens selected to illustrate the impact of tolerance. TI_{Eff} is the percentage of time spent by the DAT_{occ} profile within a TB. TI_R is the proportion of simulated subjects classified as responders

Discussion

In this paper, we integrated a Pop-PK model of MPH [12], a KPD model for NET_{occ} [37] and a PKPD model for DAT_{occ}.

DAT_{occ} Performance

Using data digitized from the literature [30, 33–35], we were able to estimate the PKPD relationship of DAT_{occ} as a function of MPH concentration. However, these digitized data had clear limitations. First, they made impossible to categorize the data by patients. Thus, for modeling purposes, we assumed that all data is provided by an average individual, as the estimation of inter-individual variability was not possible.

Second, imprecise sampling times made a clear and definitive conclusion on acute tolerance difficult. This was mainly due to an overlap between the DAT_{occ} values at 1h and 10h post-dose. The DAT_{occ} at 10h post-dose had a reported sampling time that varied between 9 and 11 hour

[35]. To assess the impact of this temporal imprecision, we compared the estimated parameters for the direct and tolerance models with and without the 10h post-dose samples (results not shown). Without these time samples, the tolerance model parameters were lower (most notably E_{max} which decreased to 74.3%) but with similar accuracy (with the exception of the RSE on the EC50start which increased to 25.8%). However, the resulting models overestimated DAT_{occ} by 40-60%. In addition, the results for the conditional weighted residuals remained the same as in Figure 3, namely that the tolerance model improved the fit for early samples compared to the direct model. Therefore, we concluded that approximating sampling times at 10 h post-dose was appropriate for our purpose.

In addition, we could not include most of the data from one study [34] in the estimation of the tolerance model. Indeed, we could only consider the 7 highest DAT_{occ} and their corresponding plasma concentrations because they were the only ones we could distinguish from the others and extract graphically. Therefore, the observations in one study [34] are only the highest values, which may impact any tolerance model.

Also, the precise formulation of the drug (and as a result its precise pharmacokinetics) was not available through the papers. Therefore, applying to these data commonly used tolerance models that involve the addition of a compartment effect (e.g., [47]) would have added unnecessary PK structural assumptions. Instead, we resorted to a descriptive tolerance model that does not account for drug-specific PK, but makes the EC_{50} time-dependent, as reported in [34], where the MPH EC_{50} at 1h post-dose is much smaller than at later sampling times.

After making every effort to extract valid information from the available data, we were able to estimate the relationship between DAT_{occ} and plasma MPH concentration with a tolerance model and a direct Michaelis-Menten model and compare them with each other. Although acute tolerance has been described on clinical scales [14–17, 22–24], or neuropsychological scores [18], this is, to our knowledge, the first attempt to account for it at the level of DAT.

In order to illustrate the differences according to the endpoint in our PKPD framework, we simulated MPH regimens (ER and IR *tid*) and computed their performance scores based on the

plasma concentration and the DAT_{occ} computed either with the direct model or with the tolerance model.

The simulations of ER doses (Concerta) show that the DAT_{occ} performance score varies according to the TDD and to the endpoint. Indeed, for Concerta $\leq$ 63mg, $Perf_{DAT,direct}$ was very close to $Perf_{PK}$, while $Perf_{DAT,tolerance}$ was slightly lower up to 36mg and higher after. Overall, for doses $\leq$ 63mg, the mean difference between MPH plasma concentration- and DAT_{occ}-based performance, regardless of the model, was less than 1%. On the other hand, for doses of Concerta $>$ 63mg, $Perf_{DAT,direct}$ was significantly lower than $Perf_{PK}$ (with a maximum difference of -13% for a TDD of 81mg), while $Perf_{DAT,tolerance}$ was much closer to $Perf_{PK}$ except for the TDD of 99mg. However, as the maximum TDD in children [48] and in adults [49] almost never exceeds 72mg, these differences may not be of clinical significance.

The PK profile of ER preparations is rigidly determined by the mechanisms of release of the drug. On the other hand, when using IR preparations taken *tid*, the PK profile may be altered as a function of doses and administration times. Performance of IR regimens increased when administration times were optimized, but this increase was minimal for performance based on plasma MPH concentration (2% on average), greater but still small for performance based on DAT_{occ} with the direct model (4%), but much more of significance with the tolerance moderator (16%). In this usual dose range (15-40 mg) the difference in performance was particularly strong (on average 15%) for $Perf_{DAT,tolerance}$ compared to $Perf_{PK}$. The increase in $Perf_{Dat,tolerance}$ for the optimized timing compared with the MTA timing suggests that a steeper slope may compensate for acute tolerance. However, Concerta was designed to mimic the plasma profile of MTA timing, the best option available at the time, but which may leave some residual acute tolerance (Figure 1 f).

Even with the limitations mentioned above for the DATocc data, the models presented in this work allow an understanding of MPH's target engagement and a preliminary exploration of the acute tolerance to MPH which, to our knowledge, has not yet been modeled in the literature. Indeed, currently available PET studies were not designed to test the existence of an acute tolerance in DATocc. With this work, we aimed to explore if current DATocc data is enough to

quantify the PKPD relationship of MPH. We conclude that further PET studies for reliable PKPD modeling should provide: randomized cross-over designs, explicit drug formulation and dosage, and exact sampling times with corresponding drug plasma concentrations. This would improve our model with an accurate assessment of interindividual variability and of acute tolerance.

NET_{occ} Performance

Because the change in NET_{occ} over time was not available, it was only possible to consider a KPD equation to calculate NET_{occ} as a function of MPH dose [37]. Furthermore, except for the lower dose of Concerta (18mg), all simulated regimens lead to a very high NET_{occ}. According to the NET_{occ} calculation in [37], a NET_{occ} of 50-70% is obtained for doses between 9.8mg-22.9mg (for a 70 kg adult). The fact that most usual therapeutic doses of MPH exceed this range is consistent with the notion of clinical overdose [42] and the therapeutic value of low doses [41–44] for some ADHD patients.

This difference between NET and DAT occupancy is related to the nearly twofold affinity of methylphenidate for NETs compared with DAT [50]. DAT is mainly responsible for DA reuptake, especially in the basal ganglia, and NET for NE reuptake in NET-rich regions (locus coeruleus, thalamus, some midbrain nuclei), as well as DA reuptake in the prefrontal cortex. Dysregulation of DA and NE functioning has been implicated in ADHD. The relative contribution of DA and NE systems in the etiology of ADHD could therefore explain the interindividual differences in effective doses of methylphenidate (in the range of 1 to 4) to treat it. By calculating the performance of different MPH regimens for DAT and NET occupancy (with or without acute tolerance), one could identify different clinical, neuropsychological, or brain functional markers that are related to dysregulation in DA, NE, or both, and thus identify among ADHD patients those who respond to a low dose and those who require higher doses. For example, it can be hypothesized that executive test scores (related to prefrontal cortex dysfunction) would be more strongly associated with $Perf_{NETocc}$ than $Perf_{DATocc}$, when tolerance is taken into account, which could identify a subgroup of ADHD patients responding to a low dose of MPH [42].

Conclusions

The advancement of DAT and NET inhibitors to treat ADHD [51, 52] confirm the need for a framework such as ours to aid in the *a priori* comparison of different ADHD drugs. We present here an analysis leading to an integrative framework for the performance assessment of MPH regiments that takes into account NET_{occ} and DAT_{occ}. Using the NET_{occ} data available in the literature, it was only possible to use a static KPD model, where NET_{occ} does not vary with time. As for the DAT_{occ} data, it was digitized from the literature, and we were able to model a PKPD relationship. Although these data carry limitations (notably the uncertainty of sampling times), we observed a trend in the data and residual errors that is consistent with acute tolerance to MPH but without being able to confidently conclude that it exists at the DAT_{occ} level. For a more definitive assessment of the acute tolerance, there is a need for a more systematic collection in the same subjects if possible, of both DAT_{occ} and NET_{occ} data following MPH administration, with precise information on its formulations, sampling times, and plasma concentration.

While objective measures of MPH performance are proposed in this work, the performance score we presented are still some steps upstream of measures of clinical efficacy (e.g. ADHD questionnaire scores). The interindividual variability in extracellular DA, which ultimately account for the therapeutic effect, is due not only to differences in MPH binding to DAT or NET, but also to differences in DA cell activity [49]. The more active DA/NE neurons are, the more DA/NE they release, and the more extracellular DA/NE accumulates from reuptake blockade. Thus, a complete model would require for some additional markers of DA and NE cell activity. Despite the complexity of the task, this work is an exploratory analysis that justifies the need for richer data geared towards the study of the two transporters involved in the mechanism of action of MPH, with a focus on the observation of acute tolerance directly at the level of these transporters.

Acknowledgments

Sara Soufsaf reports research grant from Fonds de Recherche du Québec — Santé.

Fahima Nekka reports research grant from the Natural Sciences and Engineering Research Council of Canada, and from Fonds de Recherche du Québec – Nature et Technologie.

We thank Jun Li for useful discussions and support.

References

[1] Jaeschke RR, Sujkowska E, Sowa-Kućma M. Methylphenidate for attention-deficit/hyperactivity disorder in adults: A narrative review. *Psychopharmacology* 2021; 238:2667–2691.

[2] Childress AC. Stimulants. *Child and Adolescent Psychiatric Clinics of North America* 2022; 31:373–392.

[3] Faraone SV, Buitelaar J. Comparing the efficacy of stimulants for ADHD in children and adolescents using meta-analysis. *European Child & Adolescent Psychiatry* 2010; 19:353–364.

[4] Raman SR, Man KKC, Bahmanyar S, et al. Trends in attention-deficit hyperactivity disorder medication use: A retrospective observational study using population-based databases. *The Lancet Psychiatry* 2018; 5:824–835.

[5] Medori R, Ramos-Quiroga JA, Casas M, et al. A randomized, placebo-controlled trial of three fixed dosages of prolonged-release OROS methylphenidate in adults with attention-deficit/hyperactivity disorder. *Biological Psychiatry* 2008; 63:981–989.

[6] Buitelaar JK, Ramos-Quiroga JA, Casas M, et al. Safety and tolerability of flexible dosages of prolonged-release OROS methylphenidate in adults with attention-deficit/hyperactivity disorder. *Neuropsychiatric Disease and Treatment* 2009; 5:457–466.

[7] Buitelaar JK, Kooij JJS, Ramos-Quiroga JA, et al. Predictors of treatment outcome in adults with ADHD treated with OROS methylphenidate. *Progress in Neuro-Psychopharmacology & Biological Psychiatry* 2011; 35:554–560.

[8] Cortese S, Adamo N, Del Giovane C, et al. Comparative efficacy and tolerability of medications for attention-deficit hyperactivity disorder in children, adolescents, and adults: A systematic review and network meta-analysis. *The Lancet Psychiatry* 2018; 5:727–738.

[9] Farhat LC, Flores JM, Behling E, et al. The effects of stimulant dose and dosing strategy on treatment outcomes in attention-deficit/hyperactivity disorder in children and adolescents: A meta-analysis. *Molecular Psychiatry* 2022; 27:1562–1572.

[10] Greenhill LL, Abikoff HB, Arnold LE, et al. Medication treatment strategies in the MTA Study: Relevance to clinicians and researchers. *Journal of the American Academy of Child and Adolescent Psychiatry* 1996; 35:1304–1313.

[11] Recommendations | Attention deficit hyperactivity disorder: Diagnosis and management | Guidance | NICE.

[12] Soufsaf S, Robaey P, Bonnefois G, et al. A Quantitative Comparison Approach for Methylphenidate Drug Regimens in Attention-Deficit/Hyperactivity Disorder Treatment. *J Child Adolesc Psychopharmacol*. Epub ahead of print February 2019. DOI: 10.1089/cap.2018.0093.

[13] Bonnefois G, Robaey P, Barrière O, et al. An Evaluation Approach for the Performance of Dosing Regimens in Attention-Deficit/Hyperactivity Disorder Treatment. *Journal of Child and Adolescent Psychopharmacology* 2017; 27:320–331.

[14] Teicher MH, Polcari A, Foley M, et al. Methylphenidate blood levels and therapeutic response in children with attention-deficit hyperactivity disorder: I. Effects of different dosing regimens. *Journal of Child and Adolescent Psychopharmacology* 2006; 16:416–431.

[15] Swanson JM. Long-acting stimulants: Development and dosing. *The Canadian Child and Adolescent Psychiatry Review* 2005; 14:4–9.

[16] Swanson J, Gupta S, Guinta D, et al. Acute tolerance to methylphenidate in the treatment of attention deficit hyperactivity disorder in children. *Clinical Pharmacology & Therapeutics* 1999; 66:295–305.

[17] Swanson JM, Volkow ND. Pharmacokinetic and pharmacodynamic properties of stimulants: Implications for the design of new treatments for ADHD. *Behavioural Brain Research* 2002; 130:73–78.

[18] Srinivas NR, Hubbard JW, Quinn D, et al. Enantioselective pharmacokinetics and pharmacodynamics of dl-threo-methylphenidate in children with attention deficit hyperactivity disorder. *Clinical Pharmacology and Therapeutics* 1992; 52:561–568.

[19] Volkow ND, Wang G-J, Fowler JS, et al. Imaging the effects of methylphenidate on brain dopamine: New model on its therapeutic actions for attention-deficit/hyperactivity disorder. *Biological Psychiatry* 2005; 57:1410–1415.

[20] Volkow ND, Wang G-J, Fowler JS, et al. Therapeutic Doses of Oral Methylphenidate Significantly Increase Extracellular Dopamine in the Human Brain. 5.

[21] Swanson JM, Volkow ND. Serum and brain concentrations of methylphenidate: Implications for use and abuse. *Neuroscience and Biobehavioral Reviews* 2003; 7.

[22] Teuscher NS, Sikes CR, McMahen R, et al. Population Pharmacokinetic-Pharmacodynamic Modeling of a Novel Methylphenidate Extended-Release Orally Disintegrating Tablet in Pediatric Patients With Attention-Deficit/Hyperactivity Disorder. *Journal of Clinical Psychopharmacology* 2018; 38:467–474.

[23] Gomeni R, Komolova M, Incledon B, et al. Model-Based Approach for Establishing the Predicted Clinical Response of a Delayed-Release and Extended-Release Methylphenidate for the Treatment of Attention-Deficit/Hyperactivity Disorder. *Journal of Clinical Psychopharmacology* 2020 Jul/Aug; 40:350–358.

[24] Kimko H, Gibiansky E, Gibiansky L, et al. Population pharmacodynamic modeling of various extended- release formulations of methylphenidate in children with attention deficit hyperactivity disorder via meta-analysis. *J Pharmacokinet Pharmacodyn* 2012; 16.

[25] Handelman K, Sumiya F. Tolerance to Stimulant Medication for Attention Deficit Hyperactivity Disorder: Literature Review and Case Report. *Brain Sciences* 2022; 12: 959.

[26] Weikop P, Egestad B, Kehr J. Application of triple-probe microdialysis for fast pharmacokinetic/pharmacodynamic evaluation of dopamimetic activity of drug candidates in the rat brain. *Journal of Neuroscience Methods* 2004; 140:59–65.

[27] Calipari ES, Ferris MJ, Siciliano CA, et al. Differential influence of dopamine transport rate on the potencies of cocaine, amphetamine, and methylphenidate. *ACS chemical neuroscience* 2015; 6:155–162.

[28] Nikolaus S, Larisch R, Vosberg H, et al. Pharmacological challenge and synaptic response - assessing dopaminergic function in the rat striatum with small animal single-photon emission computed tomography (SPECT) and positron emission tomography (PET). *Reviews in the Neurosciences* 2011; 22:625–645.

[29] Sachdev PS, Trollor JN. How high a dose of stimulant medication in adult attention deficit hyperactivity disorder? *The Australian and New Zealand Journal of Psychiatry* 2000; 34:645–650.

[30] Volkow ND, Gatley SJ, Hitzemann R. Dopamine Transporter Occupancies in the Human Brain Induced by Therapeutic Doses of Oral Methylphenidate. *Am J Psychiatry* 1998; 7.

[31] Fowler JS, Volkow ND, Ding Y-S, et al. Positron Emission Tomography Studies of DopamineEnhancing Drugs. 4.

[32] Volkow ND, Wang GJ, Fowler JS, et al. Blockade of striatal dopamine transporters by intravenous methylphenidate is not sufficient to induce self-reports of "high". *The Journal of Pharmacology and Experimental Therapeutics* 1999; 288:14–20.

[33] Spencer TJ, Biederman J, Ciccone PE. PET Study Examining Pharmacokinetics, Detection and Likeability, and Dopamine Transporter Receptor Occupancy of Short- and Long-Acting Oral Methylphenidate. *Am J Psychiatry* 2006; 9.

[34] Spencer TJ, Bonab AA, Dougherty DD, et al. Understanding the central pharmacokinetics of spheroidal oral drug absorption system (SODAS) dexmethylphenidate: A positron emission

tomography study of dopamine transporter receptor occupancy measured with C-11 altropane. *The Journal of Clinical Psychiatry* 2012; 73:346–352.

[35] Spencer TJ, Bonab AA, Dougherty DD, et al. A PET study examining pharmacokinetics and dopamine transporter occupancy of two long-acting formulations of methylphenidate in adults. *INTERNATIONAL JOURNAL OF MOLECULAR MEDICINE* 2010; 5.

[36] Shimizu R, Horiguchi N, Yano K, et al. Pharmacokinetic-Pharmacodynamic Modeling of Brain Dopamine Levels Based on Dopamine Transporter Occupancy after Administration of Methylphenidate in Rats. *J Pharmacol Exp Ther* 2019; 369:78–87.

[37] Hannestad J, Gallezot J-D, Planeta-Wilson B, et al. Clinically relevant doses of methylphenidate significantly occupy norepinephrine transporters in humans in vivo. *Biological Psychiatry* 2010; 68:854–860.

[38] Schmeichel BE, Berridge CW. Neurocircuitry Underlying the Preferential Sensitivity of Prefrontal Catecholamines to Low-Dose Psychostimulants. *Neuropsychopharmacology* 2013; 38: 1078–1084.

[39] Arnsten AF, Dudley AG. Methylphenidate improves prefrontal cortical cognitive function through Alpha2 adrenoceptor and dopamine D1 receptor actions: Relevance to therapeutic effects in Attention Deficit Hyperactivity Disorder. *Behavioral and brain functions: BBF* 2005; 1: 2.

[40] Berridge CW, Devilbiss DM, Andrzejewski ME, et al. Methylphenidate preferentially increases catecholamine neurotransmission within the prefrontal cortex at low doses that enhance cognitive function. *Biological Psychiatry* 2006; 60:1111–1120.

[41] Ling D, Balce K, Weiss M, et al. *Effects of low-dose versus normal-dose psychostimulants on executive functions in children with attention-deficit / hyperactivity disorder.* 2019. Epub ahead of print June 2019. DOI: 10.13140/RG.2.2.13672.39681.

[42] Ling D, Balce K, Weiss M, et al. *Patients with ADHD are being overmedicated (for optimal cognitive performance).* 2019.

[43] Diamond A. Attention-deficit disorder (attention-deficit/ hyperactivity disorder without hyperactivity): A neurobiologically and behaviorally distinct disorder from attention-deficit/hyperactivity disorder (with hyperactivity). *Development and Psychopathology* 2005; 17:807–825.

[44] Barkley RA, DuPaul GJ, McMurray MB. Attention deficit disorder with and without hyperactivity: Clinical response to three dose levels of methylphenidate. *Pediatrics* 1991; 87:519–531.

[45] Porchet HC, Benowitz NL, Sheiner LB. Pharmacodynamic model of tolerance: Application to nicotine. *The Journal of Pharmacology and Experimental Therapeutics* 1988; 244:231–236.

[46] Gomeni R, Bressolle-Gomeni F, Spencer TJ, et al. Model-Based Approach for Optimizing Study Design and Clinical Drug Performances of Extended-Release Formulations of Methylphenidate for the Treatment of ADHD. *Clinical Pharmacology and Therapeutics* 2017; 102:951–960.

[47] Dumas EO, Pollack GM. Opioid tolerance development: A pharmacokinetic/pharmacodynamic perspective. *The AAPS journal* 2008; 10:537–551.

[48] Ching C, Eslick GD, Poulton AS. Evaluation of Methylphenidate Safety and Maximum-Dose Titration Rationale in Attention-Deficit/Hyperactivity Disorder: A Meta-analysis. *JAMA pediatrics* 2019; 173:630–639.

[49] Volkow ND, Wang G-J, Fowler JS, et al. Relationship between blockade of dopamine transporters by oral methylphenidate and the increases in extracellular dopamine: Therapeutic implications. *Synapse* 2002; 43:181–187.

[50] Han DD, Gu HH. Comparison of the monoamine transporters from human and mouse in their sensitivities to psychostimulant drugs. *BMC pharmacology* 2006; 6: 6.

[51] Wigal SB, Wigal T, Hobart M, et al. Safety and Efficacy of Centanafadine Sustained-Release in Adults With Attention-Deficit Hyperactivity Disorder: Results of Phase 2 Studies. *Neuropsychiatric Disease and Treatment* 2020; 16:1411–1426.

[52] Wigal TL, Newcorn JH, Handal N, et al. A Double-Blind, Placebo-Controlled, Phase II Study to Determine the Efficacy, Safety, Tolerability and Pharmacokinetics of a Controlled Release (CR) Formulation of Mazindol in Adults with DSM-5 Attention-Deficit/Hyperactivity Disorder (ADHD). *CNS drugs* 2018; 32:289–301.

[53] Mandema JW, Wada DR. Pharmacodynamic model for acute tolerance development to the electroencephalographic effects of alfentanil in the rat. Journal of Pharmacology and Experimental Therapeutics. 1995 Dec 1;275(3):1185-94.

Supplementary information 1: VPC graphs

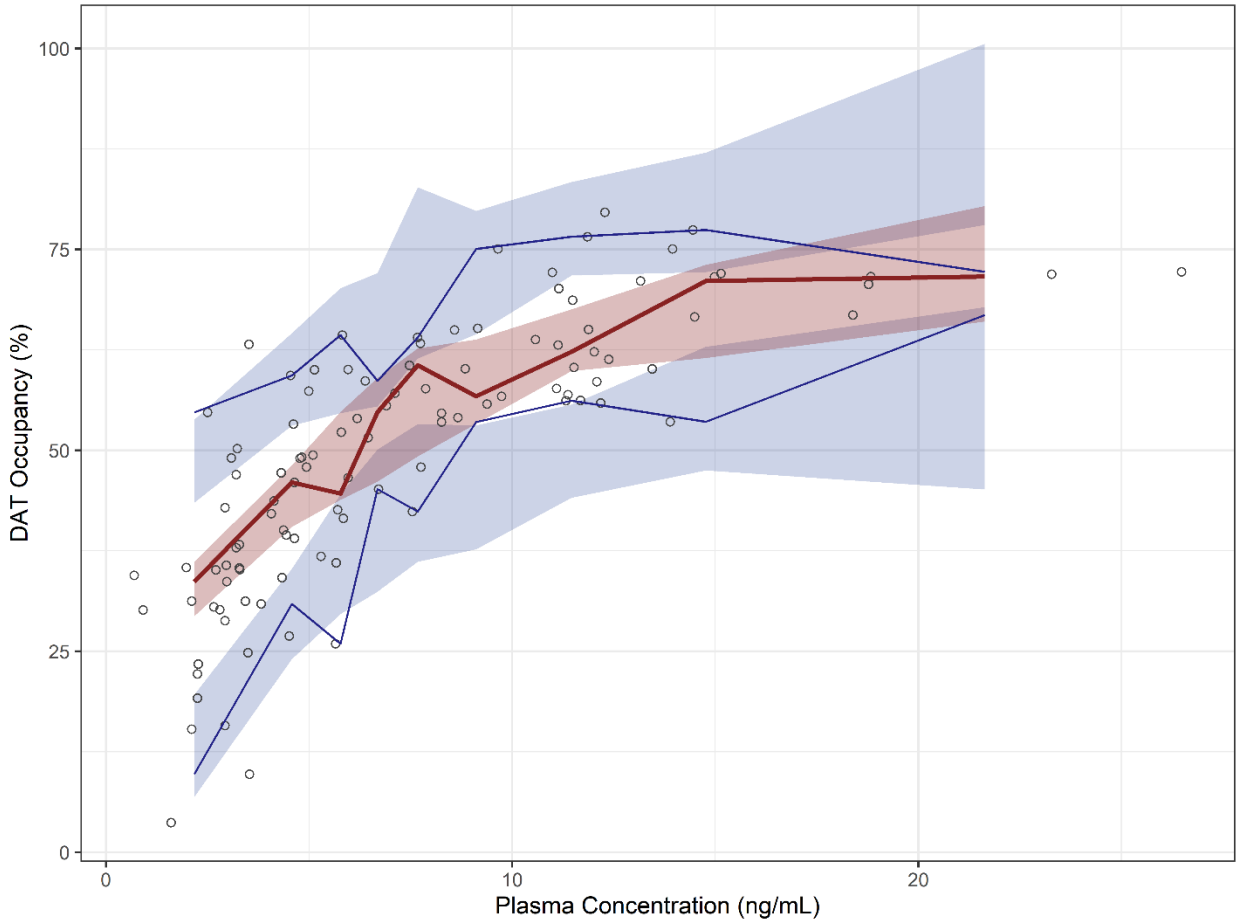

Figure 6. Direct Model: Visual Predictive Check (VPC) Validation. The observations are shown as a scatter. The solid red line is the 50th percentile of the observations. The solid blue lines are the 5th and 95th percentiles of the observations. The red shaded area is the 95% confidence interval of the 50th percentile of the predictions. The blue shaded area are the 95% confidence intervals of the 5th and 95th percentile of the predictions

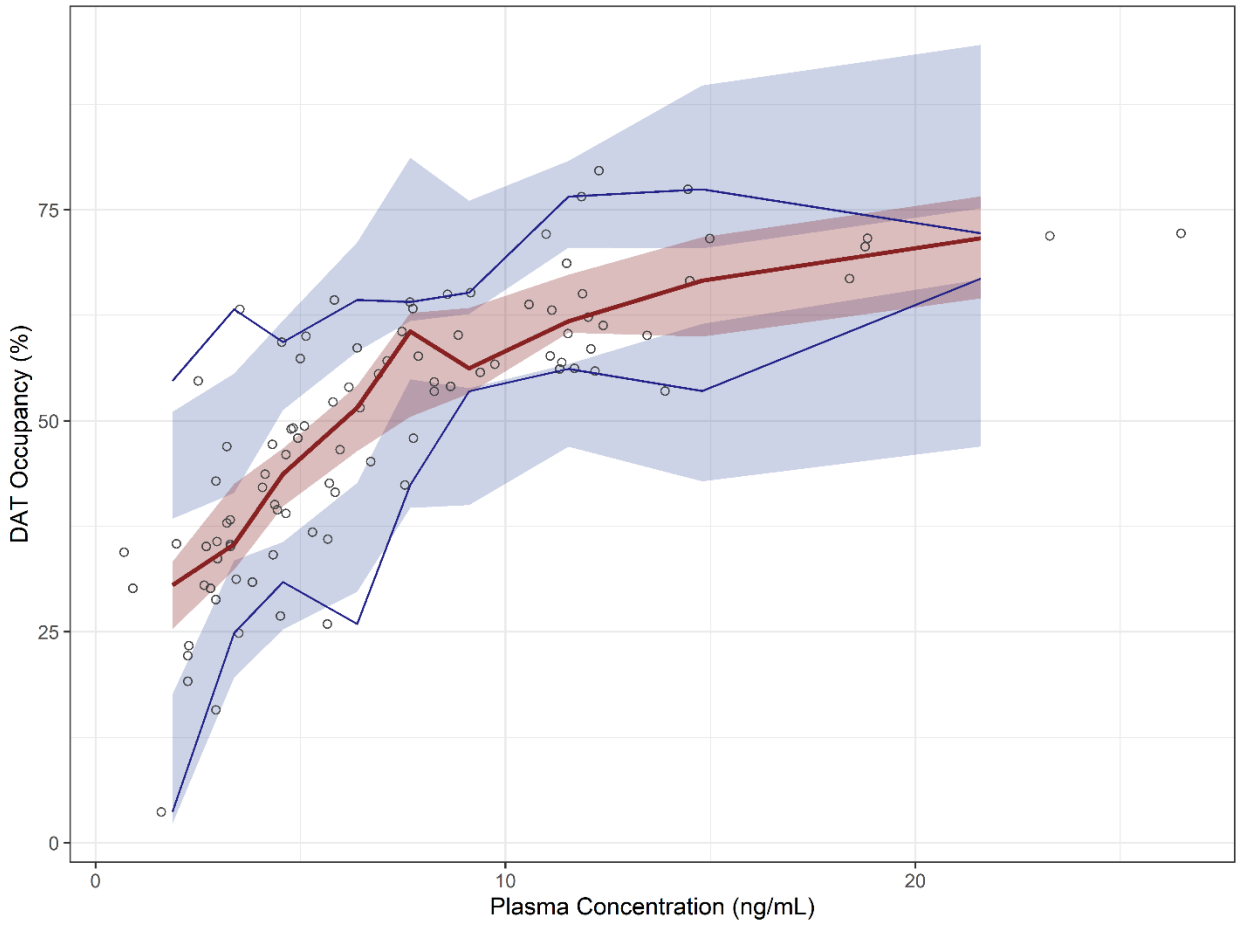

Figure 7. Tolerance Model: Visual Predictive Check (VPC) Validation. The observations are shown as a scatter. The solid red line is the 50th percentile of the observations. The solid blue lines are the 5th and 95th percentiles of the observations. The red shaded area is

the 95% confidence interval of the 50th percentile of the predictions. The blue shaded area are the 95% confidence intervals of the 5th and 95th percentile of the predictions

Supplementary information 2: Bootstrap table

Table 4. Bootstrap Analysis of Direct and Tolerance DAT models. The final estimated parameter values are presented with the 2.5% and 97.5% bootstrap confidence interval.

	Direct Model			Tolerance Model		
	Estimated Parameter Value	2.5%	97.5%	Estimated Parameter Value	5%	99.5%
OFV	1127.5	1080.3	1168.4	955.8	901.1	1025.8
Emax	89.4	83.6	96.4	85.1	81	92.3
EC50	4.7	3.8	5.7	-	-	-
EC50,start	-	-	-	2.7	2.3	3.5
ETmax	-	-	-	1	1	1
t50	-	-	-	4.6	4	6.1
Additive Residual Error	90	71.5	109.9	68.2	54.9	91.9

Supplementary information 3: Model output file

Direct Model

```
$PRED


TVEMX = THETA(1)
EMAX = TVEMX

TVEC50 = THETA(2)
EC50 = TVEC50


NUM = EMAX*CONC
DEN = EC50 + CONC
RESP =  NUM/DEN


ADD = ERR(1)

Y = RESP   +  ERR(1)

IPRED = Y

W = ADD

IRES = DV-IPRED
IF (W.EQ.0) W = 1
IWRES = IRES/W

$THETA

(0,89.4) ; EMAX
(0,4.67) ; EC50


$OMEGA  90
$COVARIANCE
 $ESTIMATION
```

Tolerance Model

```
$PRED


TVEMX = THETA(1)
EMAX = TVEMX

TVEC50S = THETA(2)
EC50S = TVEC50S

ETMAX = THETA(3)

T50 = THETA(4)

GAMMA = THETA(5);

EC50 = EC50S * (1 + (ETMAX * TIME**GAMMA) / (T50**GAMMA + TIME**GAMMA))


NUM = EMAX * CONC
DEN = EC50 + CONC
RESP =  NUM/DEN


ADD = ERR(1)

Y = RESP   +  ERR(1)

IPRED = Y

W = ADD

IRES = DV-IPRED
IF (W.EQ.0) W = 1
IWRES = IRES/W


$THETA  (0,88.1) ; EMAX
 (0,2.52) ; EC50 START
 1 FIX ; ETMAX
 (0,2.29) ; T50
 1 FIX ; GAMMA
$OMEGA  5  ;        ADD

$ESTIMATION
$COVARIANCE
```

Chapitre 6 — Can MPH target engagement be directly translated into clinical rating scales of behavior? Simulations of dopamine transporter occupancy and SKAMP clinical rating scores using population pharmacokinetic-pharmacodynamic modeling

Sara Soufsaf, M.Sc.[1], Philippe Robaey,M.D., Ph.D.[2], Fahima Nekka, Ph.D.[1]

[1] Université de Montréal, Montréal, Québec, Canada

[2]University of Ottawa, Ottawa, Ontario, Canada

Préambule

Le travail du chapitre 5 a permis de clarifier la relation entre l'occupation des DAT et les concentrations plasmatiques. Ce modèle établit une explication microscopique de la PD du MPH. Suite à la liaison du MPH aux DAT, une cascade d'évènement neurobiologiques mène aux résultats cliniques.

Ces résultats sont mesurés selon le comportement et les symptômes de TDAH.

L'occupation des DAT ainsi que ces échelles de résultats cliniques sont modélisées en fonction de la concentration plasmatique du MPH avec un modèle E_{max} qui prend en compte la tolérance aigüe du MPH avec un EC_{50} variable dans le temps.

Nous nous sommes donc intéressés à savoir si une variation dans l'occupation des DAT peut être partiellement ou complètement traduite par un changement dans les échelles de résultats cliniques. Pour ce faire, nous avons évalué la corrélation entre la pAUC sous les courbes des concentrations plasmatiques, l'occupation des DAT et les scores SKAMP. Comme la relation entre

l’échelle microscopique et macroscopique est complexe, nous avons étudié l’influence de la variabilité interindividuelle et l’impact des changements de formulation sur les deux échelles.

Nous remarquons qu’augmenter la variabilité interindividuelle réduit la corrélation entre l’occupation des DAT et les échelles de résultats cliniques, en particulier en fin de journée. Le délai entre le temps d’administration et la libération prolongée du médicament a également un impact significatif sur ces mesures.

Ce manuscrit est en préparation et présente des résultats préliminaires.

Abstract

Introduction: Methylphenidate is a drug commonly prescribed for the treatment of ADHD symptoms. It works by blocking dopamine transporters (DAT) and increasing the availability of dopamine in the synaptic cleft. MPH's efficacy can be assessed on the macroscopic level (clinical rating scales) and on the microscopic level (transporter occupancy).

Objective: To assess if change in transporter occupancy can be totally or partially translated in clinical rating scales.

Methods: With POP-PK models, POP-PD models of DAT occupancy and SKAMP clinical scores, we simulate generic drugs and compute the partial area under the curve for each of the outcomes from early to late exposure. We compute the correlation between these PK and PD measures and assess the impact of interindividual variability on the simulations. Finally, we assess how different formulations of MPH impact the DAT_{occ} and subsequently, the SKAMP scores.

Results: The correlation between the partial area under the curve of DAT occupancy and SKAMP clinical scores varies between 0.99 and 0.75, with the lowest correlation at late exposure. The delay between administration time and extended drug release has a significant impact on MPH efficacy.

Conclusion: This work provided insight into the relationship and link between DAT and SKAMP. Future work improving the POP-PD model would allow for a better understanding of this relationship.

Study Highlights

1. What is the current knowledge on the topic?

MPH's efficacy can be assessed on the macroscopic level (clinical rating scales) and on the microscopic level (transporter occupancy). Both levels are fitted to the plasma concentration of MPH with an Emax model which integrates a consideration for acute tolerance with a time-varying EC_{50}.

2. What question did this study address?

Can a change in transporter occupancy be totally or partially translated in a change in clinical rating scales?

3. What does this study add to our knowledge?

Increasing the interindividual variability reduces the correlation between transporter occupancy and clinical rating scales, specifically later in the day when the correlation is the lowest. Increasing the time delay for the extended-release drug delivery significantly impacts the transporter occupancy and clinical rating scales in the afternoon.

4. How might this change drug discovery, development and/or therapeutics?

To comprehend the mechanism of acute tolerance and the effectiveness of MPH treatment, it is crucial to understand the correlation between plasma concentration, transporter occupancy, and clinical rating scales.

Introduction

Methylphenidate (MPH) is a psychostimulant drug that is widely used for the treatment of attention-deficit hyperactivity disorder (ADHD) [1–3]. The drug works by blocking the reuptake of dopamine (DA) and norepinephrine (NE) through the dopamine transporter (DAT) and norepinephrine transporter (NET), respectively, resulting in an increased availability of DA and NE in the synaptic cleft [1]. The elevated levels of DA and NE lead to increased neurotransmission, which improves attention, focus, and impulse control in individuals with ADHD [4, 5].

The efficacy of MPH can be measured on a macroscopic and microscopic level. At the macroscopic level, the pharmacodynamics (PD) of MPH can be characterized by clinical rating scales (such as SKAMP, SNAP, ADHD-RS…) [6]. These rating scales assess the severity of the ADHD through questionnaires filled by the patient, the parents or the teachers [6]. Studies have shown that an acute tolerance is developed following MPH doses, as the clinical scores worsen in the afternoon despite similar MPH plasma concentrations as in the morning [7–10]. Multiple population pharmacokinetic-pharmacodynamic models (POP-PKPD) have already quantified the relationship

between these clinical rating scores and the MPH plasma concentration [8, 10–13]. These models use an Emax function and account for the acute tolerance to MPH.

On the microscopic level, the PD of MPH can be characterized by metrics related to its target engagement, such as dopamine DAT occupancy (DAT_{occ}), which has been quantified through positron emission tomography (PET) imaging studies [14–20]. Studies have also noted that DAT_{occ} decreased for late samples, despite similar plasma concentrations, suggesting the development of an acute tolerance on the microscopic scale as well [19, 21].

Previous studies have assessed the impact of MPH formulations on the efficacy of MPH. For instance, one study conducted a simulation study to assess the impact of the rate of absorption of MPH on its PK and on the SKAMP clinical rating scale [22]. Their findings revealed a 90% correlation between the partial AUC (pAUC) of plasma concentrations and SKAMP clinical rating scales. Similarly, another study optimized the MPH PK profile for maximal SKAMP drug effect and demonstrated that two absorption parameters were relevant: the rates of release of the drug of the dose and the time for delivering the dose [23].

By incorporating both the microscopic and macroscopic levels of drug efficacy into a unified model, researchers can gain a more comprehensive and accurate understanding of drug behavior. Drug-receptor binding, downstream signaling pathways and the physiological response of the organism to the drug may be modeled with quantitative systems pharmacology (QSP) models [24–26]. For example, a QSP study on ADHD simulated an *in silico* trial starting at the protein targets of MPH and using the ADHD-RS as an efficacy outcome [26]. In addition to QSP models, mechanistic POP-PKPD models are used to understand drug behavior [27–29]. By combining clinical outcomes with mechanistic POP-PKPD models, we can achieve a more global understanding of the connection between the microscopic and macroscopic levels of drug efficacy.

In scientific literature, no study has yet investigated the correlation between PK, DAT_{occ}, and SKAMP, which are all important factors in understanding the efficacy of MPH. The objective of our work is to explore if changes in DAT_{occ} are totally or partially translated into SKAMP. Specifically, we will use previously developed PKPD models to simulate the relationship between

plasma concentrations, clinical rating scales and DAT_{occ}. The simulations will help us evaluate how interindividual variability (IIV) or changes in MPH formulations affect the plasma concentrations, DAT_{occ} and SKAMP.

Methods

Simulations of PK and PD measures were obtained from (i) a POP-PK model with varying absorption parameter values (ii) a POP-PD model of DAT_{occ} (iii) a POP-PD model of SKAMP scores. These models are detailed below.

These three outcomes were compared for various simulated formulations of MPH. Since conventional bioequivalence metrics, such as area under the curve (AUC) and maximal concentration (C_{max}), have proven inadequate for evaluating the similarity of different extended-release (ER) formulations of MPH, the pAUC of each outcome (plasma concentrations, DAT_{occ} and SKAMP) was computed [31–34]. The pAUC was split according to the FDA guidance for the fasted state, namely 0-3h, 3-7h and 7-12h. The simulation methods and statistical analysis are summarized in Figure 1 and detailed below.

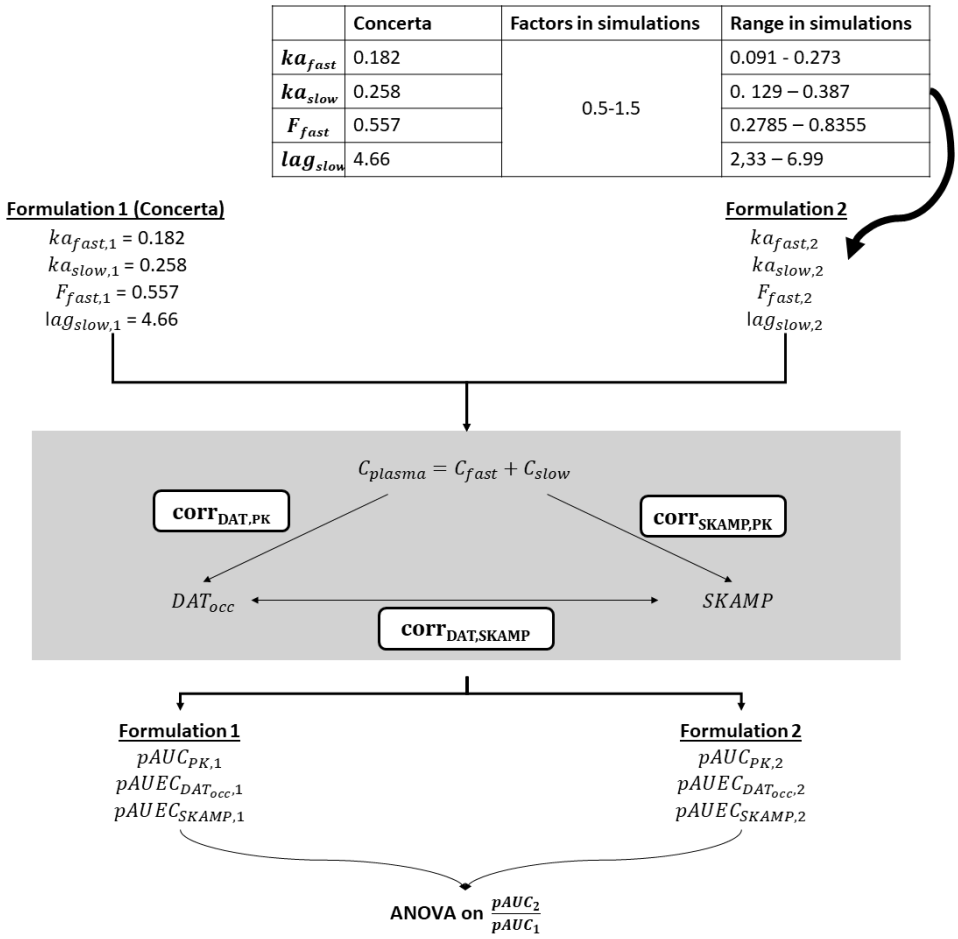

Figure 1. Illustration of the methodology. ka_{fast}: first-order absorption constant of the immediate release fraction, ka_{slow}: first-order absorption constant of the extended release fraction, F_{fast}: immediate release fraction of the formulation, F_{slow}: extended release fraction of the formulation, C_{plasma}: total plasma concentration, C_{fast}: plasma concentration for the immediate release fraction, C_{slow}: plasma concentration for the extended release fraction, DAT_{occ}: Occupancy of dopamine transporter, SKAMP: clinical rating score, pAUC: partial area under the curve, pAUEC: partial area under the effect curve, $corr_{DAT,PK}$: correlation between pAUC in DAT_{occ} and pharmacokinetics, $corr_{SKAMP,PK}$: correlation between pAUC in SKAMP and pharmacokinetics, $corr_{DAT,SKAMP}$: correlation between pAUC in DAT_{occ} and SKAMP.

Table 1. Parameter Values

Outcome	Parameter	Concerta parameter value [37]	Interindividual Variability (CV%)
PK	ka_{fast}	0.182	12.3
	ka_{slow}	0.258	29.9
	F_{fast}	0.557	9.1
	lag_{slow}	4.660	0
	Clearance	405.000	28.5
	Volume of distribution	816.000	33.3
DAT	$E_{max,DAT}$	85.080	0,12.3 or 17.5
	$EC_{50,start,DAT}$	2.680	0,12.3 or 17.5
	$ET_{max,DAT}$	1.000	0,12.3 or 17.5
	$t_{50,DAT}$	4.560	0,12.3 or 17.5
	$gamma_1$	1.000	0,12.3 or 17.5
SKAMP	$E_{max,SKAMP}$	27.800	0,12.3 or 17.5
	$EC_{50,start,SKAMP}$	7.550	0,12.3 or 17.5
	$ET_{max,SKAMP}$	1.000	0,12.3 or 17.5
	$t_{50,SKAMP}$	10.800	0,12.3 or 17.5
	$gamma_2$	4.230	0,12.3 or 17.5

POP-PKPD models

PK model

MPH plasma concentrations were simulated using a previously published ER POP-PK model, which is illustrated in Figure 2. The model splits the total dose into two fractions: the immediate release fraction (F_{fast}) and the extended release fraction (F_{slow}), which are absorbed at different rates. The immediate release fraction is rapidly absorbed into the bloodstream and produces a quick onset of the drug's effect, while the extended release fraction is slowly released over time, producing a sustained effect. Their absorption constants follow first-order kinetics, ka_{fast} and ka_{slow}, respectively. The model also includes a parameter which represents a delay time before the release of the ER fraction (lag_{slow}). Assuming that the dose is split completely between F_{fast} and F_{slow} (F_{slow} = 1 - F_{fast}), there are four PK parameters (quartet) describing the absorption of an ER formulation: F_{fast}, ka_{fast}, ka_{slow} and lag_{slow}.

In this work, we define the published absorption parameter values as those of the first formulation [37], which are given in Table 1. Using the POP-PK model described above, we simulate other formulations by varying the absorption parameter values with factors ranging from 0.5 to 1.5, by an additive step of 0.1. Thus, all other formulations are obtained with a different quartet of absorption parameter values. Since there are 4 absorption parameters, 14640 MPH formulations are simulated.

We simulate a parallel design with 40 subjects taking 54mg oral dose of MPH. The inter-individual variability (IIV) in PK parameters for all MPH formulations are identical and fixed to the values from the published model [37] (Table 1).

The concentrations are computed as:

$$C_{fast}(t) = \frac{ka_{fast}F_{fast}D}{V\left(ka_{fast} - k_e\right)}\left(e^{-k_e t} - e^{ka_{fast}t}\right)$$

$$C_{slow}(t) = \frac{ka_{slow}F_{slow}D}{V(ka_{slow} - k_e)}(e^{-k_e t} - e^{ka_{slow}t})$$

$$C_{plasma}(t) = C_{fast}(t) + C_{slow}(t)$$

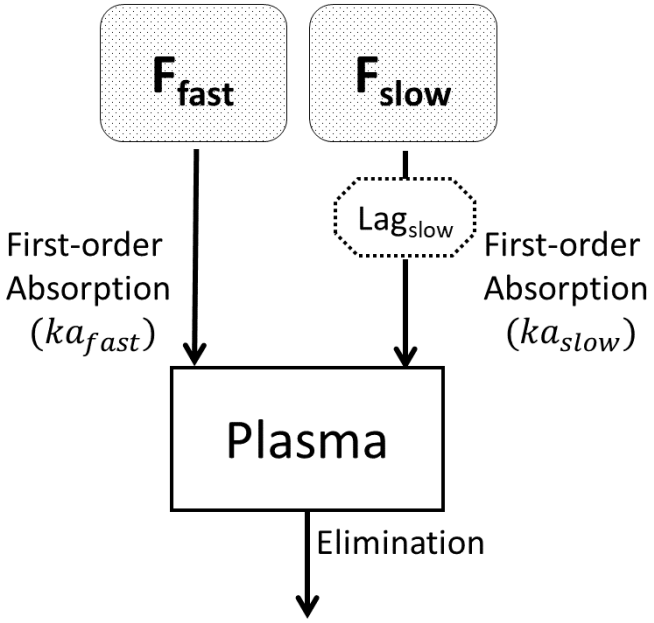

Figure 2. Illustration of the POP-PK model of Concerta. ka_{fast}: first-order absorption constant of the immediate release fraction, ka_{slow}: first-order absorption constant of the extended release fraction, F_{fast}: immediate release fraction of the formulation, F_{slow}: extended release fraction of the formulation, C_{plasma}: total plasma concentration

PD models

In this work, the PD outcomes of MPH are quantified by its target engagement and clinical rating scale scores, computed with a DAT_{occ} model and a SKAMP model, respectively. Each model is detailed below. Contrary to PK simulations, PD simulations were repeated with three levels of IIV: 0%, 12.3% and 17.5%. The IIV was applied to all parameters of the PD models and allows the assessment of variability on the PD outcomes.

DAT_{occ} model

Using a previously published model, we compute the DAT_{occ} [21]. The model takes into account the acute tolerance developed following MPH oral administration, expressed in terms of a time-varying EC_{50} :

$$DAT_{occ}(t) = \frac{E_{max,DAT} * C_{plasma}(t)}{EC_{50,DAT}(t) + C_{plasma}(t)}$$

$$EC_{50,DAT}(t) = EC_{50,start,DAT} * \left(1 + \frac{ET_{max,DAT} * t^{\gamma_1}}{t_{50,DAT}^{\gamma_1} + t^{\gamma_1}}\right)$$

where $E_{max,DAT}$ is the maximal DAT_{occ}, C_{plasma} is the plasma concentration of the drug, *t* is the time post-dose, $EC_{50,DAT}(t)$ is the concentration producing half of $E_{max,DAT}$ as a function of t, $EC_{50,start,DAT}$ is the estimated $EC_{50,DAT}$ at t=0 ($EC_{50,DAT}(t = 0)$), $ET_{max,DAT}$ is fixed to 1 [13], $t_{50,DAT}$ is the time observed for half of the increase in $EC_{50,DAT}$ from the baseline, and γ_1 is the steepness parameter representing the rate of change in $EC_{50,DAT}(t)$.

The parameter values are given in Table 1.

SKAMP model

Using a previously published model, we compute the SKAMP scores [13]. This model integrates the placebo effect, the drug effect and the acute tolerance observed following MPH oral administration. In this work, for a fair comparison between DAT_{occ} and SKAMP outcomes, only the MPH drug effect is considered. To stay consistent with the DAT_{occ}, an increase in SKAMP scores indicate an improvement in ADHD symptoms in this work:

$$SKAMP(t) = \frac{E_{max,SKAMP} * C_{plasma}(t)}{EC_{50,SKAMP}(t) + C_{plasma}(t)}$$

$$EC_{50,SKAMP}(t) = EC_{50,start,SKAMP} * \left(1 + \frac{ET_{max,SKAMP} * t^{\gamma_2}}{t_{50,SKAMP}^{\gamma_2} + t^{\gamma_2}}\right)$$

where $E_{max,SKAMP}$ is the maximal SKAMP score, C_{plasma} is the plasma concentration of the drug, *t* is the time post-dose, $EC_{50,SKAMP}(t)$ is the concentration producing half of E_{max} as a function

of t, $EC_{50,start,SKAMP}$ is the estimated $EC_{50,SKAMP}$ at t=0 ($EC_{50,SKAMP}(t=0)$), $ET_{max,SKAMP}$ is fixed to 1 [13], $t_{50,SKAMP}$ is the time observed for half of the increase in EC_{50} from the baseline, and γ_2 is the steepness parameter representing the rate of change in $EC_{50,SKAMP}(t)$.

Correlation computation

The correlation coefficient between the pAUC of each outcome from early to late exposure (0-3h, 3-7h, 7-12h) is computed. For each formulation, the correlation between its pAUC in DAT_{occ} and PK ($corr_{DAT,PK}$), the correlation between pAUC in SKAMP and PK ($corr_{SKAMP,PK}$) and the correlation between pAUC in DAT and SKAMP ($corr_{DAT,SKAMP}$) were computed.

Influence of absorption parameters

Each formulation is compared to Concerta in terms of $pAUC_{PK}$, $pAUC_{DAT}$ and $pAUC_{SKAMP}$. To assess if they both differ, we rely on the statistical computations used in the average bioequivalence, namely computing a confidence interval (CI) with an ANOVA. It is computed for $pAUC_{PK}$, $pAUC_{DAT}$ and $pAUC_{SKAMP}$.

Following an ANOVA analysis, the pAUC's 90% confidence interval is calculated as:

$$CI_{90} = \mu_2 - \mu_1 + t_{1-\alpha,n_1+n_2-2}\widehat{\sigma_w}\sqrt{\left(\frac{1}{2}\left(\frac{1}{n_1}+\frac{1}{n_2}\right)\right)}$$

$$\widehat{\sigma_w} = \sqrt{MS_{within}}$$

where μ_1 and μ_2 are the mean of the $pAUC_{PK}$, $pAUC_{DAT}$ or $pAUC_{SKAMP}$ for formulations 1 and 2, n_1 and n_2 are the number of subjects for each sequence, $\sqrt{MS_{within}}$ is the mean square error resulting from the ANOVA analysis.

The difference between both formulations, or lack thereof, is determined similarly to the average bioequivalence. If the 90% confidence interval of the ratio of $pAUC_2/pAUC_1$ falls between 0.8-1.25, the test formulation is similar to the reference formulation in terms of PK or PD (DAT_{occ} or SKAMP scores).

Results

Illustration of PK, DAT_{occ} and SKAMP scores

The plasma concentrations, DAT_{occ} and SKAMP scores curves for the first formulation (Concerta) are illustrated in Figure 3 (with the maximal level of IIV).

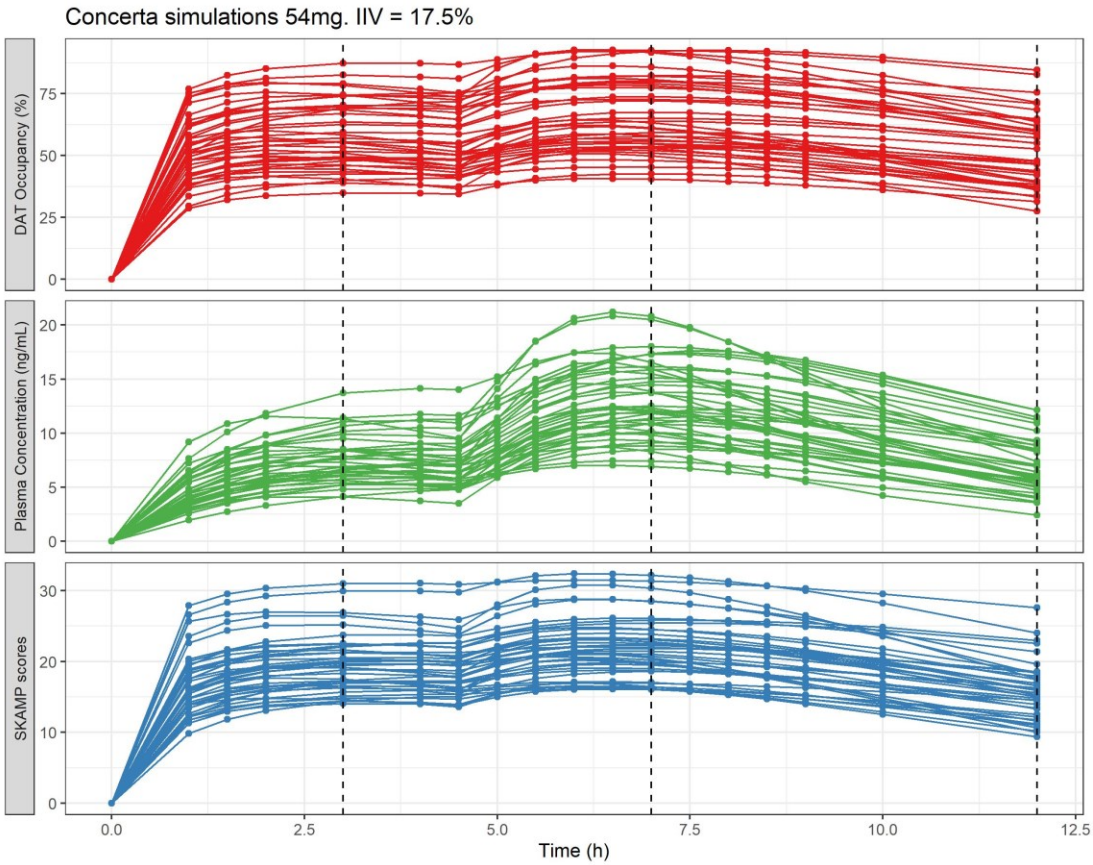

Figure 3. Plasma concentration, dopamine transporter (DAT) occupancy and SKAMP scores of the first formulation as a function of time for 40 subjects after 54mg of MPH oral administration. The vertical dashed lines represent the cut-off of partial areas under the curve (3, 7 and 12h post-dose). The interindividual variability (IIV) is equal to 17.5%

Correlation of DAT, SKAMP and PK

In this study, we first aimed to explore the relationship between PK, DAT_{occ} and SKAMP outcomes. We computed $corr_{DAT,PK}$, $corr_{SKAMP,PK}$ and $corr_{DAT,SKAMP}$, which are depicted in

Figure 4 and which values are presented in Table 2. Figure 5 illustrates the relationship between the $pAUC_{DAT}$ and $pAUC_{SKAMP}$ for each formulation.

Based on these results, it can be inferred that in the absence of IIV in PD response (IIV=0%), the correlation between PK and PD outcomes ($corr_{DAT,PK}$ and $corr_{SKAMP,PK}$) for pAUC0-3h and pAUC3-7h are comparable, with values around 0.96. The $corr_{DAT,SKAMP}$ is perfect as no IIV in PD is simulated. This can be seen in Figure 5 (a), where we observe a straight line between $pAUC_{DAT}$ and $pAUC_{SKAMP}$.

When IIV = 12.3%, all correlation coefficients decrease. In Figure 5 (b), a discernible increase in variance is evident for the 7-12h, in contrast to 0-3h or 3-7h. The decrease in correlation coefficients is particularly evident for $pAUC_{7-12h}$. Specifically, $corr_{DAT,SKAMP}$ drops by 0.14, while $corr_{DAT,PK}$ and $corr_{SKAMP,PK}$ decrease by 0.07 and 0.08, respectively. This variation is a consequence of the dynamic changes in EC_{50} through the course of the day for both SKAMP scores and DAT_{occ}. Indeed, Figure 6 reveals that the increase in $EC_{50,SKAMP}$ is substantially more pronounced than that of $EC_{50,DAT}$, driven by the higher $t_{50,SKAMP}$ and γ_2. Notably, this discrepancy in the trend of $EC_{50,SKAMP}$ and $EC_{50,DAT}$ is most salient during the 7-12h range. Figure 6 suggests that the acute tolerance observed in DAT_{occ} and SKAMP scores may not be entirely correlated. Specifically, $EC_{50,DAT}$ increases significantly in the first five hours post-dose, whereas $EC_{50,SKAMP}$ remains relatively constant at those hours. Conversely, after five hours post-dose, $EC_{50,SKAMP}$ increases at a much faster rate than $EC_{50,DAT}$.

The trends observed in simulations with IIV = 12.3% are the same as IIV = 17.5%. Specifically, all correlations decrease, with the lowest values observed for $pAUC_{7-12h}$. Moreover, $corr_{DAT,SKAMP}$ reaches its minimum value at this time interval. In Figure 5 (c), the scatter is similar to the one in Figure 5 (b). However, increasing IIV has increased the variance.

Table 2. Correlation between SKAMP and DAT and PK pAUC for different IIV values in DAT and SKAMP models. Each pAUC is obtained from a simulated clinical trial of 40 subjects taking the same simulated generic of MPH.

Interindividual variability (CV%)	**pAUC Time range**	$corr_{DAT,SKAMP}$	$corr_{DAT,PK}$	$corr_{SKAMP,PK}$
0	0-3h	1.00	0.96	0.96
	3-7h	1.00	0.96	0.95
	7-12h	1.00	0.98	0.98
12.3	0-3h	0.99	0.95	0.95
	3-7h	0.97	0.95	0.94
	7-12h	0.86	0.91	0.90
17.5	0-3h	0.97	0.95	0.94
	3-7h	0.95	0.93	0.92
	7-12h	0.75	0.85	0.84

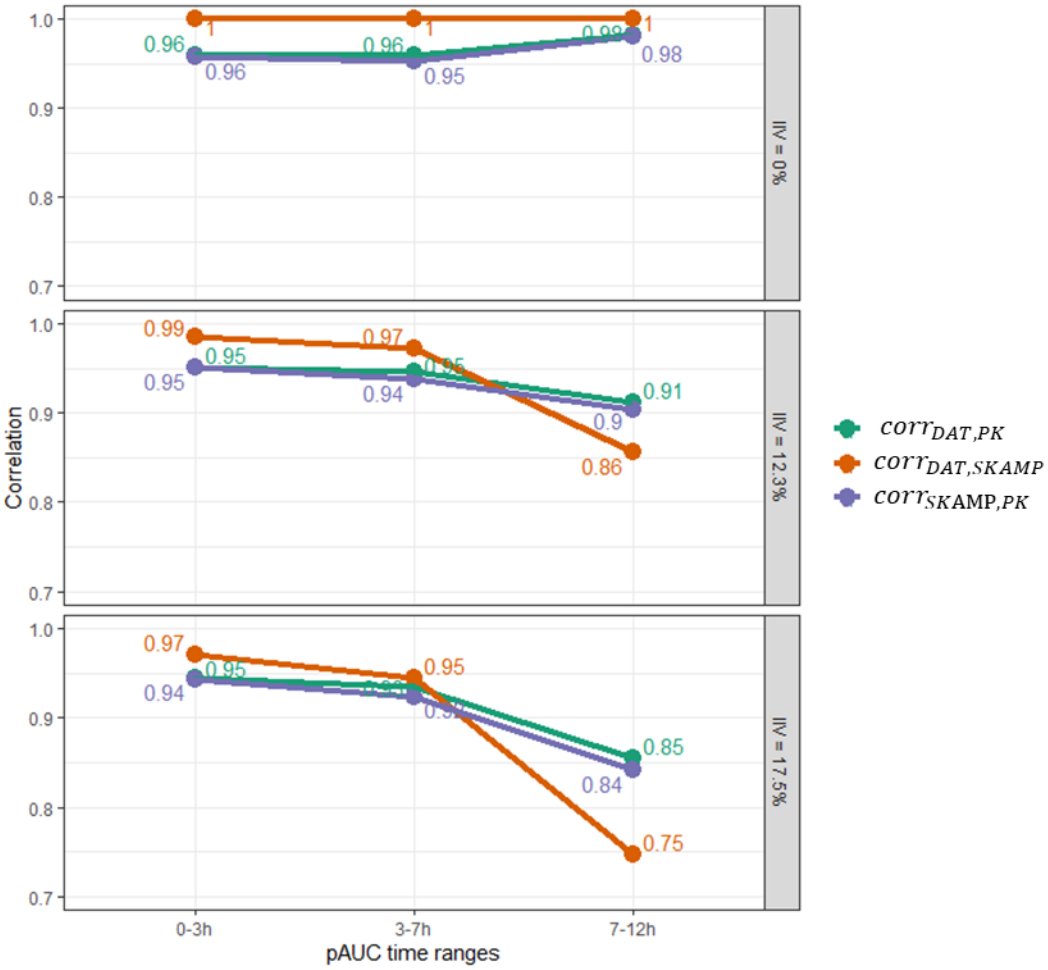

Figure 4. Correlation between the partial area under the curve (pAUC) of SKAMP, dopamine transporter (DAT) occupancy and pharmacokinetics (PK) outcomes for different interindividual variability (IIV) values. Each pAUC is obtained from a simulated clinical trial of 40 subjects taking the same formulation of MPH.

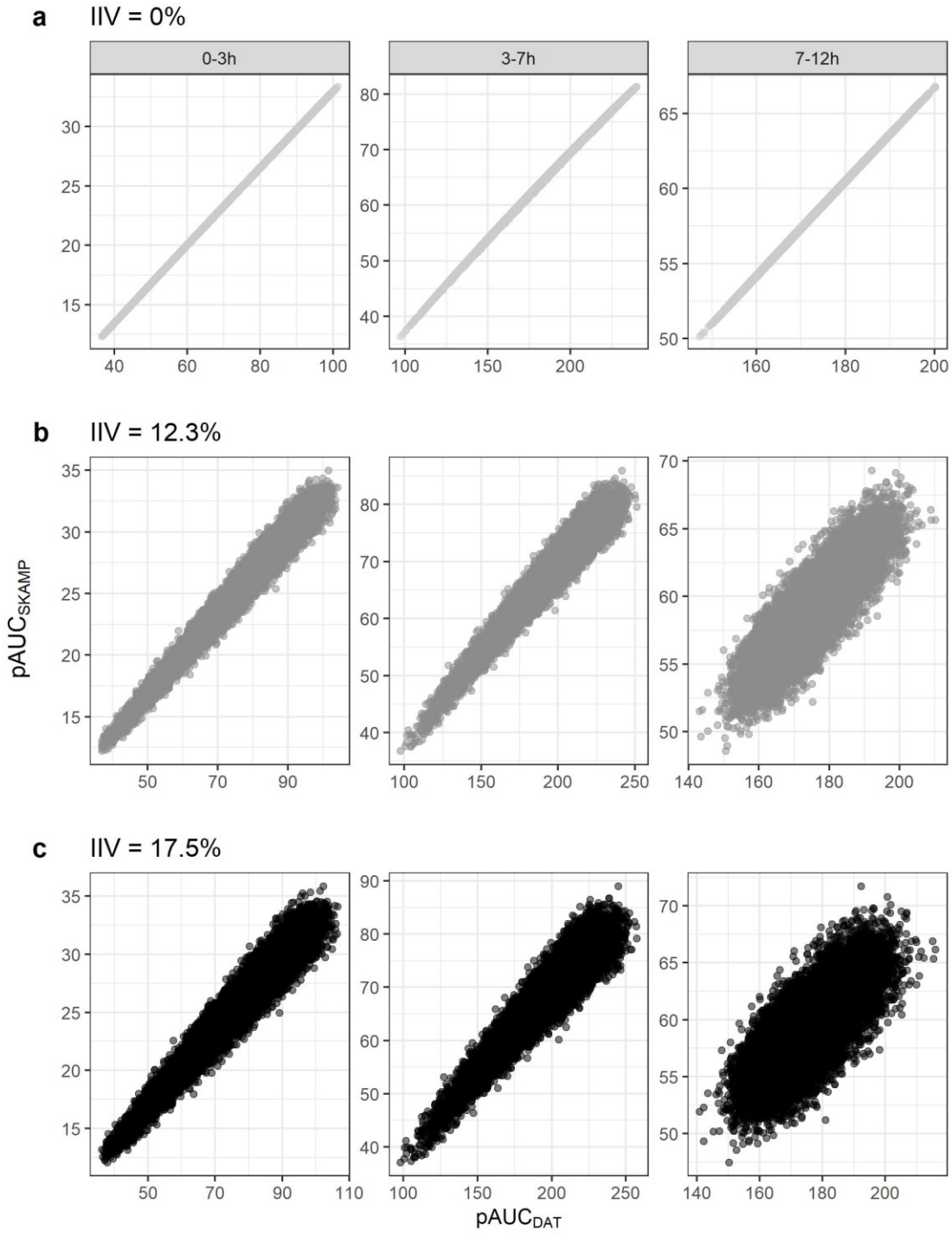

Figure 5. Partial area under the curve of SKAMP ($pAUC_{SKAMP}$) as a function of partial area under the curve of dopamine transporter occupancy ($pAUC_{DAT}$). Panels a, b, and c show the results with an interindividual variability (IIV) of 0%, 12.3% and 17.5% respectively. IIV: interindividual variability, pAUC: partial area under the curve.

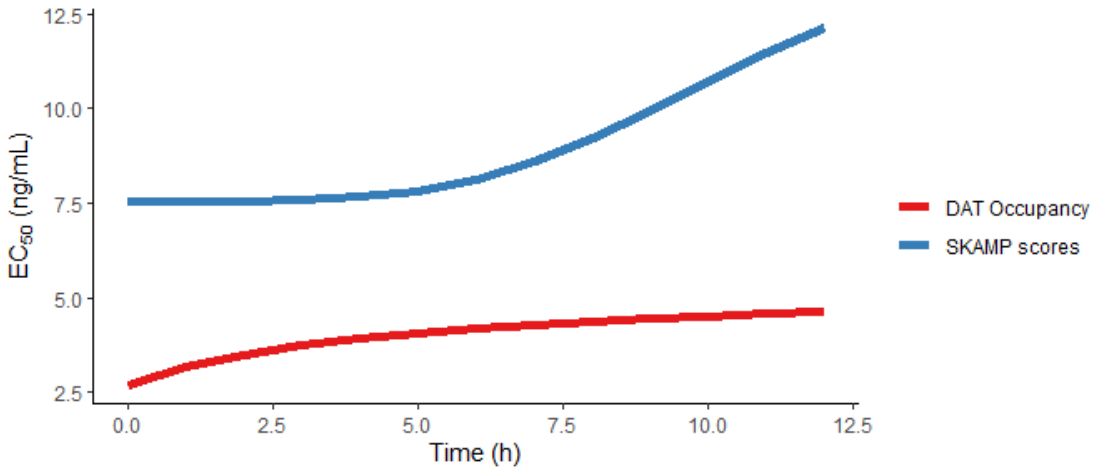

Figure 6. EC_{50} of a typical patient as a function of time. The red curve represents the EC50 of DAT_{occ} and the blue curve represents the EC50 of SKAMP scores.

Influence of PK absorption parameters on pAUC

To explore the absorption parameters that affect the similarity between MPH formulations, we assessed the percentage of test drugs that showed statistically significant differences from Concerta. Our simulations aimed to identify the absorption parameters that influence the PK, DAT_{occ} and SKAMP curves, as illustrated in Figure 7.

Analysis of PK

The simulations revealed that a large proportion of formulations differ from Concerta in PK, as depicted by the consistently highest green line in Figure 7. This is attributed to a wider range in the ratio of $\frac{pAUC_2}{pAUC_1}$ for PK outcomes compared to PD outcomes (as demonstrated by Figure S1 in the supplementary information).

Our analysis indicated that some absorption parameters had a more pronounced effect on $pAUC_{PK}$ than others, resulting in dips in Figure 7. Specifically, for $pAUC_{PK,0-3h}$, we observed that ka_{fast} and F_{fast} had a notable impact on BE. Specifically, the lowest percentage of formulations that failed BE was observed when ka_{fast} and F_{fast} were set to 0.8 and 0.7, respectively. In contrast, lag_{slow} and ka_{slow} did not affect $pAUC_{PK,0-3h}$, as evidenced by a constant percentage

of simulations across all levels of these parameters. The influence of ka_{fast} and F_{fast} on $pAUC_{PK,0-3h}$ is expected, as they are the only parameters that contribute to the PK curves before 3 hours post-dose.

For $pAUC_{PK,3-7h}$, lag_{slow} had a significant impact on the results (Figure 7). The PK curves for $lag_{slow} = 0.5$ are shown in the second row of Figure 8 (a) and help visualize the importance of lag_{slow}. It can be seen that test drugs with small values of lag_{slow} (black curves in Figure 8) will have a second release of MPH much earlier, drastically changing the $pAUC_{PK,3-7h}$ compared to the reference drug (green dashed curve in Figure 8). Moreover, we noted that an increase in F_{fast} decreased the percentage of simulations that differ from the reference drug for 3-7h. Since large values of F_{fast} indicate that a smaller fraction of the drug will be release in later times post-dose, these results are expected.

Finally, for $pAUC_{PK,7-12h}$, we found that lag_{slow} had a significant impact. However, contrary to $pAUC_{PK,3-7h}$, factors for lag_{slow} which are larger than 1 do not lead to a higher proportion of simulations that differ from Concerta. This was expected, as the reference value for lag_{slow} is 4.66, and even with the largest factor of 1.5, lag_{slow} remained below 7h post-dose. We also observed that smaller values of F_{fast} led to a plateau, while larger values increased the percentage of simulations that failed BE. Similarly to $pAUC_{PK,3-7h}$, the impact of F_{fast} on $pAUC_{PK,7-12h}$ makes sense because a smaller fraction of the drug is released at 7-12h post-dose. Furthermore, we found that reducing ka_{slow} by 25% (i.e., setting the ka_{slow} factor to 0.75) resulted in the lowest percentage of simulations that differ from the reference drug for 7-12h.

The results show that a multiplicative factor of 1 does not always result in the lowest percentage of simulations which differ from the reference drug. This can be attributed to the fact that while a specific multiplicative factor may have a value of 1, other parameters vary from 0.5-1.5 and lead to changes in the simulations compared to the reference drug. Therefore, the trends in Figure 7 have greater significance in determining which absorption parameters have an effect on pAUC compared to examining the individual PK parameter factors.

Analysis of DAT_{occ}

As can be seen in Figure 7, only F_{fast} and ka_{fast} exhibited a dip in the curve for $pAUC_{DAT,0-3h}$, which occurs approximately when the factors are 1.2. This observation is consistent with the expected behavior of the drug formulations, as F_{fast} and ka_{fast} are known to impact the absorption and bioavailability of the drug during the early stages of drug release.

In the analysis of $pAUC_{DAT,3-7h}$, we found that lag_{slow} and F_{fast} had the most significant effect, while ka_{fast} had only a minor impact. Increasing lag_{slow} more than one-fold of the reference value increases significantly the percentage of simulations which differ from Concerta. For the same reason as $pAUC_{PK,0-3h}$, the influence of lag_{slow} and F_{fast} on $pAUC_{DAT,3-7h}$ is expected. Moreover, it is worth noting that the trends observed in the PK and DAT curves are consistent with each other, except for the low values of lag_{slow}. As illustrated in Figure 8 (a), this is because a small lag_{slow} increases the plasma concentration from 3-7h significantly more compared to the DAT_{occ} at the same times.

Finally, for $pAUC_{DAT,7-12h}$, we observed that increasing F_{fast} resulted in a higher percentage of simulations which differ from Concerta, whereas increasing lag_{slow} led to a lower percentage. These findings are consistent with those for $pAUC_{PK,7-12h}$. Additionally, while ka_{fast} does not impact $pAUC_{PK,7-12h}$, it has an impact on $pAUC_{DAT,7-12h}$. This is illustrated in Figure 8 (b) and (c) which show the smallest and largest factors of ka_{fast}. We observe that the highest value of ka_{fast} produces a more abrupt slope in DAT_{occ} than the lowest values of ka_{fast}. This is not observed in plasma concentrations.

Analysis of SKAMP

The simulations conducted on the SKAMP outcome exhibited similar trends to the DAT metric, with the SKAMP results consistently being the lowest, except for $pAUC_{SKAMP,7-12h}$, where DAT_{occ} and SKAMP results are much closer.

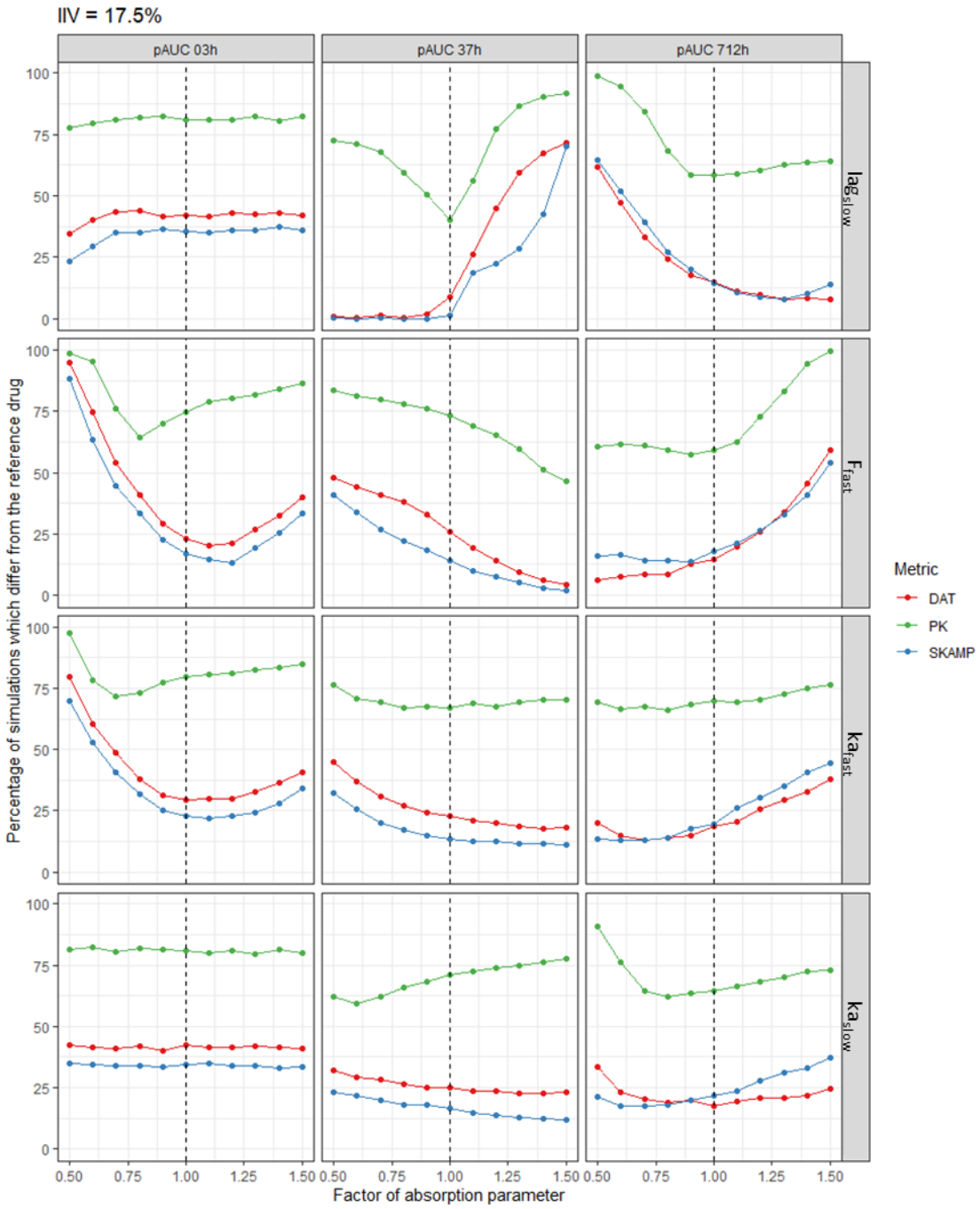

Figure 7. Percentage of simulations which differ from Concerta for each absorption parameter value. pAUC: partial area under the curve, ka_{fast}: first-order absorption constant of the immediate release fraction, ka_{slow}: first-order absorption constant of the extended release fraction, F_{fast}: immediate release fraction of the formulation, F_{slow}: extended release fraction of the formulation.

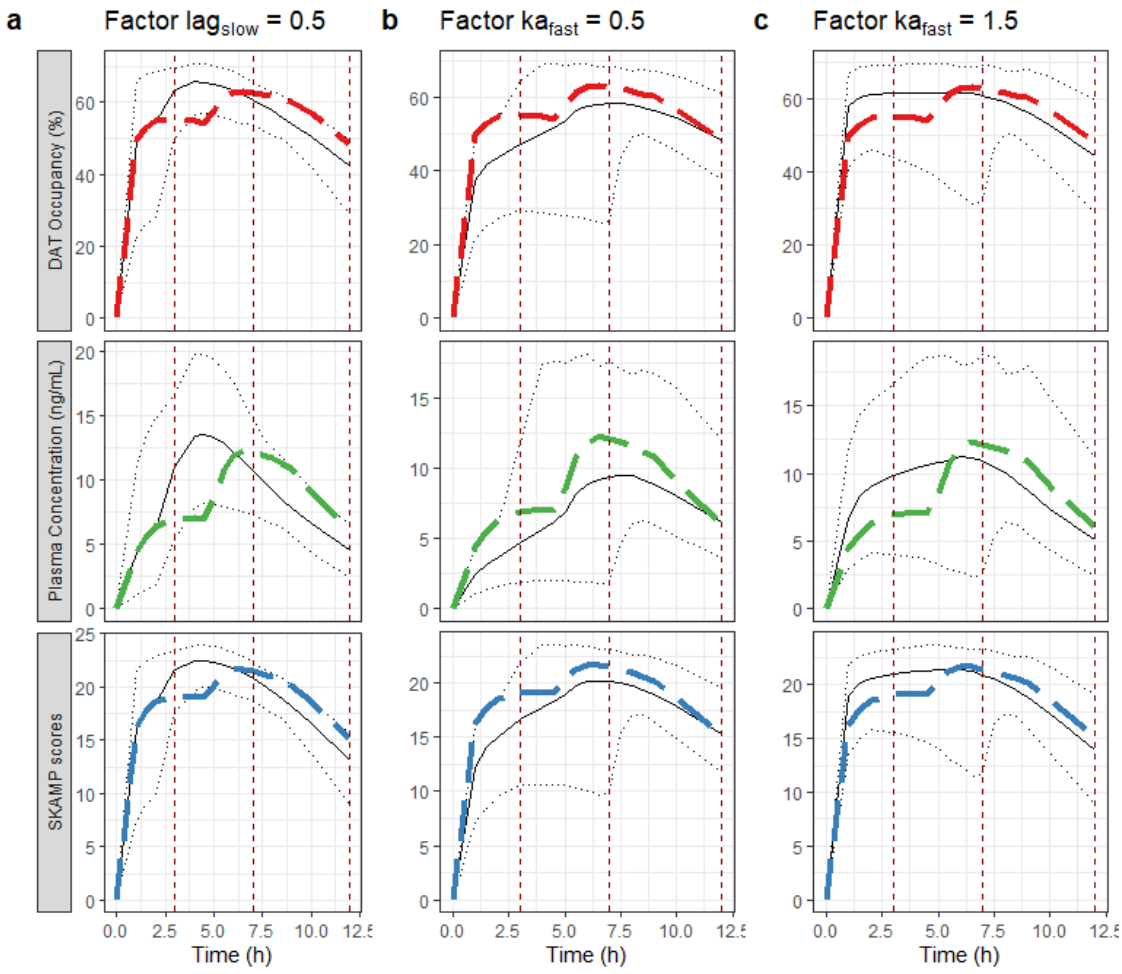

Figure 8. Plasma concentration, dopamine transporter (DAT) occupancy and SKAMP scores for Concerta and other simulations with a factor of (a) lag_{slow}=0.5, (b) ka_{fast}=0.5, (c) ka_{fast}=1.5 and interindividual variability of 0%. The colored lines represent the median of 40 subjects taking 54mg of Concerta. The solid black line represents the median values across all simulations and the dotted lines represent the minimal and maximal values. The red vertical dashed lines are the time limits 3h, 7h and 12h post-dose.

Discussion

In the cascade of neurobiological events, the initial link comprises the occupancy of DAT, while the ultimate endpoint corresponds to the SKAMP scores. In a manner akin to the game of "telephone", the objective of this study was to explore if changes at the microscopic level

(DAT_{occ}) are partially or totally translated into changes at the macroscopic level (SKAMP scores). Thus, we investigated whether changes in DAT_{occ} were correlated with changes in SKAMP scores. As well, we examined how different formulations of MPH impact the DAT_{occ} and subsequently, the SKAMP scores.

Correlations in PK and PD

Based on the findings of this study, it can be inferred that the correlation between pAUC values of any of the outcomes (PK, DAT_{occ}, and SKAMP scores) is contingent on both the IIV and the specific time frame analyzed (0-3h, 3-7h or 7-12h post-dose). The correlation coefficients were observed to decrease as IIV increases, with the weakest correlations observed for $pAUC_{7-12h}$.

When IIV $\neq 0$, we observe that $corr_{DAT,SKAMP}$ is consistently higher than $corr_{DAT,PK}$ or $corr_{SKAMP,PK}$, except for $pAUC_{7-12h}$ where we observed that $corr_{DAT,SKAMP}$ is lower. This may be attributed to the changes in EC_{50} values throughout the day for both SKAMP scores and DAT_{occ}, suggesting that the strength of the association between them weakens over time. The acute tolerance to MPH in DAT_{occ} occurs early on, while the tolerance in SKAMP scores is delayed and observed after 7 hours post-dose. This implies that the acute tolerance to MPH does not manifest at the same time for DAT_{occ} and SKAMP scores. Thus, it may be hypothesized that the acute tolerance in DAT_{occ} and SKAMP scores are not explained by the same phenomenon. An alternative hypothesis may be that a time delay between the occupancy of DAT by MPH and the onset of the effect on SKAMP scores is responsible for this discrepancy. However, since the onset of action for MPH is very short (30-120 minutes), this hypothesis is less probable. Regardless of the underlying mechanism, it is plausible to assume that the acute tolerance to MPH observed in SKAMP scores is only partially explained by the acute tolerance in DAT.

Regarding the correlation between PK and PD outcomes (DAT_{occ} and SKAMP), our findings suggest that PK of MPH may not be the most representative of PD during the 7-12 hour post-dose period. Acute tolerance is taken into account during this period, which is not possible with PK outcomes, thus resulting in a reduced correlation between PK and PD measures. As a result, the use of $pAUC_{PK,7-12h}$ as a metric for assessing the efficacy of MPH in bioequivalence trials may not be appropriate when considering the acute tolerance.

It is worth noting that previous studies analyzed $corr_{SKAMP,PK}$, with slightly different results. While our findings for IIV = 12.3% show correlation coefficients of 0.95,0.94,0.90 for $pAUC_{0-3h}$, $pAUC_{3-7h}$ and $pAUC_{7-12h}$, respectively, a previous study found correlation coefficients of 0.97, 0.8 and 0.94 for the same timeframes [22]. These differences could be attributed to a combination of factors, such as the larger IIV in our study (IIV of 10% in [22]), the differences in the absorption parameters that were varied (only ka_{fast} and ka_{slow} in [22]) and the inclusion of placebo effects in the previous study's SKAMP model.

When increasing the IIV in simulations, more variability is introduced and lead to lower correlation coefficients between different metrics. The discrepancy is observed at the time associated with the lowest $corr_{SKAMP,PK}$. While we note that $corr_{SKAMP,PK}$ is lowest for $pAUC_{7-12h}$, the results in [22] show that it is lowest for $pAUC_{3-7h}$. The authors mention that their simulations at 3-7h post-dose had a wider CI and this may have caused the drop in $corr_{SKAMP,PK}$ at 3-7h.

An important element to consider in the correlation between DAT_{occ} and SKAMP is the level of efficacy that they represent. DAT_{occ} has the advantage of being an outcome that is purely related to MPH efficacy because it is directly representative of its target engagement. On the other hand, many more confounding factors occur between oral administration of MPH and the measurement of SKAMP scores. Trying to find if DAT_{occ} can be translated into SKAMP scores might be perceived as a big jump between those two levels of efficacy because of the complex mechanistic components that exist between DAT and behavior. However, this analysis still provides insight into their correlation. For example, since we find that a change in DAT_{occ} can be partially translated in SKAMP scores, we might hypothesize that the acute tolerance observed on clinical rating scales may be partially explained by DAT_{occ}.

Influence of absorption parameters

The second part of this work aimed to investigate the impact of different MPH formulations on DAT_{occ} and subsequent changes in the SKAMP scores. Our results indicated that certain absorption parameters had a more significant influence on the PK, DAT_{occ}, and SKAMP outcomes than others. Moreover, our simulations show that $pAUC_{DAT}$ and $pAUC_{SKAMP}$ were less stringent

than $pAUC_{PK}$ when distinguishing between two formulations. For any $pAUC_{0-3h}$, we found that only ka_{fast} and F_{fast} had a discernible impact, while lag_{slow} and F_{fast} were identified as the key absorption parameters for $pAUC_{3-7h}$ and $pAUC_{7-12h}$. These results are in agreement with a previous study, which also demonstrated that decreasing absorption parameter values had a greater effect on the likelihood of bioequivalence failure compared to increasing them [22].

Limitations and future work

It is important to note that the POP-PD model used to estimate DAT_{occ} used in this study has some limitations [21]. One of them is that the model parameters were estimated using data with imprecise sampling times, which were digitally extracted from multiple studies [15, 18, 19, 20]. This has necessitated the fixing of γ_2 to 1, whereas it was was estimated in the SKAMP model. Consequentially, further studies with more precise data are warranted to validate the observed correlations between DAT_{occ} and SKAMP in this study, particularly those from 7-12h.

Exploring POP-PK models with more detailed time delays would be a valuable next step. Given the impact of lag_{slow} on PK, DAT_{occ} and SKAMP observed in our results, it would be informative to investigate the impact of a continuous release. In this work, the current PK model uses a simple delay of a number of hours during which $C_{slow}(t) = 0$. More complex models could incorporate transit compartments to simulate a gradual delay.

Finally, it is important to note that the therapeutic properties of MPH are influenced not only by DAT_{occ} but also by NET_{occ}, with MPH exhibiting even greater affinity towards NET than DAT. Given the scarcity of NET_{occ} data in existing literature, this work has exclusively focused on DAT_{occ} as the primary determinant of the clinical response to MPH. Consequently, the correlation between DAT_{occ} and SKAMP represents an incomplete representation, as NET_{occ} serves as a significant connection and driver of the clinical response.

Conclusion

This work quantified the relationship between the DAT_{occ} and the clinical outcome and provided insight into which absorption parameters are most important for optimizing the clinical and

therapeutic effects of MPH. Understanding the PK and PD profiles of different formulations of MPH is crucial for optimizing treatment outcomes for individuals with ADHD.

Acknowledgements

We wish to thank Holly Kimko and Leonid Gibiansky for sharing their code for the SKAMP model.

References

[1] Jaeschke RR, Sujkowska E, Sowa-Kućma M. Methylphenidate for attention-deficit/hyperactivity disorder in adults: A narrative review. *Psychopharmacology* 2021; 238: 2667–2691.

[2] Childress AC. Stimulants. *Child and Adolescent Psychiatric Clinics of North America* 2022; 31: 373–392.

[3] Raman SR, Man KKC, Bahmanyar S, et al. Trends in attention-deficit hyperactivity disorder medication use: A retrospective observational study using population-based databases. *The Lancet Psychiatry* 2018; 5: 824–835.

[4] Cortese S, Adamo N, Del Giovane C, et al. Comparative efficacy and tolerability of medications for attention-deficit hyperactivity disorder in children, adolescents, and adults: A systematic review and network meta-analysis. *The Lancet Psychiatry* 2018; 5: 727–738.

[5] Volkow ND, Wang G-J, Fowler JS, et al. Therapeutic Doses of Oral Methylphenidate Significantly Increase Extracellular Dopamine in the Human Brain. 5.

[6] Markowitz JT, Oberdhan D, Ciesluk A, et al. Review of Clinical Outcome Assessments in Pediatric Attention-Deficit/Hyperactivity Disorder. *Neuropsychiatric Disease and Treatment* 2020; 16: 1619–1643.

[7] Swanson JM. Long-acting stimulants: Development and dosing. *The Canadian Child and Adolescent Psychiatry Review* 2005; 14: 4–9.

[8] Swanson J, Gupta S, Guinta D, et al. Acute tolerance to methylphenidate in the treatment of attention deficit hyperactivity disorder in children. *Clinical Pharmacology & Therapeutics* 1999; 66: 295–305.

[9] Swanson JM, Volkow ND. Pharmacokinetic and pharmacodynamic properties of stimulants: Implications for the design of new treatments for ADHD. *Behavioural Brain Research* 2002; 130: 73–78.

[10] Srinivas NR, Hubbard JW, Quinn D, et al. Enantioselective pharmacokinetics and pharmacodynamics of dl-threo-methylphenidate in children with attention deficit hyperactivity disorder. *Clinical Pharmacology and Therapeutics* 1992; 52: 561–568.

[11] Teuscher NS, Sikes CR, McMahen R, et al. Population Pharmacokinetic-Pharmacodynamic Modeling of a Novel Methylphenidate Extended-Release Orally Disintegrating Tablet in Pediatric Patients With Attention-Deficit/Hyperactivity Disorder. *Journal of Clinical Psychopharmacology* 2018; 38: 8.

[12] Gomeni R, Komolova M, Incledon B, et al. Model-Based Approach for Establishing the Predicted Clinical Response of a Delayed-Release and Extended-Release Methylphenidate for the Treatment of Attention-Deficit/Hyperactivity Disorder. *Journal of Clinical Psychopharmacology* 2020 Jul/Aug; 40: 350–358.

[13] Kimko H, Gibiansky E, Gibiansky L, et al. Population pharmacodynamic modeling of various extended- release formulations of methylphenidate in children with attention deficit hyperactivity disorder via meta-analysis. *J Pharmacokinet Pharmacodyn* 2012; 16.

[14] Sachdev PS, Trollor JN. How high a dose of stimulant medication in adult attention deficit hyperactivity disorder? *The Australian and New Zealand Journal of Psychiatry* 2000; 34: 645–650.

[15] Volkow ND, Gatley SJ, Hitzemann R. Dopamine Transporter Occupancies in the Human Brain Induced by Therapeutic Doses of Oral Methylphenidate. *Am J Psychiatry* 1998; 7.

[16] Fowler JS, Volkow ND, Ding Y-S, et al. Positron Emission Tomography Studies of DopamineEnhancing Drugs. 4.

[17] Volkow ND, Wang GJ, Fowler JS, et al. Blockade of striatal dopamine transporters by intravenous methylphenidate is not sufficient to induce self-reports of "high". *The Journal of Pharmacology and Experimental Therapeutics* 1999; 288: 14–20.

[18] Spencer TJ, Biederman J, Ciccone PE. PET Study Examining Pharmacokinetics, Detection and Likeability, and Dopamine Transporter Receptor Occupancy of Short- and Long-Acting Oral Methylphenidate. *Am J Psychiatry* 2006; 9.

[19] Spencer TJ, Bonab AA, Dougherty DD, et al. Understanding the central pharmacokinetics of spheroidal oral drug absorption system (SODAS) dexmethylphenidate: A positron emission tomography study of dopamine transporter receptor occupancy measured with C-11 altropane. *The Journal of Clinical Psychiatry* 2012; 73: 346–352.

[20] Spencer TJ, Bonab AA, Dougherty DD, et al. A PET study examining pharmacokinetics and dopamine transporter occupancy of two long-acting formulations of methylphenidate in adults. *INTERNATIONAL JOURNAL OF MOLECULAR MEDICINE* 2010; 5.

[21] Soufsaf S, Robaey P, Nekka F. An exploratory analysis of the performance of methylphenidate regimens based on a PKPD model of dopamine and norepinephrine transporter occupancy. *Journal of Pharmacokinetics and Pharmacodynamics*. Epub ahead of print March 2023. DOI: 10.1007/s10928-023-09854-y.

[22] Jackson AJ, Foehl HC. A Simulation Study of the Comparative Performance of Partial Area under the Curve (pAUC) and Partial Area under the Effect Curve (pAUEC) Metrics in Crossover Versus Replicated Crossover Bioequivalence Studies for Concerta and Ritalin LA. *The AAPS Journal* 2022; 24: 80.

[23] Gomeni R, Bressolle-Gomeni F, Spencer TJ, et al. Model-Based Approach for Optimizing Study Design and Clinical Drug Performances of Extended-Release Formulations of Methylphenidate for the Treatment of ADHD. *Clinical Pharmacology and Therapeutics* 2017; 102: 951–960.

[24] Bloomingdale P, Karelina T, Ramakrishnan V, et al. Hallmarks of neurodegenerative disease: A systems pharmacology perspective. *CPT: pharmacometrics & systems pharmacology* 2022; 11: 1399–1429.

[25] Bloomingdale P, Karelina T, Cirit M, et al. Quantitative systems pharmacology in neuroscience: Novel methodologies and technologies. *CPT: pharmacometrics & systems pharmacology* 2021; 10: 412–419.

[26] Gutiérrez-Casares JR, Quintero J, Jorba G, et al. Methods to Develop an in silico Clinical Trial: Computational Head-to-Head Comparison of Lisdexamfetamine and Methylphenidate. *Frontiers in Psychiatry* 2021; 12: 741170.

[27] Shimizu R, Horiguchi N, Yano K, et al. Pharmacokinetic-Pharmacodynamic Modeling of Brain Dopamine Levels Based on Dopamine Transporter Occupancy after Administration of Methylphenidate in Rats. *J Pharmacol Exp Ther* 2019; 369: 78–87.

[28] Kielbasa W, Stratford RE Jr. Exploratory translational modeling approach in drug development to predict human brain pharmacokinetics and pharmacologically relevant clinical doses. *Drug Metab Dispos* 2012; 40: 877–83.

[29] Kielbasa W, Kalvass JC, Stratford R. Microdialysis evaluation of atomoxetine brain penetration and central nervous system pharmacokinetics in rats. *Drug Metabolism and Disposition: The Biological Fate of Chemicals* 2009; 37: 137–142.

[30] Coghill D, Banaschewski T, Zuddas A, et al. Long-acting methylphenidate formulations in the treatment of attention-deficit/hyperactivity disorder: A systematic review of head-to-head studies. 2013; 24.

[31] Chen ML, Lesko L, Williams RL. Measures of exposure versus measures of rate and extent of absorption. *Clin Pharmacokinet* 2001; 40: 565–72.

[32] U.S. Food and Drug Administration. Draft Guidance on Methylphenidate.

[33] Endrenyi L, Tothfalusi L. Do regulatory bioequivalence requirements adequately reflect the therapeutic equivalence of modified-release drug products? *Journal of Pharmacy &*

Pharmaceutical Sciences: A Publication of the Canadian Society for Pharmaceutical Sciences, Societe Canadienne Des Sciences Pharmaceutiques 2010; 13: 107–113.

[34] Chen M-L. An alternative approach for assessment of rate of absorption in bioequivalence studies. *Pharmaceutical research* 1992; 9: 1380–1385.

[35] Teicher MH, Polcari A, Foley M, et al. Methylphenidate blood levels and therapeutic response in children with attention-deficit hyperactivity disorder: I. Effects of different dosing regimens. *Journal of Child and Adolescent Psychopharmacology* 2006; 16: 416–431.

[36] Coghill D, Seth S. Effective management of attention-deficit/hyperactivity disorder (ADHD) through structured re-assessment: The Dundee ADHD Clinical Care Pathway. *Child and adolescent psychiatry and mental health* 2015; 9: 1–14.

[37] Soufsaf S, Robaey P, Bonnefois G, et al. A Quantitative Comparison Approach for Methylphenidate Drug Regimens in Attention-Deficit/Hyperactivity Disorder Treatment. *J Child Adolesc Psychopharmacol*. Epub ahead of print February 2019. DOI: 10.1089/cap.2018.0093.

Supplementary Figure

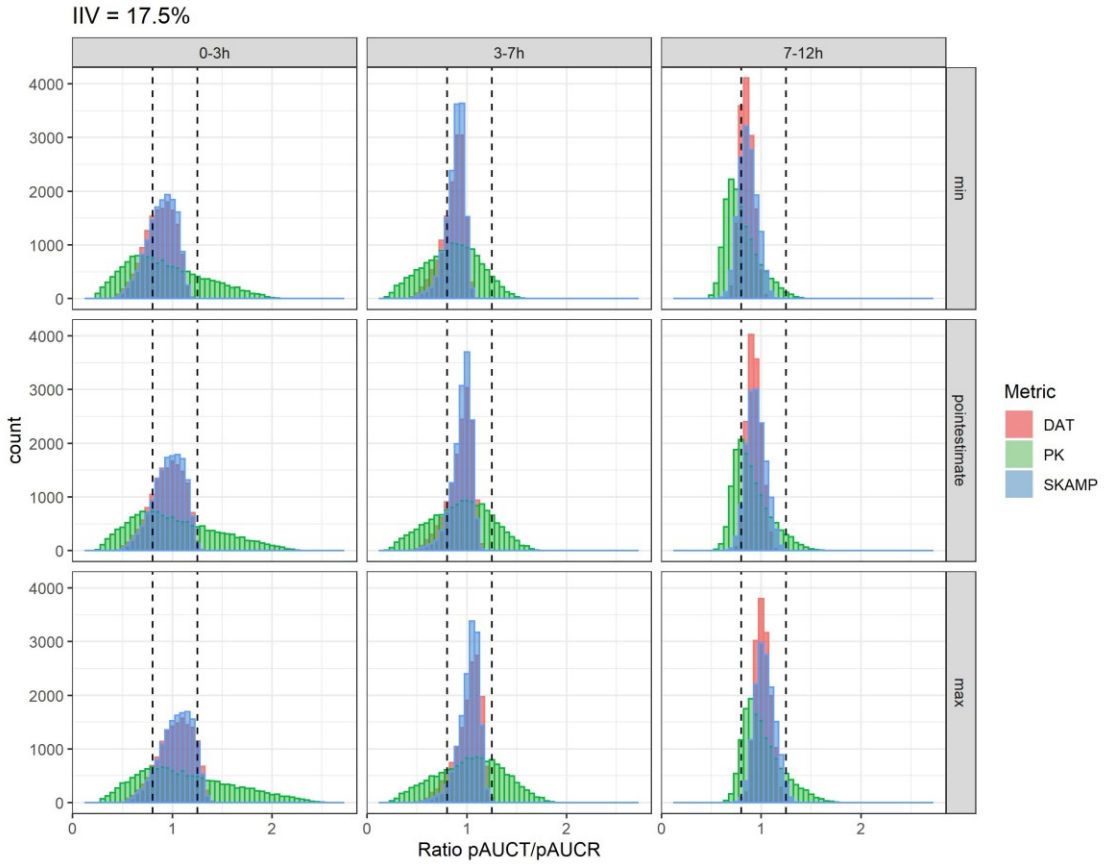

Figure S1 - Histogram of partial areas under the curve (pAUC) ratios between each formulation and Concerta for an interindividual variability (IIV) of 17.5%.

Chapitre 7 — Discussion

Le trouble déficitaire de l'attention (TDAH) est un trouble neurodéveloppemental courant chez les enfants et les adultes, et le méthylphénidate est l'un des médicaments les plus couramment prescrits pour son traitement. Cependant, comme la réponse au méthylphénidate varie considérablement d'un patient à l'autre, le processus de titration peut être long et fastidieux pour le patient. L'utilisation d'approches pharmacométriques pour optimiser l'individualisation des doses de méthylphénidate est donc une solution prometteuse.

Dans cette thèse, nous avons traité de l'optimisation des régimes posologique du méthylphénidate sous deux aspects: la pharmacocinétique et la pharmacodynamie. L'ensemble de cette thèse a donc suivi le méthylphénidate à partir de son occupation des transporteurs au niveau du cerveau jusqu'au échelles cliniques, en passant par ses concentrations plasmatiques.

Discussion générale

Au chapitre 4, nous nous sommes d'abord concentrés sur la pharmacocinétique du méthylphénidate. Ensuite aux chapitres 5 et 6, nous avons exploré la pharmacodynamie du méthylphénidate. Plus précisément, nous avons exploré la pharmacodynamique au niveau de l'occupation des transporteurs de dopamine au chapitre 5 et la pharmacodynamie sur la symptomatologie mesurée sur l'échelle des scores cliniques SKAMP au chapitre 6.

Premier article

Les premiers travaux de cette thèse découlent de nos travaux précédents concernant la comparaison statistique équitable de différents régimes de méthylphénidate (169,220). Nous nous sommes précédemment penchés sur l'interchangeabilité des médicaments génériques et novateurs (169). Ces travaux précédents proposaient une série de critères permettant de comparer différents régimes de méthylphénidate. C'est dans cette veine que s'installe le premier travail de cette thèse.

Alors que nous avions travaillé sur des méthodes statistiques pour comparer des régimes déjà approuvés, nous nous sommes interrogés sur les méthodes appliquées avant même la commercialisation.

Depuis les années 90, plusieurs chercheurs se sont posé la même question : comment peut-on s'assurer qu'un médicament générique soit interchangeable avec un médicament novateur ? La littérature traite de différentes méthodes, calculs ou approches.

Les agences réglementaires ont finalement retenu deux approches : la bioéquivalence de population et la bioéquivalence individuelle. Comme le méthylphénidate est un médicament avec une grande variabilité interindividuelle, nous nous sommes concentrés sur la bioéquivalence de population. Bien que celle-ci ait été développée pour traiter de l'interchangeabilité en bioéquivalence, l'approche présente quelques failles. En effet, telle qu'il est écrit, le critère de bioéquivalence de population permet un équilibre entre la différence des moyennes et des variances des métriques pharmacocinétique du médicament générique et du médicament novateur.

C'est dans ce contexte que s'inscrit le travail du chapitre 4, où nous avons proposé une méthode comparant les formulations de méthylphénidate avant leur commercialisation pour s'assurer de leur interchangeabilité. Nous avons adapté le critère de la PBE en y insérant un seuil maximal sur différence entre les moyennes et nous y avons introduit un poids modulable selon le médicament testé. Graphiquement, cela était représenté par un trapèze (ce qui lui a valu le nom de bioéquivalence trapézoïdale). Afin d'évaluer le comportement de la bioéquivalence trapézoïdale, nous avons effectué deux types de simulations et avons ensuite comparé ces résultats à ceux obtenus en appliquant la bioéquivalence moyenne et la bioéquivalence de population.

Les premières simulations font varier l'écart entre la moyenne (et la variance) d'une métrique de bioéquivalence pour le médicament test et le médicament de référence. Inspirées de la méthodologie de Dragalin *et al*, ces simulations ont une portée générale (216). Les simulations subséquentes portaient sur l'exemple spécifique du méthylphénidate où nous y avons varié la variabilité interindividuelle des paramètres pharmacocinétiques d'absorption.

Grâce à ces simulations, nous avons pu démontrer que la bioéquivalence trapézoïdale, tout comme la bioéquivalence de population, est sensible à des différences entre (i) la moyenne des métriques pharmacocinétiques du médicament test et du médicament générique et (ii) leurs variances.

Ces résultats ne dépendent ni de la taille d'échantillon ni de la variance interindividuelle du médicament de référence, contrairement à la bioéquivalence moyenne et la bioéquivalence de population. Finalement, la bioéquivalence trapézoïdale, contrairement à la bioéquivalence de population, ne permet pas un équilibre entre la différence des moyennes et des variances.

Bien que la métrique de la bioéquivalence trapézoïdale ne puisse être interprétée hors de la transformation logarithmique, il s'agit d'une approche qui se situe à l'intersection de la bioéquivalence moyenne et de la bioéquivalence de population.

Deuxième article

Après avoir exploré la pharmacocinétique du méthylphénidate au premier article, nous nous sommes demandé si elle représentait bien sa pharmacodynamie. Plusieurs études ont évalué cette relation et ont rapporté la présence d'une tolérance aiguë qui se développe au courant de la journée. En effet, l'efficacité du méthylphénidate, mesurée sur des échelles de mesure clinique, était réduite en fin de journée malgré des concentrations plasmatiques similaires. Bien que la tolérance aigüe ait été rapportée, sa cause exacte n'a été que théorisée, en mentionnant l'internalisation des récepteurs comme explication possible (152). Il semble par contre qu'aucune approche de modélisation ne se soit portée sur ce phénomène dans le cas du méthylphénidate.

Le deuxième article de cette thèse a traité cette hypothèse relative au rôle des transporteurs de dopamine et de norépinéphrine dans la tolérance aigüe, tous deux impliqués dans le mécanisme d'action du méthylphénidate. L'occupation des transporteurs de dopamine a été largement étudiée, sans pour autant rapporter la variabilité sous-jacente. Des efforts ont été déployés pour obtenir les données recueillies dans le cadre de ces études, sans que cela aboutisse. Nous avons donc procédé à la numérisation des données de l'occupation des transporteurs de dopamine en fonction de la concentration plasmatique. Ceci nous a permis de décrire cette relation par un modèle populationnel.

Les données concernant l'occupation des transporteurs de norépinéphrine étaient beaucoup plus limitées. Seulement une étude a porté sur l'occupation de ces transporteurs par le méthylphénidate (63), rapportant la relation entre l'occupation des transporteurs et la dose de méthylphénidate, plutôt que de sa concentration.

Grâce à ces données, nous avons développé deux modèles populationnels pour décrire l'occupation des transporteurs de dopamine : un modèle E_{max} sans et avec tolérance aigüe. Ceci nous a permis de créer un cadre d'analyse des régimes de méthylphénidate basé sur un modèle populationnel de l'occupation des transporteurs de dopamine et de norépinéphrine. Ce cadre d'analyse a été appliqué à différentes doses de méthylphénidate à libération prolongée et de régimes *t.i.d* de libération immédiate.

Le calcul de la performance de ces régimes a permis de démontrer que les doses thérapeutiques du méthylphénidate mènent à une très grande occupation des transporteurs de norépinéphrine. Ceci est attendu, sachant que le méthylphénidate a une affinité plus grande pour ces transporteurs. Cette étude ouvre donc la porte à la notion de surdosage de certains patients. L'utilisation des petites doses est présentement explorée dans une étude clinique (143,144).

Troisième article

L'analyse du deuxième article se plaçait au niveau moléculaire de la pharmacodynamie du méthylphénidate. Le troisième article nous a mené vers l'analyse du niveau clinique du méthylphénidate. Nous nous sommes intéressés à savoir si des changements au niveau de l'occupation des transporteurs de dopamine peuvent être traduits en un changement en effet clinique. Afin de tester cette hypothèse, nous avons simulé différentes formulations de méthylphénidate et défini leurs bénéfices cliniques par l'aire sous la courbe partielle de (i) l'occupation des transporteurs de dopamine et (ii) l'aire sous la courbe partielle des scores cliniques SKAMP. Nous avons étudié l'impact de la variabilité interindividuelle sur cette corrélation.

Nous observons que la pharmacocinétique est un bon représentant de la pharmacodynamie dans les premières heures de la journée. Par contre, cette corrélation diminue à partir de 7h post-dose.

Ces résultats pointent vers le rôle de la tolérance aigüe dans la séparation qui se produit dans la journée entre la pharmacocinétique et la pharmacodynamie.

Nos résultats démontrent aussi une grande corrélation entre l'occupation des transporteurs de dopamine et les scores SKAMP qui y sont associés. Il existe une relation proportionnelle entre l'occupation des transporteurs de dopamine et les scores cliniques. Toutefois, cette corrélation diminue aussi à partir de 7 heures après l'administration du traitement, et devient plus faible que les corrélations observées entre la pharmacocinétique et la pharmacodynamie. Ces résultats nous portent à croire que le phénomène de tolérance aigüe observé sur les transporteurs de dopamine n'est pas le même qui explique la tolérance aigüe observée sur les scores SKAMP.

Nous avons également exploré l'impact de la modification de certains aspects de la formulation sur la pharmacocinétique et la pharmacodynamie du méthylphénidate. Nos résultats confirment les travaux précédents de Jackson *et al.* selon lesquels la constante d'absorption de la libération rapide du méthylphénidate affecte les premières heures post-dose et que la constante d'absorption de la partie de libération prolongée affecte les dernières heures en pharmacocinétique (221). Notre analyse révèle en plus que la constante d'absorption de la partie rapide affecte également la pharmacodynamie, et fait ressortir le temps de délai avant la libération lente comme paramètre important pour les temps de 3 à 12 h post-dose.

En somme, les résultats pointent vers les limites de la pharmacocinétique à représenter la pharmacodynamie du méthylphénidate en fin de journée, malgré leur forte corrélation en début de journée. Cette étude peut servir de guide dans la détermination d'un profil de libération idéal du méthylphénidate pour optimiser l'effet clinique.

Limites et amélioration future des travaux

Le but global de de cette thèse était de développer des approches quantitatives pour l'individualisation du méthylphénidate. Par ces travaux, nous pouvons dire que nous avons défriché un peu ce chemin en apportant notre contribution aux niveaux suivants:

- une approche pour contrôler la variabilité interindividuelle permise en PK,

- une analyse exploratoire pharmacocinétique-pharmacodynamique pour l'évaluation de la tolérance aigüe au méthylphénidate et une analyse comparative de la performance d'un régime de MPH,
- une analyse de la traduction de l'occupation des transporteurs de dopamine en scores SKAMP.

Malgré les résultats prometteurs obtenus dans cette thèse, certaines limites devront être prises en compte dans de futurs explorations. Tout d'abord, nos travaux ont testé la bioéquivalence trapézoïdale en utilisant diverses simulations ainsi que des données cliniques portant sur le méthylphénidate. Bien que cette méthode puisse être comparable à la bioéquivalence moyenne et à la bioéquivalence de population, d'autres méthodes n'ont pas été prises en compte. On peut citer en particulier la méthode basée sur la divergence de Kullback-Leibler, une approche agrégée, qui a été proposée pour corriger les problèmes de la bioéquivalence de population (216). Il serait également intéressant de comparer les résultats de la bioéquivalence trapézoïdale à ceux des approches désagrégées (215). Il convient également de noter qu'il serait envisageable d'élargir le champ d'application de cette étude au-delà de celui de la thèse, en appliquant la méthode de la bioéquivalence trapézoïdale à des médicaments inhalés pour lesquels l'utilisation de la bioéquivalence de population est recommandée dans les guides de la FDA (222–224).

Ensuite, le modèle pharmacocinétique-pharmacodynamique de l'occupation des transporteurs de dopamine a été développé à l'aide de données extraites numériquement de la littérature. Ceci nous a permis d'estimer la valeur des paramètres du modèle pour un sujet typique. Cependant, en raison de la nature de ces données, nous ne pouvions pas distinguer les valeurs spécifiques à chaque sujet, et par le fait même, d'estimer la variabilité interindividuelle dans notre modèle. De plus, nous avons eu recours à une estimation du temps d'administration de certaines données lorsque seulement l'intervalle était donné. D'autres données n'ont pas pu être incluses dans l'analyse car leurs temps de prélèvement étaient inconnus. Cumulées, ces limites nous ont uniquement permis de détecter des traces de tolérance aigüe au niveau de l'occupation des transporteurs de dopamine, sans pouvoir la confirmer avec certitude. Par ailleurs, les données sur l'occupation des transporteurs de norépinéphrine n'étaient pas publiées avec suffisamment d'informations pour pouvoir établir un modèle dynamique de l'occupation des transporteurs de

norépinéphrine. Ainsi, notre analyse s'est limitée à un calcul statique de l'occupation des transporteurs de norépinéphrine, supposée constante à travers la journée. Par conséquent, des études cliniques analysant l'occupation des transporteurs de dopamine et des transporteurs de norépinéphrine seraient nécessaires pour approfondir l'analyse et enrichir les résultats produits lors de ce projet de thèse. Ces études devraient être conçues de manière à recueillir des données appropriées pour construire un modèle pharmacocinétique-pharmacodynamique de l'occupation des transporteurs. D'ailleurs, les autres cibles pharmacologiques du méthylphénidate (ex. les récepteurs alpha-2) n'ont pas été considérées dans cette thèse.

Finalement, l'impact des covariables potentielles, telles que l'âge et le sexe, sur les scores cliniques SKAMP n'a pas été étudié. Par soucis de simplicité, nos simulations ne s'appliquent que pour un groupe de sujets homogènes : des hommes à jeun prenant la même dose de 54mg et ayant le même sous-type de TDAH. Cependant, il est bien connu que l'âge et la prise concomitante de nourriture peuvent avoir un impact significatif sur la pharmacocinétique du méthylphénidate, tandis que le sexe et le sous-type de TDAH peuvent affecter la pharmacodynamie de ce médicament. Ainsi, l'étude de l'impact de ces covariables sur l'efficacité des régimes de méthylphénidate serait extrêmement pertinent pour une application clinique plus large.

Conclusion

En somme, cette thèse contribue à une meilleure compréhension de la pharmacocinétique et de la pharmacodynamie du méthylphénidate. Elle ouvre la voie à de futures recherches pour explorer davantage différents volets pharmacologiques et cliniques dans le contexte du TDAH. Avec l'ère de la médecine de précision qui cogne à nos portes et la pharmacométrie rendue beaucoup plus accessible grâce aux outils web, l'histoire du méthylphénidate ne fait que commencer.

Références bibliographiques

1. Faraone SV, Banaschewski T, Coghill D, Zheng Y, Biederman J, Bellgrove MA, et al. The World Federation of ADHD International Consensus Statement: 208 Evidence-based conclusions about the disorder. Neuroscience & Biobehavioral Reviews. 2021 Sep 1;128:789–818.

2. Lange KW, Reichl S, Lange KM, Tucha L, Tucha O. The history of attention deficit hyperactivity disorder. Atten Defic Hyperact Disord. 2010 Dec;2(4):241–55.

3. Still GF. The Goulstonian Lectures. Some abnormal psychical conditions in children. 1902;1008–12.

4. Bradley C. The behavior of children receiving benzedrine. AJP. 1937 Nov;94(3):577–85.

5. Polanczyk GV, Willcutt EG, Salum GA, Kieling C, Rohde LA. ADHD prevalence estimates across three decades: an updated systematic review and meta-regression analysis. International Journal of Epidemiology. 2014 Apr 1;43(2):434–42.

6. Willcutt EG. The Prevalence of DSM-IV Attention-Deficit/Hyperactivity Disorder: A Meta-Analytic Review. Neurotherapeutics. 2012 Jul 1;9(3):490–9.

7. Simon V, Czobor P, Bálint S, Mészáros Á, Bitter I. Prevalence and correlates of adult attention-deficit hyperactivity disorder: meta-analysis. The British Journal of Psychiatry. 2009 Mar;194(3):204–11.

8. Fayyad J, Sampson NA, Hwang I, Adamowski T, Aguilar-Gaxiola S, Al-Hamzawi A, et al. The descriptive epidemiology of DSM-IV Adult ADHD in the World Health Organization World Mental Health Surveys. ADHD Atten Def Hyp Disord. 2017 Mar 1;9(1):47–65.

9. Stahl SM 1951, Grady MM, Muntner N. Stahl's essential psychopharmacology : neuroscientific basis and practical applications [Internet]. Fifth edition. Cambridge, United Kingdom ; Cambridge University Press; 2021. (Cambridge medicine). Available from: https://www.r2library.com/resource/title/110883857X

10. Pan YQ, Qiao L, Xue XD, Fu JH. Association between ANKK1 (rs1800497) polymorphism of DRD2 gene and attention deficit hyperactivity disorder: A meta-analysis. Neuroscience Letters. 2015 Mar 17;590:101–5.

11. Grünblatt E, Werling AM, Roth A, Romanos M, Walitza S. Association study and a systematic meta-analysis of the VNTR polymorphism in the 3'-UTR of dopamine transporter gene and attention-deficit hyperactivity disorder. J Neural Transm. 2019 Apr 1;126(4):517–29.

12. Grünblatt E, Nemoda Z, Werling AM, Roth A, Angyal N, Tarnok Z, et al. The involvement of the canonical Wnt-signaling receptor LRP5 and LRP6 gene variants with ADHD and sexual

dimorphism: Association study and meta-analysis. American Journal of Medical Genetics Part B: Neuropsychiatric Genetics. 2019;180(6):365–76.

13. Liu YS, Dai X, Wu W, Yuan F fen, Gu X, Chen JG, et al. The Association of SNAP25 Gene Polymorphisms in Attention Deficit/Hyperactivity Disorder: a Systematic Review and Meta-Analysis. Mol Neurobiol. 2017 Apr 1;54(3):2189–200.

14. Bruxel EM, Moreira-Maia CR, Akutagava-Martins GC, Quinn TP, Klein M, Franke B, et al. Meta-analysis and systematic review of ADGRL3 (LPHN3) polymorphisms in ADHD susceptibility. Mol Psychiatry. 2021 Jun;26(6):2277–85.

15. Bonvicini C, Cortese S, Maj C, Baune BT, Faraone SV, Scassellati C. DRD4 48 bp multiallelic variants as age-population-specific biomarkers in attention-deficit/hyperactivity disorder. Transl Psychiatry. 2020 Feb 19;10(1):1–19.

16. Bonvicini C, Faraone SV, Scassellati C. Attention-deficit hyperactivity disorder in adults: A systematic review and meta-analysis of genetic, pharmacogenetic and biochemical studies. Mol Psychiatry. 2016 Jul;21(7):872–84.

17. Li JJ. The positive end of the polygenic score distribution for ADHD: a low risk or a protective factor? Psychological Medicine. 2021 Jan;51(1):102–11.

18. Demontis D, Walters GB, Athanasiadis G, Walters R, Therrien K, Nielsen TT, et al. Genome-wide analyses of ADHD identify 27 risk loci, refine the genetic architecture and implicate several cognitive domains. Nat Genet. 2023 Feb;55(2):198–208.

19. Nilsen FM, Tulve NS. A systematic review and meta-analysis examining the interrelationships between chemical and non-chemical stressors and inherent characteristics in children with ADHD. Environmental Research. 2020 Jan 1;180:108884.

20. Froehlich TE, Lanphear BP, Auinger P, Hornung R, Epstein JN, Braun J, et al. Association of Tobacco and Lead Exposures With Attention-Deficit/Hyperactivity Disorder. Pediatrics. 2009 Dec 1;124(6):e1054–63.

21. Braun JM, Kahn RS, Froehlich T, Auinger P, Lanphear BP. Exposures to Environmental Toxicants and Attention Deficit Hyperactivity Disorder in U.S. Children. Environmental Health Perspectives. 2006 Dec;114(12):1904–9.

22. Chen MH, Pan TL, Wang PW, Hsu JW, Huang KL, Su TP, et al. Prenatal Exposure to Acetaminophen and the Risk of Attention-Deficit/Hyperactivity Disorder: A Nationwide Study in Taiwan. J Clin Psychiatry. 2019 Sep 10;80(5):15264.

23. Ystrom E, Gustavson K, Brandlistuen RE, Knudsen GP, Magnus P, Susser E, et al. Prenatal Exposure to Acetaminophen and Risk of ADHD. Pediatrics. 2017 Nov 1;140(5):e20163840.

24. Christensen J, Pedersen L, Sun Y, Dreier JW, Brikell I, Dalsgaard S. Association of Prenatal Exposure to Valproate and Other Antiepileptic Drugs With Risk for Attention-Deficit/Hyperactivity Disorder in Offspring. JAMA Network Open. 2019 Jan 4;2(1):e186606.

25. Franz AP, Bolat GU, Bolat H, Matijasevich A, Santos IS, Silveira RC, et al. Attention-Deficit/Hyperactivity Disorder and Very Preterm/Very Low Birth Weight: A Meta-analysis. Pediatrics. 2018 Jan 1;141(1):e20171645.

26. Momany AM, Kamradt JM, Nikolas MA. A Meta-Analysis of the Association Between Birth Weight and Attention Deficit Hyperactivity Disorder. J Abnorm Child Psychol. 2018 Oct 1;46(7):1409–26.

27. Lindström K, Lindblad F, Hjern A. Preterm Birth and Attention-Deficit/Hyperactivity Disorder in Schoolchildren. Pediatrics. 2011 May 1;127(5):858–65.

28. Sucksdorff M, Lehtonen L, Chudal R, Suominen A, Joelsson P, Gissler M, et al. Preterm Birth and Poor Fetal Growth as Risk Factors of Attention-Deficit/Hyperactivity Disorder. Pediatrics. 2015 Sep 1;136(3):e599–608.

29. Maher GM, Dalman C, O'Keeffe GW, Kearney PM, McCarthy FP, Kenny LC, et al. Association between preeclampsia and attention-deficit hyperactivity disorder: a population-based and sibling-matched cohort study. Acta Psychiatrica Scandinavica. 2020;142(4):275–83.

30. Maher GM, O'Keeffe GW, Kearney PM, Kenny LC, Dinan TG, Mattsson M, et al. Association of Hypertensive Disorders of Pregnancy With Risk of Neurodevelopmental Disorders in Offspring: A Systematic Review and Meta-analysis. JAMA Psychiatry. 2018 Aug 1;75(8):809–19.

31. Jenabi E, Bashirian S, Khazaei S, Basiri Z. The maternal prepregnancy body mass index and the risk of attention deficit hyperactivity disorder among children and adolescents: a systematic review and meta-analysis. Korean J Pediatr. 2019 Jun 14;62(10):374–9.

32. Sanchez CE, Barry C, Sabhlok A, Russell K, Majors A, Kollins SH, et al. Maternal pre-pregnancy obesity and child neurodevelopmental outcomes: a meta-analysis. Obesity Reviews. 2018;19(4):464–84.

33. Andersen CH, Thomsen PH, Nohr EA, Lemcke S. Maternal body mass index before pregnancy as a risk factor for ADHD and autism in children. Eur Child Adolesc Psychiatry. 2018 Feb 1;27(2):139–48.

34. Ouyang L, Fang X, Mercy J, Perou R, Grosse SD. Attention-Deficit/Hyperactivity Disorder Symptoms and Child Maltreatment: A Population-Based Study. The Journal of Pediatrics. 2008 Dec 1;153(6):851–6.

35. Choi Y, Shin J, Cho KH, Park EC. Change in household income and risk for attention deficit hyperactivity disorder during childhood: A nationwide population-based cohort study. Journal of Epidemiology. 2017 Feb 1;27(2):56–62.

36. Larsson H, Sariaslan A, Långström N, D'Onofrio B, Lichtenstein P. Family income in early childhood and subsequent attention deficit/hyperactivity disorder: a quasi-experimental study. Journal of Child Psychology and Psychiatry. 2014;55(5):428–35.

37. Keilow M, Wu C, Obel C. Cumulative social disadvantage and risk of attention deficit hyperactivity disorder: Results from a nationwide cohort study. SSM - Population Health. 2020 Apr 1;10:100548.

38. Do I have ADHD? [Internet]. 2017 [cited 2022 Dec 27]. Available from: https://www.youtube.com/watch?v=j7F7Pil9tVQ

39. Faraone SV. The scientific foundation for understanding attention-deficit/hyperactivity disorder as a valid psychiatric disorder. EuropChild & Adolescent Psych. 2005 Feb 1;14(1):1–10.

40. Ebenezer IS. Neuropsychopharmacology and therapeutics [Internet]. Chichester, West Sussex ; Wiley-Blackwell; 2015. Available from: http://site.ebrary.com/id/11064539

41. Faraone SV, Asherson P, Banaschewski T, Biederman J, Buitelaar JK, Ramos-Quiroga JA, et al. Attention-deficit/hyperactivity disorder. Nat Rev Dis Primers. 2015 Aug 6;1(1):1–23.

42. van Ewijk H, Heslenfeld DJ, Zwiers MP, Buitelaar JK, Oosterlaan J. Diffusion tensor imaging in attention deficit/hyperactivity disorder: a systematic review and meta-analysis. Neuroscience & Biobehavioral Reviews. 2012;36(4):1093–106.

43. Nakao T, Radua J, Rubia K, Mataix-Cols D. Gray Matter Volume Abnormalities in ADHD: Voxel-Based Meta-Analysis Exploring the Effects of Age and Stimulant Medication. AJP. 2011 Nov;168(11):1154–63.

44. Arnsten AFT. Toward a New Understanding of Attention-Deficit Hyperactivity Disorder Pathophysiology. CNS Drugs. 2009 Nov 1;23(1):33–41.

45. Lukito S, Norman L, Carlisi C, Radua J, Hart H, Simonoff E, et al. Comparative meta-analyses of brain structural and functional abnormalities during cognitive control in attention-deficit/hyperactivity disorder and autism spectrum disorder. Psychological Medicine. 2020 Apr;50(6):894–919.

46. Norman LJ, Carlisi C, Lukito S, Hart H, Mataix-Cols D, Radua J, et al. Structural and Functional Brain Abnormalities in Attention-Deficit/Hyperactivity Disorder and Obsessive-Compulsive Disorder: A Comparative Meta-analysis. JAMA Psychiatry. 2016 Aug 1;73(8):815–25.

47. Hart H, Radua J, Nakao T, Mataix-Cols D, Rubia K. Meta-analysis of Functional Magnetic Resonance Imaging Studies of Inhibition and Attention in Attention-deficit/Hyperactivity Disorder: Exploring Task-Specific, Stimulant Medication, and Age Effects. JAMA Psychiatry. 2013 Feb 1;70(2):185–98.

48. Cortese S, Kelly C, Chabernaud C, Proal E, Di Martino A, Milham MP, et al. Toward Systems Neuroscience of ADHD: A Meta-Analysis of 55 fMRI Studies. AJP. 2012 Oct;169(10):1038–55.

49. Plichta MM, Scheres A. Ventral–striatal responsiveness during reward anticipation in ADHD and its relation to trait impulsivity in the healthy population: A meta-analytic review of the fMRI literature. Neuroscience & Biobehavioral Reviews. 2014 Jan 1;38:125–34.

50. Luman M, Tripp G, Scheres A. Identifying the neurobiology of altered reinforcement sensitivity in ADHD: a review and research agenda. Neuroscience & Biobehavioral Reviews. 2010;34(5):744–54.

51. Sonuga-Barke EJS, Fairchild G. Neuroeconomics of Attention-Deficit/Hyperactivity Disorder: Differential Influences of Medial, Dorsal, and Ventral Prefrontal Brain Networks on Suboptimal Decision Making? Biological Psychiatry. 2012 Jul 15;72(2):126–33.

52. Sonuga-Barke E, Bitsakou P, Thompson M. Beyond the Dual Pathway Model: Evidence for the Dissociation of Timing, Inhibitory, and Delay-Related Impairments in Attention-Deficit/Hyperactivity Disorder. Journal of the American Academy of Child & Adolescent Psychiatry. 2010 Apr 1;49(4):345–55.

53. Véronneau-Veilleux F, Robaey P, Ursino M, Nekka F. A mechanistic model of ADHD as resulting from dopamine phasic/tonic imbalance during reinforcement learning. Front Comput Neurosci. 2022;16:849323.

54. Bear MF, Connors BW, Paradiso MA, Nieoullon A (1948 . . .). Neurosciences : à la découverte du cerveau [Internet]. 4e édition. Montrouge: Editions Pradel, John Libbey Eurotext; 2016. Available from: http://catalogue.bnf.fr/ark:/12148/cb451786111

55. Berridge CW, Waterhouse BD. The locus coeruleus–noradrenergic system: modulation of behavioral state and state-dependent cognitive processes. Brain Research Reviews. 2003 Apr 1;42(1):33–84.

56. Hunt R. Medscape. 2006 [cited 2022 Dec 27]. Functional Roles of Norepinephrine and Dopamine in ADHD. Available from: http://www.medscape.org/viewarticle/523887

57. Aston-Jones G, Rajkowski J, Cohen J. Role of locus coeruleus in attention and behavioral flexibility. Biological Psychiatry. 1999 Nov 1;46(9):1309–20.

58. Pliszka SR, McCRACKEN JT, Maas JW. Catecholamines in Attention-Deficit Hyperactivity Disorder: Current Perspectives. Journal of the American Academy of Child & Adolescent Psychiatry. 1996 Mar 1;35(3):264–72.

59. Vanicek T, Spies M, Rami-Mark C, Savli M, Höflich A, Kranz GS, et al. The norepinephrine transporter in attention-deficit/hyperactivity disorder investigated with positron emission tomography. JAMA Psychiatry. 2014 Dec 1;71(12):1340–9.

60. Sigurdardottir HL, Kranz GS, Rami-Mark C, James GM, Vanicek T, Gryglewski G, et al. Effects of norepinephrine transporter gene variants on NET binding in ADHD and healthy controls investigated by PET. Human Brain Mapping. 2016;37(3):884–95.

61. Arnsten AFT, Li BM. Neurobiology of Executive Functions: Catecholamine Influences on Prefrontal Cortical Functions. Biological Psychiatry. 2005 Jun 1;57(11):1377–84.

62. Fusar-Poli P, Rubia K, Rossi G, Sartori G, Balottin U. Striatal dopamine transporter alterations in ADHD: pathophysiology or adaptation to psychostimulants? A meta-analysis. American Journal of Psychiatry. 2012;169(3):264–72.

63. Hannestad J, Gallezot JD, Planeta-Wilson B, Lin SF, Williams WA, van Dyck CH, et al. Clinically relevant doses of methylphenidate significantly occupy norepinephrine transporters in humans in vivo. Biol Psychiatry. 2010 Nov 1;68(9):854–60.

64. Morón JA, Brockington A, Wise RA, Rocha BA, Hope BT. Dopamine uptake through the norepinephrine transporter in brain regions with low levels of the dopamine transporter: evidence from knock-out mouse lines. J Neurosci. 2002 Jan 15;22(2):389–95.

65. Woods D, Wolraich M, Pierce K, DiMarco L, Muller N, Sachdeva R. Considerations and Evidence for an ADHD Outcome Measure. Academic Pediatrics. 2014 Sep 1;14(5, Supplement):S54–60.

66. Markowitz JT, Oberdhan D, Ciesluk A, Rams A, Wigal SB. Review of Clinical Outcome Assessments in Pediatric Attention-Deficit/Hyperactivity Disorder. Neuropsychiatr Dis Treat. 2020;16:1619–43.

67. Epstein JN, Weiss MD. Assessing Treatment Outcomes in Attention-Deficit/Hyperactivity Disorder: A Narrative Review. Prim Care Companion CNS Disord. 2012 Nov 29;14(6):26661.

68. Teuscher NS, Sikes CR, McMahen R, Engelking D. Population Pharmacokinetic-Pharmacodynamic Modeling of a Novel Methylphenidate Extended-Release Orally Disintegrating Tablet in Pediatric Patients With Attention-Deficit/Hyperactivity Disorder. Journal of Clinical Psychopharmacology. 2018;38(5):8.

69. Gomeni R, Komolova M, Incledon B, Faraone SV. Model-Based Approach for Establishing the Predicted Clinical Response of a Delayed-Release and Extended-Release Methylphenidate for the Treatment of Attention-Deficit/Hyperactivity Disorder. J Clin Psychopharmacol. 2020 Aug;40(4):350–8.

70. Gomeni R, Bressolle-Gomeni F, Spencer TJ, Faraone SV, Fang L, Babiskin A. Model-Based Approach for Optimizing Study Design and Clinical Drug Performances of Extended-Release Formulations of Methylphenidate for the Treatment of ADHD. Clin Pharmacol Ther. 2017 Dec;102(6):951–60.

71. Kimko H, Gibiansky E, Gibiansky L, Starr HL, Berwaerts J, Massarella J, et al. Population pharmacodynamic modeling of various extended- release formulations of methylphenidate in children with attention deficit hyperactivity disorder via meta-analysis. J Pharmacokinet Pharmacodyn. 2012;16.

72. Teuscher NS, Adjei A, Findling RL, Greenhill LL, Kupper RJ, Wigal S. Population pharmacokinetics of methylphenidate hydrochloride extended-release multiple-layer beads in pediatric subjects with attention deficit hyperactivity disorder. Drug Des Devel Ther. 2015;9:2767–75.

73. Swanson JM, Lerner M, Wigal T, Steinhoff K, Greenhill L, Posner K, et al. The use of a laboratory school protocol to evaluate concepts about efficacy and side effects of new formulations of stimulant medications. J Atten Disord. 2002 Apr 1;6(1_suppl):73–88.

74. Wigal SB, Wigal TL. The Laboratory School Protocol: Its Origin, Use, and New Applications. J Atten Disord. 2006 Aug 1;10(1):92–111.

75. Wigal SB, Gupta S, Guinta D, Swanson JM. Reliability and validity of the SKAMP rating scale in a laboratory school setting. Psychopharmacology Bulletin. 1998;34(1):47–54.

76. DuPaul GJ, Power TJ, Anastopoulos AD, Reid R. ADHD rating scale? 5 for children and adolescents: checklists, norms, and clinical interpretation. Guilford Publications; 2016.

77. Spencer TJ, Biederman J, Ciccone PE. PET Study Examining Pharmacokinetics, Detection and Likeability, and Dopamine Transporter Receptor Occupancy of Short- and Long-Acting Oral Methylphenidate. Am J Psychiatry. 2006;9.

78. Spencer TJ, Bonab AA, Dougherty DD, Martin J, McDONNELL T, Fischman AJ. A PET study examining pharmacokinetics and dopamine transporter occupancy of two long-acting formulations of methylphenidate in adults. INTERNATIONAL JOURNAL OF MOLECULAR MEDICINE. 2010;5.

79. Spencer TJ, Bonab AA, Dougherty DD, Mirto T, Martin J, Clarke A, et al. Understanding the central pharmacokinetics of spheroidal oral drug absorption system (SODAS) dexmethylphenidate: a positron emission tomography study of dopamine transporter receptor occupancy measured with C-11 altropane. J Clin Psychiatry. 2012 Mar;73(3):346–52.

80. Volkow ND, Gatley SJ, Hitzemann R. Dopamine Transporter Occupancies in the Human Brain Induced by Therapeutic Doses of Oral Methylphenidate. Am J Psychiatry. 1998;7.

81. Morgan P, Van Der Graaf PH, Arrowsmith J, Feltner DE, Drummond KS, Wegner CD, et al. Can the flow of medicines be improved? Fundamental pharmacokinetic and pharmacological principles toward improving Phase II survival. Drug Discovery Today. 2012 May 1;17(9):419–24.

82. Zhang Y, Fox GB. PET imaging for receptor occupancy: meditations on calculation and simplification. J Biomed Res. 2012 Mar;26(2):69–76.

83. Passchier J, Gee A, Willemsen A, Vaalburg W, van Waarde A. Measuring drug-related receptor occupancy with positron emission tomography. Methods. 2002 Jul 1;27(3):278–86.

84. Aoyama T, Kotaki H, Sawada Y, Iga T. Pharmacokinetics and pharmacodynamics of methylphenidate enantiomers in rats. Psychopharmacology (Berl). 1996 Sep;127(2):117–22.

85. Shimizu R, Horiguchi N, Yano K, Sakuramoto M, Kanegawa N, Shinohara S, et al. Pharmacokinetic-Pharmacodynamic Modeling of Brain Dopamine Levels Based on Dopamine Transporter Occupancy after Administration of Methylphenidate in Rats. J Pharmacol Exp Ther. 2019 Apr;369(1):78–87.

86. Berridge CW, Devilbiss DM, Andrzejewski ME, Arnsten AFT, Kelley AE, Schmeichel B, et al. Methylphenidate preferentially increases catecholamine neurotransmission within the prefrontal cortex at low doses that enhance cognitive function. Biol Psychiatry. 2006 Nov 15;60(10):1111–20.

87. Kielbasa W, Stratford RE Jr. Exploratory translational modeling approach in drug development to predict human brain pharmacokinetics and pharmacologically relevant clinical doses. Drug Metab Dispos. 2012 May;40(5):877–83.

88. Kielbasa W, Kalvass JC, Stratford R. Microdialysis evaluation of atomoxetine brain penetration and central nervous system pharmacokinetics in rats. Drug Metab Dispos. 2009 Jan;37(1):137–42.

89. Canadian A. Resource Alliance (CADDRA): Canadian ADHD Practice Guidelines. Toronto, Ontario: CADDRA. 2018;

90. Dalrymple RA, McKenna Maxwell L, Russell S, Duthie J. NICE guideline review: Attention deficit hyperactivity disorder: diagnosis and management (NG87). Arch Dis Child Educ Pract Ed. 2020 Oct 1;105(5):289.

91. Farhat LC, Flores JM, Behling E, Avila-Quintero VJ, Lombroso A, Cortese S, et al. The effects of stimulant dose and dosing strategy on treatment outcomes in attention-deficit/hyperactivity disorder in children and adolescents: a meta-analysis. Mol Psychiatry. 2022 Mar;27(3):1562–72.

92. Bymaster FP, Katner JS, Nelson DL, Hemrick-Luecke SK, Threlkeld PG, Heiligenstein JH, et al. Atomoxetine increases extracellular levels of norepinephrine and dopamine in prefrontal cortex of rat: a potential mechanism for efficacy in attention deficit/hyperactivity disorder. Neuropsychopharmacology. 2002 Nov;27(5):699–711.

93. Arnsten AFT, Steere JC, Hunt RD. The Contribution of α2-Noradrenergic Mechanisms to Prefrontal Cortical Cognitive Function: Potential Significance for Attention-Deficit Hyperactivity Disorder. Archives of General Psychiatry. 1996 May 1;53(5):448–55.

94. Faraone SV, Glatt SJ. A Comparison of the Efficacy of Medications for Adult Attention-Deficit/Hyperactivity Disorder Using Meta-Analysis of Effect Sizes. J Clin Psychiatry. 2009 Dec 29;71(6):3475.

95. Catalá-López F, Hutton B, Núñez-Beltrán A, Page MJ, Ridao M, Saint-Gerons DM, et al. The pharmacological and non-pharmacological treatment of attention deficit hyperactivity disorder in children and adolescents: A systematic review with network meta-analyses of randomised trials. PLOS ONE. 2017 Jul 12;12(7):e0180355.

96. Faraone SV, Buitelaar J. Comparing the efficacy of stimulants for ADHD in children and adolescents using meta-analysis. Eur Child Adolesc Psychiatry. 2010 Apr;19(4):353–64.

97. Joseph A, Ayyagari R, Xie M, Cai S, Xie J, Huss M, et al. Comparative efficacy and safety of attention-deficit/hyperactivity disorder pharmacotherapies, including guanfacine extended release: a mixed treatment comparison. Eur Child Adolesc Psychiatry. 2017 Aug 1;26(8):875–97.

98. Stuhec M, Munda B, Svab V, Locatelli I. Comparative efficacy and acceptability of atomoxetine, lisdexamfetamine, bupropion and methylphenidate in treatment of attention deficit hyperactivity disorder in children and adolescents: A meta-analysis with focus on bupropion. Journal of Affective Disorders. 2015 Jun 1;178:149–59.

99. Duong S, Chung K, Wigal SB. Metabolic, toxicological, and safety considerations for drugs used to treat ADHD. Expert Opinion on Drug Metabolism & Toxicology. 2012 May 1;8(5):543–52.

100. Vaughan B, Kratochvil CJ. Pharmacotherapy of Pediatric Attention-Deficit/Hyperactivity Disorder. Child and Adolescent Psychiatric Clinics. 2012 Oct 1;21(4):941–55.

101. Martinez-Raga J, Ferreros A, Knecht C, de Alvaro R, Carabal E. Attention-deficit hyperactivity disorder medication use: factors involved in prescribing, safety aspects and outcomes. Therapeutic Advances in Drug Safety. 2017 Mar 1;8(3):87–99.

102. Avelar AJ, Juliano SA, Garris PA. Amphetamine augments vesicular dopamine release in the dorsal and ventral striatum through different mechanisms. Journal of Neurochemistry. 2013;125(3):373–85.

103. Covey DP, Juliano SA, Garris PA. Amphetamine Elicits Opposing Actions on Readily Releasable and Reserve Pools for Dopamine. PLOS ONE. 2013 May 3;8(5):e60763.

104. Easton N, Steward C, Marshall F, Fone K, Marsden C. Effects of amphetamine isomers, methylphenidate and atomoxetine on synaptosomal and synaptic vesicle accumulation and

release of dopamine and noradrenaline in vitro in the rat brain. Neuropharmacology. 2007 Feb 1;52(2):405–14.

105. Riddle EL, Hanson GR, Fleckenstein AE. Therapeutic doses of amphetamine and methylphenidate selectively redistribute the vesicular monoamine transporter-2. European Journal of Pharmacology. 2007 Sep 24;571(1):25–8.

106. Sulzer D, Chen TK, Lau YY, Kristensen H, Rayport S, Ewing A. Amphetamine redistributes dopamine from synaptic vesicles to the cytosol and promotes reverse transport. J Neurosci. 1995 May 1;15(5):4102–8.

107. Drevets WC, Gautier C, Price JC, Kupfer DJ, Kinahan PE, Grace AA, et al. Amphetamine-induced dopamine release in human ventral striatum correlates with euphoria. Biological Psychiatry. 2001 Jan 15;49(2):81–96.

108. Myers RL. The 100 Most Important Chemical Compounds: A Reference Guide [Internet]. Greenwood Press; 2007. Available from: https://books.google.ca/books?id=a4DuGVwyN6cC

109. Panizzon L. La preparazione di piridil- e piperidil-arilacetonitrili e di alcuni prodotti di trasformazione (Parte Ia). Helvetica Chimica Acta. 1944 Jan 1;27(1):1748–56.

110. Bachmann CJ, Wijlaars LP, Kalverdijk LJ, Burcu M, Glaeske G, Schuiling-Veninga CCM, et al. Trends in ADHD medication use in children and adolescents in five western countries, 2005–2012. European Neuropsychopharmacology. 2017 May 1;27(5):484–93.

111. Wolraich ML, Hagan JF, Allan C, Chan E, Davison D, Earls M, et al. Clinical practice guideline for the diagnosis, evaluation, and treatment of attention-deficit/hyperactivity disorder in children and adolescents. Pediatrics. 2019;144(4).

112. Kooij J, Bijlenga D, Salerno L, Jaeschke R, Bitter I, Balazs J, et al. Updated European Consensus Statement on diagnosis and treatment of adult ADHD. European psychiatry. 2019;56(1):14–34.

113. Jaeschke RR, Sujkowska E, Sowa-Kućma M. Methylphenidate for attention-deficit/hyperactivity disorder in adults: a narrative review. Psychopharmacology (Berl). 2021 Oct;238(10):2667–91.

114. Nikolaus S, Wirrwar A, Antke C, Arkian S, Schramm N, Müller HW, et al. Quantitation of dopamine transporter blockade by methylphenidate: first in vivo investigation using [123I] FP-CIT and a dedicated small animal SPECT. European journal of nuclear medicine and molecular imaging. 2005;32(3):308–13.

115. Volkow N, Fowler J, Gatley S, Dewey S, Wang G, Logan J, et al. Comparable changes in synaptic dopamine induced by methylphenidate and by cocaine in the baboon brain. Synapse. 1999;31(1):59–66.

116. Kuczenski R, Segal DS. Effects of methylphenidate on extracellular dopamine, serotonin, and norepinephrine: comparison with amphetamine. Journal of neurochemistry. 1997;68(5):2032–7.

117. Schiffer WK, Volkow N, Fowler J, Alexoff D, Logan J, Dewey S. Therapeutic doses of amphetamine or methylphenidate differentially increase synaptic and extracellular dopamine. Synapse. 2006;59(4):243–51.

118. Young KA, Liu Y, Gobrogge KL, Dietz DM, Wang H, Kabbaj M, et al. Amphetamine alters behavior and mesocorticolimbic dopamine receptor expression in the monogamous female prairie vole. Brain research. 2011;1367:213–22.

119. Dresel SHJ, Kung MPT, Huang X, Plössl K, Hou C, Shiue CY, et al. In vivo imaging of serotonin transporters with [99mTc]TRODAT-1 in nonhuman primates. Eur J Nucl Med. 1999 Apr 1;26(4):342–7.

120. Federici M, Geracitano R, Bernardi G, Mercuri NB. Actions of methylphenidate on dopaminergic neurons of the ventral midbrain. Biological Psychiatry. 2005 Feb 15;57(4):361–5.

121. Gatley SJ, Pan D, Chen R, Chaturvedi G, Ding YS. Affinities of methylphenidate derivatives for dopamine, norepinephrine and serotonin transporters. Life Sciences. 1996 Feb 16;58(12):PL231–9.

122. Markowitz JS, DeVane CL, Pestreich LK, Patrick KS, Muniz R. A Comprehensive In Vitro Screening of d-, l-, and dl-threo-Methylphenidate: An Exploratory Study. Journal of Child and Adolescent Psychopharmacology. 2006 Dec;16(6):687–98.

123. Nikolaus S, Larisch R, Vosberg H, Beu M, Wirrwar A, Antke C, et al. Pharmacological challenge and synaptic response - assessing dopaminergic function in the rat striatum with small animal single-photon emission computed tomography (SPECT) and positron emission tomography (PET). Rev Neurosci. 2011;22(6):625–45.

124. Wall SC, Gu H, Rudnick G. Biogenic amine flux mediated by cloned transporters stably expressed in cultured cell lines: amphetamine specificity for inhibition and efflux. Molecular pharmacology. 1995;47(3):544–50.

125. Eshleman AJ, Carmolli M, Cumbay M, Martens CR, Neve KA, Janowsky A. Characteristics of drug interactions with recombinant biogenic amine transporters expressed in the same cell type. J Pharmacol Exp Ther. 1999 May;289(2):877–85.

126. Giros B, Wang YM, Suter S, McLeskey SB, Pifl C, Caron MG. Delineation of discrete domains for substrate, cocaine, and tricyclic antidepressant interactions using chimeric dopamine-norepinephrine transporters. Journal of Biological Chemistry. 1994;269(23):15985–8.

127. Gu H, Wall S, Rudnick G. Stable expression of biogenic amine transporters reveals differences in inhibitor sensitivity, kinetics, and ion dependence. Journal of Biological Chemistry. 1994;269(10):7124–30.

128. Andrews GD, Lavin A. Methylphenidate increases cortical excitability via activation of alpha-2 noradrenergic receptors. Neuropsychopharmacology. 2006;31(3):594–601.

129. Jain R, Katic A. Current and investigational medication delivery systems for treating attention-deficit/hyperactivity disorder. The Primary Care Companion for CNS Disorders. 2016;18(4):27471.

130. Faraone SV. The pharmacology of amphetamine and methylphenidate_ Relevance to the neurobiology of attention-deficit/hyperactivity disorder and other psychiatric comorbidities. Neuroscience and Biobehavioral Reviews. 2018;16.

131. Greenhill LL, Abikoff HB, Arnold LE, Cantwell DP, Conners CK, Elliott G, et al. Medication treatment strategies in the MTA Study: relevance to clinicians and researchers. J Am Acad Child Adolesc Psychiatry. 1996 Oct;35(10):1304–13.

132. Markowitz JS, Straughn AB, Patrick KS. Advances in the pharmacotherapy of attention-deficit-hyperactivity disorder: Focus on methylphenidate formulations. Pharmacotherapy: The Journal of Human Pharmacology and Drug Therapy. 2003;23(10):1281–99.

133. Childress AC, Komolova M, Sallee FR. An update on the pharmacokinetic considerations in the treatment of ADHD with long-acting methylphenidate and amphetamine formulations. Expert opinion on drug metabolism & toxicology. 2019;15(11):937–74.

134. Chan YP, Swanson JM, Soldin SS, Thiessen JJ, Macleod SM, Logan W. Methylphenidate hydrochloride given with or before breakfast: II. Effects on plasma concentration of methylphenidate and ritalinic acid. Pediatrics. 1983 Jul;72(1):56–9.

135. Kimko HC, Cross JT, Abernethy DR. Pharmacokinetics and Clinical Effectiveness of Methylphenidate. Clin Pharmacokinet. 1999 Dec 1;37(6):457–70.

136. Spiller HA, Hays HL, Aleguas A. Overdose of Drugs for Attention-Deficit Hyperactivity Disorder: Clinical Presentation, Mechanisms of Toxicity, and Management. CNS Drugs. 2013 Jul 1;27(7):531–43.

137. Hungund B, Perel J, Hurwic M, Sverd J, Winsberg B. Pharmacokinetics of methylphenidate in hyperkinetic children. British Journal of Clinical Pharmacology. 1979;8(6):571–6.

138. Volkow ND, Ding YS, Fowler JS, Wang GJ, Logan J, Gatley JS, et al. Is methylphenidate like cocaine?: Studies on their pharmacokinetics and distribution in the human brain. Archives of general psychiatry. 1995;52(6):456–63.

139. Ding YS, Fowler JS, Volkow ND, Gatley SJ, Logan J, Dewey SL, et al. Pharmacokinetics and in vivo specificity of [LLC]dl-threo-methylphenidate for the presynaptic dopaminergic neuron. Synapse. 1994;18(2):152–60.

140. Markowitz JS, Straughn AB, Patrick KS, DeVane CL, Pestreich L, Lee J, et al. Pharmacokinetics of methylphenidate after oral administration of two modified-release formulations in healthy adults. Clinical pharmacokinetics. 2003;42:393–401.

141. Schmeichel BE, Berridge CW. Neurocircuitry Underlying the Preferential Sensitivity of Prefrontal Catecholamines to Low-Dose Psychostimulants. Neuropsychopharmacology. 2013 May;38(6):1078–84.

142. Arnsten AF, Dudley AG. Methylphenidate improves prefrontal cortical cognitive function through alpha2 adrenoceptor and dopamine D1 receptor actions: Relevance to therapeutic effects in Attention Deficit Hyperactivity Disorder. Behav Brain Funct. 2005 Apr 22;1(1):2.

143. Ling D, Balce K, Weiss M, Murray C, Diamond A. Effects of low-dose versus normal-dose psychostimulants on executive functions in children with attention-deficit / hyperactivity disorder. 2019.

144. Ling D, Balce K, Weiss M, Murray C, Diamond A. Patients with ADHD are being overmedicated (for optimal cognitive performance). 2019.

145. Diamond A. Attention-deficit disorder (attention-deficit/ hyperactivity disorder without hyperactivity): a neurobiologically and behaviorally distinct disorder from attention-deficit/hyperactivity disorder (with hyperactivity). Dev Psychopathol. 2005;17(3):807–25.

146. Barkley RA, DuPaul GJ, McMurray MB. Attention deficit disorder with and without hyperactivity: clinical response to three dose levels of methylphenidate. Pediatrics. 1991 Apr;87(4):519–31.

147. University of British C. Low-dose vs. Normal-dose Psychostimulants on Executive Functions in Individuals With ADHD. 2024.

148. Handelman K, Sumiya F. Tolerance to Stimulant Medication for Attention Deficit Hyperactivity Disorder: Literature Review and Case Report. Brain Sci. 2022 Jul 22;12(8):959.

149. Swanson J, Gupta S, Guinta D, Flynn D, Agler D, Lerner M, et al. Acute tolerance to methylphenidate in the treatment of attention deficit hyperactivity disorder in children. Clinical Pharmacology & Therapeutics. 1999;66(3):295–305.

150. Srinivas NR, Hubbard JW, Quinn D, Midha KK. Enantioselective pharmacokinetics and pharmacodynamics of dl-threo-methylphenidate in children with attention deficit hyperactivity disorder. Clin Pharmacol Ther. 1992 Nov;52(5):561–8.

151. Swanson JM, Volkow ND. Pharmacokinetic and pharmacodynamic properties of stimulants: implications for the design of new treatments for ADHD. Behav Brain Res. 2002 Mar 10;130(1–2):73–8.

152. Swanson JM, Volkow ND. Serum and brain concentrations of methylphenidate: implications for use and abuse. Neuroscience and Biobehavioral Reviews. 2003;7.

153. Swanson JM. Long-acting stimulants: development and dosing. Can Child Adolesc Psychiatr Rev. 2005 Aug;14(Suppl 1):4–9.

154. Castells X, Ramon M, Cunill R, Olivé C, Serrano D. Relationship between treatment duration and efficacy of pharmacological treatment for ADHD: a meta-analysis and meta-regression of 87 randomized controlled clinical trials. Journal of attention disorders. 2021;25(10):1352–61.

155. Safer DJ, Allen RP. Absence of tolerance to the behavioral effects of methylphenidate in hyperactive and inattentive children. The Journal of pediatrics. 1989;115(6):1003–8.

156. Matthijssen AFM, Dietrich A, Bierens M, Kleine Deters R, van de Loo-Neus GH, van den Hoofdakker BJ, et al. Continued benefits of methylphenidate in ADHD after 2 years in clinical practice: a randomized placebo-controlled discontinuation study. American Journal of Psychiatry. 2019;176(9):754–62.

157. Ross DC, Fischhoff J, Davenport B. Treatment of ADHD when tolerance to methylphenidate develops. Psychiatric Services. 2002;53(1):102–102.

158. Cunill R, Castells X, Tobias A, Capellà D. Efficacy, safety and variability in pharmacotherapy for adults with attention deficit hyperactivity disorder: a meta-analysis and meta-regression in over 9000 patients. Psychopharmacology. 2016;233:187–97.

159. Swanson JM, Hinshaw SP, Arnold LE, Gibbons RD, Marcus S, Hur K, et al. Secondary evaluations of MTA 36-month outcomes: propensity score and growth mixture model analyses. Journal of the American Academy of Child & Adolescent Psychiatry. 2007;46(8):1003–14.

160. Sibley MH, Arnold LE, Swanson JM, Hechtman LT, Kennedy TM, Owens E, et al. Variable patterns of remission from ADHD in the multimodal treatment study of ADHD. American Journal of Psychiatry. 2022;179(2):142–51.

161. Yang X, Morris SM, Gearhart JM, Ruark CD, Paule MG, Jr WS, et al. Development of a Physiologically Based Model to Describe the Pharmacokinetics of Methylphenidate in Juvenile and Adult Humans and Nonhuman Primates. PLOS ONE. 2014;9(9):30.

162. Qian Y, Markowitz JS. Prediction of Carboxylesterase 1-mediated In Vivo Drug Interaction between Methylphenidate and Cannabinoids using Static and Physiologically Based Pharmacokinetic Models. Drug Metab Dispos. 2022 Jul;50(7):968–79.

163. Xiao J, Shi J, Thompson BR, Smith DE, Zhang T, Zhu HJ. Physiologically-Based Pharmacokinetic Modeling to Predict Methylphenidate Exposure Affected by Interplay Among Carboxylesterase 1 Pharmacogenetics, Drug-Drug Interactions, and Sex. J Pharm Sci. 2022 Sep;111(9):2606–13.

164. Gutiérrez-Casares JR, Quintero J, Jorba G, Junet V, Martínez V, Pozo-Rubio T, et al. Methods to Develop an in silico Clinical Trial: Computational Head-to-Head Comparison of Lisdexamfetamine and Methylphenidate. Front Psychiatry. 2021;12:741170.

165. Lyauk YK, Stage C, Bergmann TK, Ferrero-Milliani L, Bjerre D, Thomsen R, et al. Population Pharmacokinetics of Methylphenidate in Healthy Adults Emphasizing Novel and Known Effects of Several Carboxylesterase 1 (CES1) Variants. Clin Transl Sci. 2016 Dec;9(6):337–45.

166. Shader RI, Harmatz JS, Oesterheld JR, Parmelee DX, Sallee FR, Greenblatt DJ. Population pharmacokinetics of methylphenidate in children with attention-deficit hyperactivity disorder. J Clin Pharmacol. 1999 Aug;39(8):775–85.

167. Simon N. Analyse pharmacocinétique et pharmacodynamique par approche de population. Solal Ed. 2011;

168. Bonate PL. Pharmacokinetic-pharmacodynamic modeling and simulation [Internet]. 2nd ed. New York: Springer; 2011. Available from: http://site.ebrary.com/id/10481377

169. Soufsaf S, Robaey P, Bonnefois G, Nekka F, Li J. A Quantitative Comparison Approach for Methylphenidate Drug Regimens in Attention-Deficit/Hyperactivity Disorder Treatment. J Child Adolesc Psychopharmacol. 2019 Feb 4;

170. Owen JS, Fiedler-Kelly J. Introduction to population pharmacokinetic/pharmacodynamic analysis with nonlinear mixed effects models. Hoboken, New Jersey: Wiley; 2014. p.

171. Soufsaf S, Li J. Amélioration de l'usage des psychostimulants en TDAH pédiatrique par des régimes médicamenteux axés sur le bien-être des patients : approche par modélisation et simulation [Internet]. [[Montréal]]: Université de Montréal; 2017. Available from: http://hdl.handle.net/1866/20553

172. Boroujerdi M (19. . . . .). Pharmacokinetics : principles and applications. New York: McGraw-Hill Medical Pub. Division; 2001.

173. Gabrielsson J. Pharmacokinetic and pharmacodynamic data analysis : concepts and applications. 5th edition, revised and expanded.. Stockholm : Apotekarsocieteten; 2016. (Weiner D, editor. Pharmacokinetic & pharmacodynamic data analysis).

174. Upton RN, Mould DR. Basic concepts in population modeling, simulation, and model-based drug development: part 3-introduction to pharmacodynamic modeling methods. CPT Pharmacometrics Syst Pharmacol. 2014 Jan 2;3(1):e88.

175. Mandema JW, Wada DR. Pharmacodynamic model for acute tolerance development to the electroencephalographic effects of alfentanil in the rat. J Pharmacol Exp Ther. 1995 Dec 1;275(3):1185.

176. US-FDA,CDER: CFR Code of Federal Regulations Title 21 Part 314.3. Definitions. [Internet]. [cited 2023 Feb 4]. Available from: https://www.ecfr.gov/current/title-21/chapter-I/subchapter-D/part-314/subpart-A/section-314.3

177. Hauschke D, Steinijans V, Pigeot I. Bioequivalence studies in drug development : methods and applications [Internet]. Chichester, England ; Hoboken, NJ: Wiley,; 2007. 1 online resource (xi, 311 pages). (Statistics in practice). Available from: http://onlinelibrary.wiley.com/book/10.1002/9780470094778 Accès réservé UdeM Conditions d'utilisation: https://bib.umontreal.ca/public/bib/conditions-utilisation/conditions-utilisation-fiche_006.pdf

178. U.S. Food and Drug Administration. FDA. FDA; 2019 [cited 2021 May 21]. Abbreviated New Drug Application (ANDA). Available from: https://www.fda.gov/drugs/types-applications/abbreviated-new-drug-application-anda

179. Coghill D, Banaschewski T, Zuddas A, Pelaz A, Gagliano A, Doepfner M. Long-acting methylphenidate formulations in the treatment of attention-deficit/hyperactivity disorder: a systematic review of head-to-head studies. 2013;24.

180. Endrenyi L, Tothfalusi L. Do regulatory bioequivalence requirements adequately reflect the therapeutic equivalence of modified-release drug products? J Pharm Pharm Sci. 2010 May 10;13(1):107–13.

181. Chen ML. An alternative approach for assessment of rate of absorption in bioequivalence studies. Pharmaceutical research. 1992;9:1380–5.

182. U.S. Food and Drug Administration. Draft Guidance on Methylphenidate [Internet]. 2018. Available from: https://www.accessdata.fda.gov/drugsatfda_docs/psg/Methylphenidate_draft_Orally%20disintegrating%20tab%20ER_RLD%20205489_RC07-18.pdf

183. Bois FY, Tozer TN, Hauck WW, Chen ML, Patnaik R, Williams RL. Bioequivalence: performance of several measures of rate of absorption. Pharm Res. 1994 Jul;11(7):966–74.

184. Elze M, Potthast H, Blume H. Metrics of absorption: data base analysis. In 1995. p. 61–71.

185. Endrenyi L, Csizmadia F, Tothfalusi L, Chen ML. Metrics comparing simulated early concentration profiles for the determination of bioequivalence. Pharm Res. 1998 Aug;15(8):1292–9.

186. Endrenyi L, Tothfalusi L, Zha J. Metrics assessing absorption rates: principles, and determination of bioequivalence in the steady state. BioInternational. 1995;94.

187. Endrenyi L, Yan W. Variation of Cm, and C^/AUC in investigations of bioequivalence. Int J Clin Pharmacol Ther Toxicol. 1993;31:184–9.

188. Endrenyi L, Fritsch S, Yan W. Cmax/AUC is a clearer measure than Cmax for absorption rates in investigations of bioequivalence. International journal of clinical pharmacology, therapy, and toxicology. 1991;29(10):394–9.

189. Lacey L, Keene O, Duquesnoy C, Bye A. Evaluation of different indirect measures of rate of drug absorption in comparative pharmacokinetic studies. Journal of pharmaceutical sciences. 1994;83(2):212–5.

190. Lacey LF, Bye A, Keene ON. Glaxo's experience of different absorption rate metrics of immediate release and extended release dosage forms. Drug information journal. 1995;29(3):821–40.

191. Reppas C, Lacey LF, Keene ON, Macheras P, Bye A. Evaluation of different metrics as indirect measures of rate of drug absorption from extended release dosage forms at steady-state. Pharmaceutical research. 1995;12:103–7.

192. Steinijans VW, Sauter R, Hauschke D, Elze M. Metrics to characterize concentration-time profiles in single-and multiple-dose bioequivalence studies. Drug information journal. 1995;29(3):981–7.

193. Steinijans V. Pharmacokinetic characteristics of controlled release products and their biostatistical analysis. Paperback APV. 1989;22:99–115.

194. Chen ML, Lesko L, Williams RL. Measures of exposure versus measures of rate and extent of absorption. Clin Pharmacokinet. 2001;40(8):565–72.

195. Schall R, Luus HG, Steinijans VW, Hauschke D. Choice of characteristics and their bioequivalence ranges for the comparison of absorption rates of immediate-release drug formulations. Int J Clin Pharmacol Ther. 1994 Jul;32(7):323–8.

196. Yue CS, Ozdin D, Selber-Hnatiw S, Ducharme MP. Opportunities and Challenges Related to the Implementation of Model--Based Bioequivalence Criteria. CLINICAL PHARMACOLOGY. 2019;105(2):13.

197. Zhao L, Kim M, Zhang L, Lionberger R. Generating model integrated evidence for generic drug development and assessment. Clinical Pharmacology & Therapeutics. 2019;105(2):338–49.

198. Research C for DE and. U.S. Food and Drug Administration. FDA; 2022 [cited 2023 Mar 27]. Population Pharmacokinetics. Available from: https://www.fda.gov/regulatory-information/search-fda-guidance-documents/population-pharmacokinetics

199. U.S. Food and Drug Administration. Guidance for industry. Statistical Approaches to Establishing Bioequivalence [Internet]. FDA: Rockville, MD; 2001 [cited 2020 Oct 22]. Available from: https://www.fda.gov/regulatory-information/search-fda-guidance-documents/statistical-approaches-establishing-bioequivalence

200. Food and Drug Administration. In vivo bioequivalence studies based on population and individual bioequivalence approaches. Guidance for Industry. Rockville, MD; 1997.

201. Food and Drug Administration. Average, population and individual approaches to establishing bioequivalence. Rockville, MD; 1999.

202. Food and Drug Administration. BA and BE studies for orally administered drug products: General considerations. Rockville, MD; 1999.

203. Nardi R, Masina M, Cioni G, Leandri P, Zuccheri P. Generic- equivalent drugs use in internal and general medicine patients: distrust, confusion, lack of certainties or of knowledge? Part 2. Misconceptions, doubts and critical aspects when using generic drugs in the real world. Italian Journal of Medicine. 2014;8:88–98.

204. Toutain PL. Bioequivalence: Some challenges and issues [Internet]. Paris; 2008. Available from: http://physiologie.envt.fr/spip/IMG/ppt/final_Bioequivalence_web_CVMP_paris_2008.ppt

205. Nakai K, Fujita M, Tomita M. Comparison of average and population bioequivalence approach. Int J Clin Pharmacol Ther. 2002 Sep;40(9):431–8.

206. Barrett JS, Batra V, Chow A, Cook J, Gould AL, Heller AH, et al. PhRMA perspective on population and individual bioequivalence. J Clin Pharmacol. 2000 Jun;40(6):561–70.

207. Zariffa NM, Patterson SD. Population and individual bioequivalence: lessons from real data and simulation studies. J Clin Pharmacol. 2001 Aug;41(8):811–22.

208. Hauck WW, Chen ML, Hyslop T, Patnaik R, Schuirmann D, Williams R. Mean difference vs. variability reduction: tradeoffs in aggregate measures for individual bioequivalence. FDA Individual Bioequivalence Working Group. Int J Clin Pharmacol Ther. 1996 Dec;34(12):535–41.

209. Sheiner LB. Bioequivalence revisited. Stat Med. 1992 Sep 30;11(13):1777–88.

210. Hauck WW, Anderson S. Measuring switchability and prescribability: when is average bioequivalence sufficient? J Pharmacokinet Biopharm. 1994 Dec;22(6):551–64.

211. Steinijans VW. Some conceptual issues in the evaluation of average, population, and individual bioequivalence. Drug Information Journal. 2001;35:893–9.

212. Hauschke D, Steinijans VW. The U.S. draft guidance regarding population and individual bioequivalence approaches: comments by a research-based pharmaceutical company. 2000;6.

213. Hsuan FC. Some statistical considerations on the FDA draft guidance for individual bioequivalence. Statistics in Medicine. 2000;19:2879–84.

214. Midha KK. Individual and Average Bioequivalence of Highly Variable Drugs and Drug Products. 1997;86(11):5.

215. Vuorinen J, Turunen J. A simple three-step procedure for parametric and nonparametric assessment of bioequivalence. Drug Information Journal. 1997;31:167–80.

216. Dragalin V, Fedorov V, Patterson S, Jones B. Kullback–Leibler divergence for evaluating bioequivalence. Statistics in Medicine. 2003;22(6):913–30.

217. Patterson S. A review of the development of biostatistical design and analysis techniques for assessing in vivo bioequivalence: Part two. Indian Journal of Pharmaceutical Sciences. 2001;63(3):169.

218. Soufsaf S, Nekka F, Li J. Trapezoid bioequivalence: A rational bioavailability evaluation approach on account of the pharmaceutical-driven balance of population average and variability. CPT Pharmacometrics Syst Pharmacol. 2022 Apr;11(4):482–93.

219. Soufsaf S, Robaey P, Nekka F. An exploratory analysis of the performance of methylphenidate regimens based on a PKPD model of dopamine and norepinephrine transporter occupancy. J Pharmacokinet Pharmacodyn. 2023 Mar 17;

220. Bonnefois G, Robaey P, Barrière O, Li J, Nekka F. An Evaluation Approach for the Performance of Dosing Regimens in Attention-Deficit/Hyperactivity Disorder Treatment. Journal of Child and Adolescent Psychopharmacology. 2017 May 1;27(4):320–31.

221. Jackson AJ, Foehl HC. A Simulation Study of the Comparative Performance of Partial Area under the Curve (pAUC) and Partial Area under the Effect Curve (pAUEC) Metrics in Crossover Versus Replicated Crossover Bioequivalence Studies for Concerta and Ritalin LA. AAPS J. 2022 Jul 8;24(4):80.

222. Chen S, Morgan B, Beresford H, Burmeister Getz E, Christopher D, Långström G, et al. Performance of the Population Bioequivalence (PBE) Statistical Test with Impactor Sized Mass Data. AAPS PharmSciTech. 2019 Aug 23;20(7):296.

223. U.S. Food and Drug Administration. Draft guidance on budesonide [Internet]. 2012. Available from: https://www.accessdata.fda.gov/drugsatfda_docs/psg/Budesonide_Inhalation_Sus_20929_RC_09-12.pdf

224. Morgan B, Strickland H. Performance properties of the population bioequivalence approach for in vitro delivered dose for orally inhaled respiratory products. AAPS J. 2014 Jan;16(1):89–100.